

GEOMETRIC OPTIMAL CONTROL WITH AN APPLICATION TO IMAGING
IN NUCLEAR MAGNETIC RESONANCE

A DISSERTATION SUBMITTED TO THE GRADUATE DIVISION OF THE
UNIVERSITY OF HAWAII AT MĀNOA IN PARTIAL FULFILLMENT OF THE
REQUIREMENTS FOR THE DEGREE OF

DOCTOR OF PHILOSOPHY

IN

MATHEMATICS

DECEMBER 2013

By

John Marriott

Dissertation Committee:

Monique Chyba, Chairperson

Bernard Bonnard

Sarah Post

George Wilkens

Andrew Stenger

We certify that we have read this dissertation and that, in our opinion, it is satisfactory in scope and quality as a dissertation for the degree of Doctor of Philosophy in Mathematics.

DISSERTATION
COMMITTEE

Chairperson

Copyright 2013 by

John Marriott

ACKNOWLEDGMENTS

I would first like to thank those who I could not have done this without. On the academic side, my advisers and collaborators, Bernard Bonnard, Monique Chyba, Alain Jacquemard, Urszula Ledzewicz, Gautier Picot, Heinz Schättler, and George Wilkens, have demonstrated a depth of knowledge and patience that have been instrumental in my development as a mathematician and a researcher. I also thank my committee members, Sarah Post and Andrew Stenger, for their feedback on this manuscript and evaluation of the results therein.

On the personal side, I would of course be nowhere without the support and love from my family: Joe, Jane, Levi, Penelope, Simone, and Stacy Marriott.

As for pecuniary matters, I thank the National Science Foundation for funding of grants that I have been supported by, under the Division of Mathematical Sciences and the GK-12 program, and the Graduate Student Organization at the University of Hawai'i for for travel reimbursement

There are many other teachers, mentors, friends, and family that have been integral to my success. To all of you, listed or not, my gratitude is inexpressible.

ABSTRACT

This work addresses the contrast problem in nuclear magnetic resonance as a Mayer problem in optimal control. This is a problem motivated by improving the visible contrast in magnetic resonance imaging, in which the magnetization of the nuclei of the substances imaged are first prepared by being set to a particular configuration by an external magnetic field, the control. In particular we examine the contrast problem by saturation, wherein the magnetization of the first substance is set to zero. This system is modeled by a pair of Bloch equations representing the evolution of the magnetization vectors of the nuclei of two different substances, both influenced by the same control field.

The Pontryagin maximum principle is used to reduce the problem to the analysis of so-called singular trajectories of the system, and we apply the tools of geometric optimal control. We explore the exceptional singular trajectories in detail. In this case the singular control, which is generically a feedback of the state and adjoint vectors of the Hamiltonian system, is a feedback of only the state for this problem, characterizing exceptional singular trajectories as solutions of an ordinary differential equation in the state variables.

We introduce the concept of feedback equivalent control systems and results concerning quadratic differential equations, and compute a set of invariants for the quadratic approximation of exceptional singular flow to distinguish the different cases occurring in physical experiments. Additionally, Gröbner bases are employed to make an algebraic-geometric classification of the equilibrium and singular points of the exceptional dynamics.

TABLE OF CONTENTS

Acknowledgments	iv
Abstract	v
List of Tables	ix
List of Figures	x
1 Introduction	1
2 Optimality Conditions of the Contrast Problem by Saturation	11
2.1 Preliminaries	11
2.1.1 Bi-input case	11
2.1.2 Single-input case	12
2.1.3 Collinear set	13
2.1.4 Optimal control structure	14
2.2 The single-spin case	15
2.2.1 Experimental result	18
2.3 Optimality conditions	18
2.3.1 Geometric interpretation	19
2.3.2 Classification of extremals	20
2.3.3 Conjugate point algorithms	23
2.4 Symmetry of revolution	25
2.5 Generated Lie algebra	29
2.5.1 Restriction to a single spin	29
2.5.2 Lie algebra of the coupled system	32
3 Classification of the Singular Flow: the Exceptional Case	35
3.1 The exceptional flow—equilibria and attractivity	35

3.2	Feedback classification	40
3.2.1	Definitions	40
3.2.2	Application to the exceptional case	42
3.2.3	Quadratic differential equations	45
3.3	Quadratic approximation at the north pole	49
3.3.1	Non-isolated equilibria	51
3.3.2	Ray solutions	55
3.4	Quadratic approximation at the origin	59
3.4.1	Non-isolated equilibria	62
3.4.2	Ray solutions	63
3.5	Algebraic geometric classification	64
3.5.1	Gröbner bases	65
3.5.2	Analysis of the set S	66
3.5.3	Analysis of the surface S'	69
3.6	Classification	84
4	Conclusion	86
A	Physical Model	87
B	Optimal Control Theory	91
B.1	Calculus of variations	91
B.2	Optimal control problem statement	95
B.3	Pontryagin maximum principle	96
B.4	Optimal control computation	98
B.4.1	Definitions	98
B.4.2	Single-input case	99
B.4.3	Bi-input case	101
B.5	Second-order conditions	102

B.5.1 Legendre–Clebsch condition	103
B.5.2 Conjugate points	103
Bibliography	106

LIST OF TABLES

1.1	Parameter values for the four experimental substances.	5
2.1	Brackets of A , C_{ij} , H_{ij} , and T_{ij}	31
3.1	Attractors in continuation of Λ_{gw} to Λ_{wf}	39
3.2	Invariant values for the four sets of parameters.	59

LIST OF FIGURES

1.1	A contrast imaging experiment.	2
2.1	Collinear set.	13
2.2	Maximum steady-state (non-saturation) contrast for parameter set Λ_{do}	14
2.3	Synthesis of single-spin transfer to origin.	18
2.4	Optimal versus heuristic solution of single-spin transfer.	19
2.5	Optimal solution in a Mayer problem.	20
2.6	Behaviors of extremals in the fold case.	21
2.7	Non-smooth extremal of order zero extremal arcs.	23
2.8	Exceptional trajectory and conjugate point for parameter set Λ_{wc}	25
2.9	Exceptional trajectory and conjugate point for parameter set Λ_{do}	25
2.10	Exceptional trajectory and conjugate point for parameter set Λ_{gw}	26
2.11	Exceptional trajectory and conjugate point for parameter set Λ_{wf}	26
3.1	Exceptional trajectories reaching the equilibrium for Λ_{wc}	36
3.2	Exceptional trajectories reaching the equilibrium for Λ_{do}	37
3.3	Exceptional trajectories reaching the equilibrium for Λ_{wf}	37
3.4	Exceptional trajectory for Λ_{gw}	38
3.5	Exceptional trajectory for Λ_{gw}	38
3.6	Attractors in continuation of Λ_{gw} to Λ_{wf}	40
3.7	Classification of the flow of Q_N^π	55
3.8	The roots of $\{D, \nabla D\}$ in the translated system.	69
3.9	Projections of the singular set Ξ for parameter set Λ_{wc}	73
3.10	Projection on (y_2, z_2) of the singular set Ξ for parameter set Λ_{wc}	74

3.11 Singularity Ω_+	74
3.12 Singularity Ω'	74
3.13 Singularity at O for parameter set Λ_{wc}	76
3.14 Components of $p_1(y_1, z_1) = 0$ and $p_2(y_1, z_1, z_2) = 0$ in the interior of the Bloch ball. .	80
3.15 Projections of the singular set Ξ for parameter set Λ_{do}	81
3.16 Components of $p_1(y_1, z_1) = 0$ and $p_2(y_1, z_1, z_2) = 0$ in the interior of the Bloch ball. .	83
3.17 Projections of the singular set Ξ for parameter set Λ_{gw}	83
3.18 Projections of the singular set Ξ for parameter set Λ_{wf}	84
3.19 Partial phase portrait of the vector field X_r^e	85
A.1 Cone precession of a nuclear magnetic moment μ about a magnetic field \mathcal{B}	88
A.2 Behavior of the components of the Bloch equation.	90
A.3 Behavior of Bloch equation in the yz -plane.	90

CHAPTER 1

INTRODUCTION

The central goal of this work is to analyze the contrast problem in nuclear magnetic resonance imaging with the tools of geometric optimal control theory. In broad terms, the first step of the imaging process is to set the atomic nuclei of two distinct substances being imaged to a particular quantum state. The objective of the contrast problem is to optimize this preparatory step in terms of maximizing the visual contrast between the substances when imaged.

Motivation

Since its introduction in the 1940s, nuclear magnetic resonance (NMR) has become an essential tool in chemistry. Through interaction with a magnetic field, NMR allows the manipulation and observation of nuclear spins, which correspond to the magnetization vector of the nucleus.

Applications include NMR spectroscopy, used to determine molecular structures; quantum computing, where NMR is a promising avenue for the construction of a scalable quantum computer [55] and the advancement of control technology enables sophisticated control fields so that complex quantum algorithms may be implemented [30]; and magnetic resonance imaging (MRI), which is a quotidian tool in medical diagnosis. Thus NMR is a standard tool in experimentation and application of quantum control. On the other hand, it is well-suited for theoretical analysis due to the existence of low-dimensional physical models with excellent accuracy in experimentation. This study is therefore interesting as a practical application of geometric techniques in quantum control, and a pragmatic motivation is that advancement of the problem can lead to improved medical imaging techniques.

The focus of this work is a problem in MRI: the *contrast imaging problem*. In imaging, the magnitude of a nucleus' magnetization vector is used to assign its brightness on a gray scale: zero magnetization appears as black, and a maximum magnetization appears as white. When imaging a pair of heterogeneously mixed substances in MRI, one aspect of image quality is the distinction between the two substances, e.g., white and gray cerebral matter in an MRI brain scan. By manipulation of nuclear spins through an external magnetic field, the means of *control* in this setting, the objective is to separate the magnitudes of the magnetization vectors of the two substances as much as possible, thereby maximizing the visual contrast between the two when imaged: the ideal

configuration would be to have each atomic nucleus of the first substance at zero magnetization, and each of the second at maximum magnetization. Both substances are subjected to the *same external control fields* but *respond differently* since they have different physical parameters. The difference in physical parameters of the substances enables the separation of the magnetizations, and the difficulty is posed by the fact that both are simultaneously controlled by with the same signal.

In a laboratory setting, the experiment is set up as follows: the two substances are in separate test tubes of diameter 5 mm and 8 mm, with the smaller test tube suspended inside the larger. A horizontal cross-section is imaged. Figure 1.1 shows an experimentally-produced image before and after the contrast-producing control is applied [38]. Before the control is applied, both magnetizations are at the equilibrium, which has maximum modulus, and so both samples appear as white. The control sets the first magnetization to zero (black), and the remaining magnetization of the second substance gives the image its contrast.

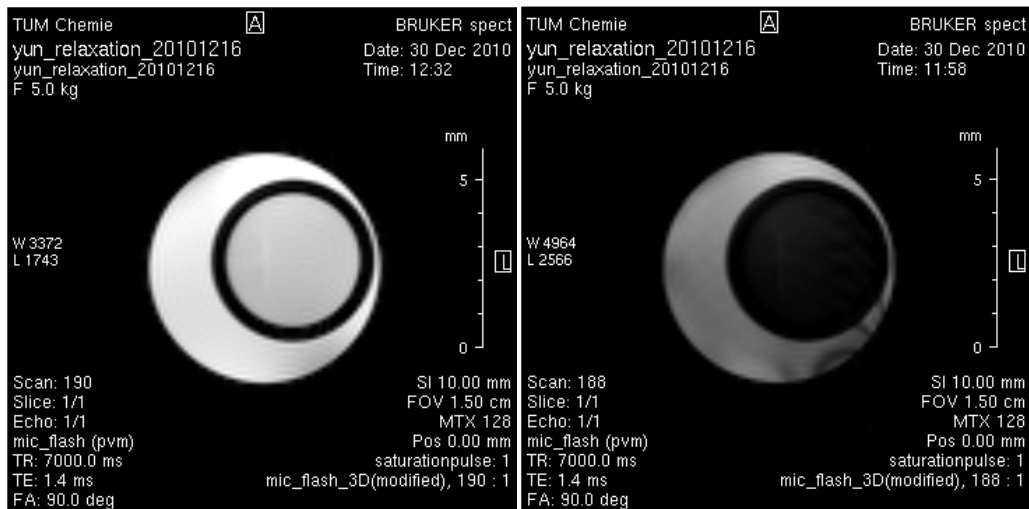


Figure 1.1: Result of a contrast imaging experiment. The image before the control is applied is shown on the left, and the resulting image after the control is applied is shown on the right. At rest, both are at equilibrium (white), so there is zero contrast. The control sets the inner sample to zero magnetization (black), and the remaining magnetization of the outer sample gives the visual contrast.

This particular formulation, in which the magnetization of the first substance has been set to zero, or *saturated*, entirely removes the visual contribution of that substance and therefore reduces the contrast problem to that of maximizing the magnetization of the second substance. This special case of the contrast problem, the *contrast problem by saturation*, is the problem addressed in this

work.

Problem statement

The derivation and full detail of the physical model is given in Appendix A [41].

For a single substance, the magnetization vector of a nucleus is represented by $q := (x, y, z)^T$ belonging to the *Bloch ball* $B := \{q : |q| \leq 1\}$. Its dynamics are described by the Bloch equation,

$$\dot{q} = f(q, u, \gamma, \Gamma) = \begin{cases} \dot{x} = -\Gamma x + u_2 z \\ \dot{y} = -\Gamma y - u_1 z \\ \dot{z} = \gamma(1 - z) + u_1 y - u_2 x, \end{cases} \quad (1.1)$$

where the parameter pair (γ, Γ) are physical constants (corresponding to relaxation times T_1 and T_2 , see Appendix A) for the particular substance, and the control, $u = (u_1, u_2)$, is the external magnetic field which the nuclei are influenced by, which has bounded magnitude; here we set $|u| \leq 1$. The point $(0, 0, 1)$ is a globally attractive equilibrium point of the uncontrolled ($u \equiv 0$) system, and as such is taken as the initial state value. Notice that the controls u_1 and u_2 act by rotation about the x - and y -axes, respectively.

Remark 1. The parameters γ and Γ of a substance are subject to the physical constraint $2\Gamma \geq \gamma \geq 0$ [51]. With this constraint, the Bloch ball is invariant for the dynamics. We additionally assume that $\gamma > 0$ (corresponding to finite relaxation times).

Since in the contrast problem we are concerned with the behavior of a pair of substances, we now extend this notation. The two state variables are denoted q_1 and q_2 , with respective parameters (γ_1, Γ_1) and (γ_2, Γ_2) . The system dynamics, simply two copies of (1.1), are

$$\begin{aligned} \dot{q}_1 &= f(q_1, u, \gamma_1, \Gamma_1) \\ \dot{q}_2 &= f(q_2, u, \gamma_2, \Gamma_2). \end{aligned} \quad (1.2)$$

In this case, we write the state variable as $q = (q_1, q_2)$. This abuse of notation will follow the convention $q = (x, y, z)^T$ when only considering one spin particle, and $q = (q_1, q_2) = ((x_1, y_1, z_1), (x_2, y_2, z_2))^T$ when considering two.

The system (1.2) can be split into *drift* and *control* vector fields and written as

$$\dot{q} = F_0(q) + u_1 F_1(q) + u_2 F_2(q). \quad (1.3)$$

We define B_i and S_i to be the closed unit ball and unit sphere in coordinate q_i , respectively, and the points N_i and O_i to be point $(0, 0, 1)$ and the origin in coordinate q_i , respectively. The state space of the contrast problem is $B := B_1 \times B_2$, and the boundary of this state space is $B_1 \times S_2 \cup B_2 \times S_1$. Further, we denote the north pole as $N := N_1 \times N_2$ and the origin $O := O_1 \times O_2$.

The contrast problem falls in the domain of optimal control theory: we wish to find, among all controls producing saturation of the first magnetization, a control that maximizes the magnitude of the second magnetization. In this framework, the problem can be stated as follows.

Problem 2 (Contrast problem by saturation). *Starting from the equilibrium point $q(0) = N$, reach in a transfer time T , which can be fixed or free, the final state $q_1(T) = O_1$ while minimizing $J(u) = -|q_2(T)|^2$, subject to the dynamics (1.2) where u is a measurable function with bound $|u| \leq 1$.*

A subcase of this problem is the *single-input case*, with $u_2 \equiv 0$. Here, the state is restricted to the $y_i z_i$ -planes, so the state coordinate is simply written $q_i = (y_i, z_i)$. Although the general case is treated, *this work primarily deals with the single-input case*. In this case we write (1.3) simply as $\dot{q} = F(q) + uG(q)$.

Remark 3. In experimentation, a magnetization is in fact measured by reading the magnitude of its projection in the xy -plane (instead of ideally reading each of its coordinates). For the contrast problem by saturation, this is irrelevant: after reaching a position satisfying the terminal state condition, a final rotation can be made to place q_2 in the xy -plane while leaving q_1 at O_1 .

Physical parameter values

We consider four sets of substance parameters representing substances used in an experimental setting. A set of parameters is denoted $\Lambda = ((\gamma_1, \Gamma_1), (\gamma_2, \Gamma_2))$. The values for a particular substance are $\gamma = 1/(T_1 \cdot \omega_{\max})$ and $\Gamma = 1/(T_2 \cdot \omega_{\max})$, where we take $\omega_{\max} = 32.3$ for consistency with experimentation [37] and other numerical work [12]. The parameter values for the four pairs of substances are listed in Table 1.1.

Notice that for parameter sets Λ_{wc} and Λ_{wf} , both with water as the first spin, we have $\gamma_1 = \Gamma_1$; for parameter set Λ_{do} we have $\gamma_1 = \gamma_2$. Various combinations of γ and Γ will commonly appear in

Table 1.1: Parameter values for the four experimental substances. The relaxation times T_1 and T_2 are given, and $\gamma = 1/(T_1 \cdot 32.3)$, $\Gamma = 1/(T_2 \cdot 32.3)$ are written both as decimal values and as rational numbers with a denominator common to the values in a parameter set. The first line of a given parameter set gives the values γ_1 and Γ_1 , and the second line gives γ_2 and Γ_2 .

Parameter set	substance	T_1	T_2	γ	Γ
Λ_{wc}	water	2.5	2.5	$\gamma_1 = \frac{12}{969} \simeq 0.0124$	$\Gamma_1 = \frac{12}{969} \simeq 0.0124$
	cerebrospinal fluid	2.0	0.3	$\gamma_2 = \frac{15}{969} \simeq 0.0155$	$\Gamma_2 = \frac{100}{969} \simeq 0.1032$
Λ_{do}	deoxygenated blood	1.35	0.05	$\frac{200}{8721} \simeq 0.0229$	$\frac{5400}{8721} \simeq 0.6192$
	oxygenated blood	1.35	0.2	$\frac{200}{8721} \simeq 0.0229$	$\frac{1350}{8721} \simeq 0.1548$
Λ_{gw}	gray cerebral matter	0.92	0.1	$\frac{29250}{869193} \simeq 0.0337$	$\frac{269100}{869193} \simeq 0.3096$
	white cerebral matter	0.78	0.09	$\frac{34500}{869193} \simeq 0.0397$	$\frac{299000}{869193} \simeq 0.3440$
Λ_{wf}	water	2.5	2.5	$\frac{4}{323} \simeq 0.0124$	$\frac{4}{323} \simeq 0.0124$
	fat tissue	0.2	0.1	$\frac{50}{323} \simeq 0.1548$	$\frac{100}{323} \simeq 0.3096$

later calculations, leading to the following definitions for $i = 1, 2$: $\delta_i := \gamma_i - \Gamma_i$, $\eta_i := 2\Gamma_i - \gamma_i$, and $\mu_i := 2\gamma_i - \Gamma_i$.

Maximum principle

The Pontryagin Maximum Principle is the foundational result of optimal control theory. We give its statement for the contrast problem here; a full discussion is available in Appendix B.

We denote the target *set of terminal constraints* by $N = \{q \in B : \Psi(q) = 0\}$ where $\Psi(q) = |q_1|$. A given control $u(\cdot)$ yields a unique solution $q(\cdot)$ to (1.2), and we call the pair (q, u) an *admissible controlled trajectory*. As defined in Problem 2, $J(u) = -|q_2(T)|$ is the cost functional to minimize.

Proposition 4 (Pontryagin Maximum Principle). *Let $u(\cdot)$ be a control whose associated trajectory $q(\cdot)$, both defined on $[0, T]$, is optimal for the contrast problem. Denoting $H(q, p, u) = \langle p, F(q) + uG(q) \rangle$ as the control Hamiltonian function, there exists $p(\cdot) : [0, T] \rightarrow \mathbb{R}^4$ and a constant p^0 such that for almost every $t \in [0, T]$,*

(i) *The pair (p^0, p) is nonzero for all $t \in [0, T]$ (nontriviality condition)*

(ii) *$\frac{dq}{dt} = \frac{\partial H}{\partial p}(q, p, u)$, $\frac{dp}{dt} = -\frac{\partial H}{\partial q}(q, p, u)$ (Hamiltonian dynamics)*

(iii) *$H(t, q, p, u) = \max_{|v| \leq 1} H(t, q, p, v)$ for all $t \in [0, T]$ (maximization condition)*

$$(iv) \quad p(T) = p^0 \frac{\partial J}{\partial q}(q(T)) + \sum_{i=1}^k \sigma_i \frac{\partial \Psi_i}{\partial q_i}(q(T)), \quad \sigma = (\sigma_1, \dots, \sigma_k), \quad p^0 \leq 0 \quad (\text{transversality condition})$$

Tuples (q, p, p^0, u) which satisfy the Hamiltonian dynamics and maximization condition of Proposition 4 are called *extremal lifts* and if they additionally satisfy the transversality condition and the problem's boundary conditions they are called *BC-extremals*. We commonly use the coordinate z to denote an extremal lift. When p^0 and u are understood, we may omit them and just write $z = (x, p)$. An extremal lift is *normal* if $p^0 \neq 0$ and *abnormal* if $p^0 = 0$.

Since the dynamics are time-invariant, H as a function of t along an extremal is constant and furthermore if the final time is not fixed then H is zero along an extremal by the transversality condition.

We also note that in this problem, the cost is defined only in terms of the final state value, and so it is known as a *Mayer problem* in optimal control. For such a problem, we have that in an extremal, $p(t) \neq 0$ for all $t \in [0, T]$ by the nontriviality condition.

Optimal control computation in the single-input case

Let us now discuss the computation of an optimal control in the single-input contrast problem with dynamics written as $\dot{q} = F(q) + uG(q)$. By the maximization condition of the maximum principle, for an optimal control $u(\cdot)$ with associated trajectory $q(\cdot)$ we have that for all $t \in [t_0, t_f]$

$$H(t, p^0, p(t), q(t), u(t)) = \max_{|v| \leq 1} H(t, p^0, p(t), q(t), v) = \langle p(t), F(q(t)) \rangle + \max_{|v| \leq 1} v \langle p(t), G(q(t)) \rangle$$

so in particular the maximization of H over $v \in [-1, 1]$ amounts to maximizing just the quantity $v \langle p, G \rangle$ and to this end we define the *switching function* $\Phi(t) := \langle p(t), G(q(t)) \rangle$ and the *switching manifold* $\Sigma := \{(q, p) : \langle p, G(q) \rangle = 0\}$. Clearly, if $\Phi(t)$ is nonzero, $u(t) = \text{sgn } \Phi(t)$, i.e., $u(t) = \pm 1$, and if $\Phi(t) = 0$ this condition gives no immediate information about the value of $u(t)$. If this occurs only at a point, i.e., $\Phi(t) = 0$ but $\dot{\Phi}(t)$ exists and is nonzero, then $u(t)$ is defined everywhere on a neighborhood of t except at the point t , which is sufficient to define u on this interval. Aside from situations where the the times t such that $\Phi(t) = 0$ accumulate, we call such a control *bang-bang*.

If however $\Phi(t) = 0$ on an interval, then we are in the so-called *singular* case and the value of the control is found by the using fact that since Φ is identically zero, all derivatives are also zero. It can be shown (Lemma 94) that the derivatives of Φ are neatly captured by the Lie bracket: $\dot{\Phi} = \langle p, [F, G] \rangle + u \langle p, [G, G] \rangle = \langle p, [F, G] \rangle$. Hence, $\langle p, G \rangle$ and $\langle p, [F, G] \rangle$ are necessarily zero in the

singular case, leading us to define the *singular manifold* $\Sigma' := \{(q, p) : \langle p, G(q) \rangle = \langle p, [F, G](q) \rangle = 0\}$.

In order to calculate the singular control, we use $0 = \dot{\Phi} = \langle p, [F, G] \rangle$, and differentiating once more gives $0 = \ddot{\Phi} = \langle p, [F, [F, G]] \rangle + u \langle p, [G, [F, G]] \rangle$. If $\langle p, [G, [F, G]] \rangle \neq 0$, this gives the value of the singular control u_s ,

$$u_s(t) := -\frac{\langle p, [F, [F, G]] \rangle}{\langle p, [G, [F, G]] \rangle}. \quad (1.4)$$

This is called a *singular control of order 1*, higher orders occurring when $\langle p, [G, [F, G]] \rangle$ is zero and further differentiation is required to compute the value of u .

Singular flow in the single-input case

We denote the Hamiltonian vector field $\langle p, F \rangle(q)$ as $H_F(q)$. On Hamiltonian vector fields, we have the *Poisson bracket* which, in coordinates, is $\{H_1, H_2\}(q, p) = \langle p, [F_1, F_2](q) \rangle$.

In the single input case we can write the order one singular control value as

$$u_s(q, p) = -\frac{\mathcal{D}'(q, p)}{\mathcal{D}(q, p)} \quad (1.5)$$

where $\mathcal{D} = \{H_G, \{H_F, H_G\}\}$ and $\mathcal{D}' = \{H_F, \{H_F, H_G\}\}$. Denoting the extremal $z = (q, p)$, associated singular extremals are solutions of the Hamiltonian equation $\dot{z} = \vec{H}_s(z)$ constrained to the set $\Sigma' = \{z : H_G = \{H_F, H_G\} = 0\}$, where $H_s := H_F + u_s H_G$. This defines a Hamiltonian vector field on $\Sigma' \setminus \{z : \mathcal{D} = 0\}$. In this case we can desingularize u_s by the time reparameterization $ds = dt/\mathcal{D}(z(t))$, so that

$$\frac{dq}{ds} = \mathcal{D}F - \mathcal{D}'G, \quad \frac{dp}{ds} = -p \left(\mathcal{D} \frac{\partial F}{\partial q} - \mathcal{D}' \frac{\partial G}{\partial q} \right),$$

restricted to Σ' .

Since the state is dimension four, the two relations $H_G = 0$ and $\{H_F, H_G\} = 0$ (implying that $p \in \ker(G, [F, G])$, a rank two space off the collinear set of G and $[F, G]$), along with the fact that $p(\cdot)$ is unique only up to a scalar factor reduce (1.5) to the form

$$\frac{dq}{dt} = F(q) - \frac{\mathcal{D}'(q, \zeta)}{\mathcal{D}(q, \zeta)} G(q)$$

where ζ is a one-dimension, time-dependent parameter whose dynamics are deduced from the adjoint

equation.

If the final time is free then $H = H_F + uH_G$ is identically zero. Since in the singular case $H_G \equiv 0$, this leads to the additional constraint $H_F \equiv 0$. This is called the *exceptional* case since it is intrinsic to the system in the sense that it is an abnormal extremal of any system with these state dynamics, regardless of cost. With this, we can eliminate the adjoint entirely.

Proposition 5. *In the single-input contrast problem, the exceptional singular control is given by*

$$u_s^e = -\frac{D'(q)}{D(q)}$$

where

$$D = \det(F, G, [F, G], [G, [F, G]]) \quad \text{and} \quad D' = \det(F, G, [F, G], [F, [F, G]]), \quad (1.6)$$

outside of $\{q : D(q) = 0\}$.

Proof. In the singular case, $H_G = 0$. Differentiating,

$$\dot{H}_G = \langle p, [F, G] \rangle + u \langle p, [G, G] \rangle = 0 \Rightarrow \langle p, [F, G] \rangle = 0$$

$$\ddot{H}_G = \langle p, [F, [F, G]] \rangle + u \langle p, [G, [F, G]] \rangle = 0.$$

Also $H_F = \langle p, F \rangle = 0$, so p is orthogonal to each of F , G , $[F, G]$, and $[F, [F, G]] + u[G, [F, G]]$. By the nontriviality condition of the maximum principle p is not identically zero, therefore these four vectors must be linearly dependent, i.e., $\det(F, G, [F, G], [F, [F, G]] + u[G, [F, G]]) = 0$. Splitting this, we have $\det(F, G, [F, G], [F, [F, G]]) + u \det(F, G, [F, G], [G, [F, G]]) = 0$, which completes the proof. \square

In the exceptional case we denote the vector field X_s^e , defined as

$$\frac{dq}{dt} = F(q) - \frac{D'(q)}{D(q)}G(q),$$

which can be reparameterized by $ds = dt/D(q(t))$ giving the smooth vector field $X_r^e = DF - D'G$.

Remark 6. Summarizing, we see that in the single-input contrast problem with free final time, the singular extremals are necessarily exceptional singular extremals. In this case, the exceptional singular control is defined only in terms of the state, which reduces the exceptional trajectories to

the flow of an ordinary differential equation in the state variables. Furthermore, the exceptional singular extremals are extremals of any optimal control problem sharing the state dynamics of the contrast problem, regardless of cost.

Previous and current results

An early application of optimal control theory to general NMR pulse design was the gradient ascent pulse engineering, GRAPE, algorithm [33]. It is a numerical approach based on the maximum principle, operating in the spirit of steepest descent methods. The basic idea of this algorithm is, given an initial guess of a control duration and value on this time interval, to calculate $\frac{\partial H}{\partial u}$ to iteratively update $u(\cdot)$ to improve the resulting cost. Flexibility is allowed in the cost functional to combine state, duration, and energy penalties.

A step closer to the problem addressed here was the application of geometric methods in optimal control to the control of a single spin particle, which will be discussed in more detail in §2.2. This work resulted in a marked improvement over the existing heuristic techniques, and demonstrated the efficacy of geometric optimal control and the key role of singular extremals in the NMR setting [10, 15]. A comparison of the GRAPE algorithm and the geometric methods in the saturation of a single spin, along with experimental implementation, is given by Lapert, et al. [37].

In the contrast problem, recent numerical work has employed shooting and continuation methods, implemented in the HAMPATH software [18] to obtain locally optimal solutions [12]. The basic idea of this method is that, given a fixed control structure and boundary conditions, homotopy and simple shooting methods are used to identify a singular arc satisfying the maximum principle. This is used to initialize a multiple shooting method corresponding to a particular control structure along a path of zeroes (of the function constraining the shooting) which converges to a local optimum. This work is a thorough numerical treatment of the fixed-time, single-input contrast problem by saturation.

Ongoing work is done to frame the contrast problem in various numerical schemes for cross-validation [11]. The first of these is a direct method implemented in the BOCOP toolbox [2]. This approach transforms the infinite-dimensional optimal control problem into a finite-dimensional non-linear optimization problem by discretization, and applying the optimization tools provided by BOCOP to obtain solutions. The second method poses the optimal control problem as convex, finite-dimensional relaxations in the form of linear matrix inequalities [39]. A feature of this method is

that it can establish lower bounds on the cost and so it can verify global optimality of solutions. Finally, the GRAPE algorithm has been applied to the contrast problem, accompanied by experimental implementation [38].

A promising aspect of these various numerical implementations is that the obtained solutions are comparable in performance. The numerical difference is negligible when compared to the loss of accuracy in experimentation [36]. Given the good agreement of the results of these methods, they can be evaluated by their performance in obtaining solutions. An effective combination in terms of speed and precision is the use of BOCOP to obtain a first estimate, followed by HAMPATH, initialized with this first estimate, to refine the control.

Synopsis

In Chapter 2, examine various properties of the contrast problem: geometric properties, which include the set of points where the drift and control vector fields are collinear and the symmetry of revolution of the problem; optimality conditions, which are derived from application of the maximum principle; and the Lie algebra generated by the drift and control vector fields of the state dynamics.

In Chapter 3 we study exceptional case in detail. We first examine properties of the flow of the exceptional singular dynamics. We then introduce the notion of feedback equivalence in control systems and compute a set of partial invariants with respect to parameter values. Finally we make an algebraic-geometric classification of the singularities of the sets $\{q : D(q) = 0\}$ and $\{q : D(q) = D'(q) = 0\}$, where D and D' are as in (1.6).

Notes

This work will follow the convention that the state variable x will be used when stating general results, and the state variable q will be used when discussing the contrast problem in particular.

Also note that the parameter variables γ and Γ and the related constants δ , η , and μ (and the subscripted versions of these) defined above will be used globally and uniquely to denote these quantities.

CHAPTER 2

OPTIMALITY CONDITIONS OF THE CONTRAST PROBLEM BY SATURATION

In this chapter we analyze various properties of the contrast problem. In particular a major goal of the analysis is to classify various properties of the system with respect to the four physical parameters.

2.1 Preliminaries

We first restate the contrast problem by saturation, and detail the problem statement in the single-input subcase.

2.1.1 Bi-input case

The bi-input case is the general statement of the problem as originally stated.

Problem 7 (Bi-input contrast problem by saturation). *Starting from the equilibrium point $q(0) = N$, reach in a transfer time T , which can be fixed or free, the final state $q_1(T) = O_1$ while minimizing $J(u) = -|q_2(T)|^2$, subject to the dynamics (1.2) where u is measurable and $|u| \leq 1$.*

The Hamiltonian dynamics are

$$\left\{ \begin{array}{l} \dot{x}_1 = -\Gamma_1 x_1 + u_2 z_1 \\ \dot{y}_1 = -\Gamma_1 y_1 - u_1 z_1 \\ \dot{z}_1 = \gamma_1(1 - z_1) + u_1 y_1 - u_2 x_1 \\ \dot{x}_2 = -\Gamma_2 x_2 + u_2 z_2 \\ \dot{y}_2 = -\Gamma_2 y_2 - u_1 z_2 \\ \dot{z}_2 = \gamma_2(1 - z_2) + u_1 y_2 - u_2 x_2 \end{array} \right. \quad \left\{ \begin{array}{l} \dot{p}_{x_1} = \Gamma_1 p_{x_1} + u_2 p_{z_1} \\ \dot{p}_{y_1} = \Gamma_1 p_{y_1} - u_1 p_{z_1} \\ \dot{p}_{z_1} = \gamma_1 p_{z_1} + u_1 p_{y_1} - u_2 p_{x_1} \\ \dot{p}_{x_2} = \Gamma_2 p_{x_2} + u_2 p_{z_2} \\ \dot{p}_{y_2} = \Gamma_2 p_{y_2} - u_1 p_{z_2} \\ \dot{p}_{z_2} = \gamma_2 p_{z_2} + u_1 p_{y_2} - u_2 p_{x_2} \end{array} \right. \quad (2.1)$$

The state dynamics can be written in the form

$$\dot{q} = F_0(q) + u_1 F_1(q) + u_2 F_2(q) \quad (2.2)$$

where the drift F_0 and the control vector fields F_1 and F_2 are given below.

Listed here are the Lie brackets, up to length three, of the vector fields F_0 , F_1 , and F_2 . Since the first three entries of each bracket contain only q_1 , γ_1 , and Γ_1 terms, the last three entries only q_2 , γ_2 , and Γ_2 terms, and these sets of terms differ only by the subscript 1 or 2, we write only three entries of each vector, e.g., $F_1 = (0, -z_1, y_1, 0, -z_2, y_2)^T$ is written as $F_1 = (0, -z_i, y_i)^T$.

$$\begin{aligned}
F_0 &= \begin{pmatrix} -\Gamma_i x_i \\ -\Gamma_i y_i \\ \gamma_i(1 - z_i) \end{pmatrix} & F_1 &= \begin{pmatrix} 0 \\ -z_i \\ y_i \end{pmatrix} & F_2 &= \begin{pmatrix} z_i \\ 0 \\ -x_i \end{pmatrix} \\
[F_0, F_1] &= \begin{pmatrix} 0 \\ \gamma_i - \delta_i z_i \\ -\delta_i y_i \end{pmatrix} & [F_0, F_2] &= \begin{pmatrix} -\gamma_i + \delta_i z_i \\ 0 \\ \delta_i x_i \end{pmatrix} & [F_1, F_2] &= \begin{pmatrix} -y_i \\ x_i \\ 0 \end{pmatrix} \\
[[F_0, F_1], F_0] &= \begin{pmatrix} 0 \\ \gamma_i \eta_i + \delta_i^2 z_i \\ -\delta_i^2 y_i \end{pmatrix} & [[F_0, F_1], F_1] &= \begin{pmatrix} 0 \\ -2\delta_i y_i \\ -\gamma_i + 2\delta_i z_i \end{pmatrix} & [[F_0, F_1], F_2] &= \begin{pmatrix} y_i \delta_i \\ x_i \delta_i \\ 0 \end{pmatrix} \\
[[F_0, F_2], F_0] &= \begin{pmatrix} -\gamma_i \eta_i - \delta_i^2 z_i \\ 0 \\ \delta_i^2 x_i \end{pmatrix} & [[F_0, F_2], F_2] &= \begin{pmatrix} -2\delta_i x_i \\ 0 \\ -\gamma_i + 2\delta_i z_i \end{pmatrix} & [[F_1, F_2], F_2] &= -F_1 \\
& & & & [[F_1, F_2], F_1] &= F_2
\end{aligned}$$

2.1.2 Single-input case

In the single-input case we have $u_2 \equiv 0$, implying that $x_i \equiv 0$ since $x_i(0) = 0$. In this case we write the state coordinate as $q = ((y_1, z_1), (y_2, z_2))$ and the control as u .

The Hamiltonian dynamics are identical to (2.1) with the x_i and u_2 removed,

$$\begin{cases} \dot{y}_1 = -\Gamma_1 y_1 - u z_1 \\ \dot{z}_1 = \gamma_1(1 - z_1) + u y_1 \\ \dot{y}_2 = -\Gamma_2 y_2 - u z_2 \\ \dot{z}_2 = \gamma_2(1 - z_2) + u y_2 \end{cases} \quad \begin{cases} \dot{p}_{y_1} = \Gamma_1 p_{y_1} - u p_{z_1} \\ \dot{p}_{z_1} = \gamma_1 p_{z_1} + u p_{y_1} \\ \dot{p}_{y_2} = \Gamma_2 p_{y_2} - u p_{z_2} \\ \dot{p}_{z_2} = \gamma_2 p_{z_2} + u p_{y_2} \end{cases} \quad (2.3)$$

and in the single-input case we denote the vector fields F_0 and F_1 as F and G respectively, so the dynamics can be written $\dot{q} = F(q) + uG(q)$.

As with the bi-input case, we write the vector field $G = (-z_1, y_1, -z_2, y_2)$ as $(-z_i, y_i)$. The Lie brackets up to length three are

$$\begin{aligned} F &= \begin{pmatrix} -\Gamma_i y_i \\ \gamma_i(1 - z_i) \end{pmatrix}, & G &= \begin{pmatrix} -z_i \\ y_i \end{pmatrix}, & [F, G] &= \begin{pmatrix} \gamma_i - \delta_i z_i \\ -\delta_i y_i \end{pmatrix}, \\ [F, [F, G]] &= \begin{pmatrix} -\gamma_i \eta_i - \delta_i^2 z_i \\ \delta_i^2 y_i \end{pmatrix}, & \text{and} & [G, [F, G]] &= \begin{pmatrix} 2\delta_i y_i \\ \gamma_i - 2_i \delta_i z_i \end{pmatrix}. \end{aligned} \quad (2.4)$$

2.1.3 Collinear set

Here we define the *collinear set* of the single-input system,¹ the set of points where the vector fields F and G are collinear. This set is characterized by three relations,

$$\Gamma_1 y_1^2 = \gamma_1 z_1(1 - z_1), \quad \Gamma_2 y_2^2 = \gamma_2 z_2(1 - z_2), \quad \text{and} \quad \Gamma_1 y_1 z_2 = \Gamma_2 y_2 z_1,$$

i.e., a point in the collinear set lies on two ellipses in (y_1, z_1) - and (y_2, z_2) -coordinates and satisfies an additional compatibility relation. This is shown in Figure 2.1.

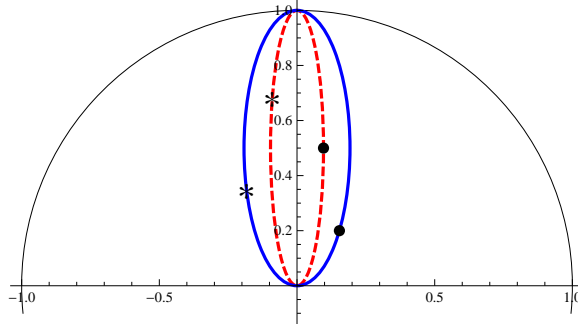


Figure 2.1: Collinear set, illustrated with parameters Λ_{do} . The ellipses containing points in the collinear set are shown, the ellipse in coordinates (y_1, z_1) is a dashed red line, the ellipse in coordinates (y_2, z_2) is a solid blue line, and the (y_1, z_1) - and (y_2, z_2) -planes are overlaid. Two points of the collinear set are shown, with matching markers between the two projections representing a point in the set.

Intuitively, the points of the collinear set are equilibrium points of the state dynamics (2.3) under some fixed control value $u = \bar{u}$, or conversely that a given constant $\bar{u} \in \mathbb{R}$ yields an equilibrium point (\bar{q}_1, \bar{q}_2) in this collinear set. It can be shown using a Lyapunov function that such an equilibrium

¹The collinear set of the bi-input system is the set where F_0 is collinear to a linear combination of F_1 and F_2 , which is a revolution of the collinear set in the single-input case about the z -axis.

point is globally attractive and asymptotically stable.

Such geometric aspects as the collinear set were highly relevant in NMR applications before the 1960s since most applications used continuous-wave spectrometers [26, 41]. Further significance of the collinear set in NMR imaging is discussed in an article of Garon, Glaser, and Sugny [27].

For our problem, it can be used to give a lower bound on the achievable contrast in terms of the parameter values.

A fixed \bar{u} yields the equilibrium point (\bar{q}_1, \bar{q}_2) , and the contrast (*not* a contrast by saturation) can be evaluated at this point: it is the absolute value of the differences of the magnitudes of the projections of \bar{q}_1 and \bar{q}_2 onto the y -axis. Recalling that a rotation may be performed to, in this case, re-align the y -axis in order to maximize this value, this lower bound is found by finding among all $\bar{u} \in \mathbb{R}$ the value which maximizes this difference between the projections of \bar{q}_1 and \bar{q}_2 on some axis.² This is illustrated for parameters Λ_{do} in Figure 2.2. For these, the bound given by this calculation is 0.294, while a locally optimal solution to the contrast problem by saturation obtained by numerical methods achieves a contrast of 0.466 [12].

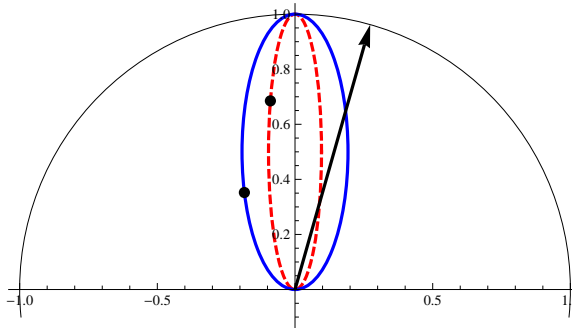


Figure 2.2: Maximum steady-state (non-saturation) contrast for parameter set Λ_{do} . The control value is $\bar{u} = 0.081$, with a corresponding contrast of 0.346. The axis upon which the contrast is maximized is shown as the black arrow.

2.1.4 Optimal control structure

As described in the introduction, extremals are concatenations of bang and singular arcs (see §B.4 for more detail), and in the contrast problem we have the following result which in particular guides numerical control optimization.

Lemma 8. *In terms of number of concatenated arcs, the simplest BC-extremals of the contrast*

²This axis is either parallel to the displacement vector $\bar{q}_1 - \bar{q}_2$, or orthogonal to the shorter of \bar{q}_1 and \bar{q}_2 .

problem are of the form bang-singular.

Proof. The initial point is an equilibrium of the singular dynamics (seen by direct computation of u_s by (1.4)), so the initial control is necessarily a bang, which can be set as $u = +1$ or $u = -1$ due to symmetry. This initial bang arc does not generically meet the boundary condition $q_1(T) = O_1$, and a bang-bang sequence does not either. There exist BC-extremals of the form bang-singular (we will see these in numerical examples), and therefore these are the simplest in terms of number of concatenated arcs. \square

2.2 The single-spin case

A limit case of the contrast problem by saturation with fixed final time T is when T approaches T_{\min} , the duration of a time-optimal transfer of the first spin from N_1 to O_1 . The time-minimal transfer of a single spin has further significance, shown by the following proposition.

Proposition 9. *The time-minimal solution of the transfer of the first spin from N_1 to O_1 can be embedded as an abnormal extremal solution of the contrast problem by saturation.*

Proof. Suppose that (q_1, p_1, u) is the extremal lift of the time-minimal solution of the transfer from $q_1(0) = N_1$ to $q_1(T_{\min}) = O_1$ of a single spin. Let $q_2(0) = N_2$ and $p_2(0) = \mathbf{0}$. The corresponding extremal $q = (q_1, q_2)$ and $p = (p_1, p_2)$, $p_i = (p_{y_i}, p_{z_i})$, is a BC-extremal which satisfies the transversality condition, since by the dynamics of p , given in (2.3), we clearly have $p_2 \equiv \mathbf{0}$ and in particular $p_2(T_{\min}) = \mathbf{0}$, satisfying the transversality condition with $p^0 = 0$. \square

Therefore the time-minimal transfer in the single-spin problem is of particular interest. In previous work the single-spin case was studied in detail, providing time- and energy-minimal solutions to arbitrary points, in the integrable [15] and generic [10] cases. We now review the relevant results of this work.

For the remainder of this section we will discuss only a single spin, so no subscripts will be written. We additionally assume that $2\Gamma > 3\gamma$, which holds for all experimental parameters except water (for which $\Gamma = \gamma$), and also that $\eta > 0$, which holds for all experimental parameters. Since the initial condition, $q(0) = (0, 0, 1)$, is on the z -axis of revolution of the system, the state can be restricted to the yz -plane ($x = 0$) of B with the control restricted to $u = u_1$ ($u_2 = 0$), amounting to a fixed orientation of the control field.

Hence the state variable is $q = (y, z)$ and we write the dynamics as

$$\dot{q} = F(q) + uG(q), \quad (2.5)$$

where F and G (and their Lie brackets) are as given in §2.1.2, with control bound $|u| \leq 1$. The problem is then stated as follows.

Problem 10 (Single-spin transfer to origin). *From the equilibrium point $q(0) = (0, 1)$, reach the final state $q(T) = (0, 0)$ while minimizing the transfer time T , subject to the dynamics (2.5) with $|u| \leq 1$.*

We will see that the optimal control synthesis is a concatenation of bang and singular arcs, so let us first examine the singular extremals of the system. These are found by setting $\Phi = \dot{\Phi} = 0$ (where Φ is the switching function, defined in §B.4.2), which is $\langle p, G \rangle = \langle p, [F, G] \rangle = 0$. By the nontriviality condition of the maximum principle, $0 \neq p \in \ker(G, [F, G])$, implying that $\det(G, [F, G]) = 0$. Hence singular arcs are contained in the set of points satisfying $\det(G, [F, G]) = 0$, namely

$$\det \begin{pmatrix} -z & \gamma - \delta z \\ y & -\delta y \end{pmatrix} = y(2\delta z - \gamma) = 0,$$

where we recall that $\delta = \gamma - \Gamma$. Hence the singular arcs are the line $y = 0$ and the line $z = z_s$, $z_s := \gamma/2\delta$, where $-1 < z_s < 0$ by the assumption that $2\Gamma > 3\gamma$.

As given in Chapter 1, we have that $\langle p, [F, [F, G]] + u_s [G, [F, G]] \rangle = 0$, and similar to the determination of the singular manifold, we have $\det(G, [F, [F, G]] + u_s [G, [F, G]]) = 0$. By multilinearity of the determinant, this gives $\det(G, [F, [F, G]]) + u_s \det(G, [G, [F, G]]) = 0$ which provides the value of the control as a function of the state:

$$u_s = -\frac{\det(G, [F, [F, G]])}{\det(G, [G, [F, G]])} = \frac{\gamma\eta y}{2\delta(y^2 - z^2) + \gamma z} \quad (2.6)$$

outside the set where $\det(G, [G, [F, G]]) = 0$. Thus on the singular line $y = 0$, $u_s = 0$ and the dynamics are

$$\dot{y} = 0, \quad \dot{z} = \gamma(1 - z)$$

which approaches the equilibrium N along the vertical axis. On the singular line $z = \gamma/2\delta$, the

control is $u_s = \gamma\eta/2\delta y$ and the dynamics are

$$\dot{y} = -\Gamma y - \frac{\delta^2\eta}{4\delta^2 y}, \quad \dot{z} = 0,$$

which satisfies $\text{sgn}(\dot{y}) = -\text{sgn}(y)$ due to the assumptions on the parameters γ and Γ , so the flow is toward the vertical axis along this horizontal line. As $y \rightarrow 0$, $|u_s| \rightarrow \infty$ so the control eventually becomes inadmissible as the state moves inward.

In order to classify the time-optimality of the flow along a singular arc, we use the strengthened Legendre–Clebsch condition, that $\langle p, [G, [F, G]] \rangle > 0$ along a an optimal solution (see §B.5 for more detail), which can be given in terms of just the state in the two-dimensional case. Using the relation between the determinant and the inner product of the columns of a matrix, the singular case condition $\langle p, G \rangle = 0$, and fact that $\langle p, F \rangle > 0$ (by the assumption of a normal extremal), we have that

$$\text{sgn} \langle p, [G, [F, G]] \rangle = \text{sgn}(\det(G, F) \det(G, [G, [F, G]])),$$

which for this case is

$$\det(G, F) \det(G, [G, [F, G]]) = -(\Gamma y^2 + \gamma z(z-1))(z(\gamma - 2\delta z) + 2\delta y^2).$$

On the horizontal singular line this is $-2\Gamma\delta y^4 + \gamma^3(1 - \frac{\gamma}{2\delta})y^2$, which is positive, and on the vertical singular line it is $\gamma z^2(1-z)(\gamma - 2\delta z)$ which is positive for $z > z_s$. Therefore singular extremals are small-time minimizing on the horizontal singular line and on the vertical singular line for $z > z_s$.

Further work is needed to give the full synthesis of an optimal control, but the above results present the key factors of this synthesis. The locally-optimal trajectory is a concatenation of arcs $\sigma_+\sigma_h\sigma_+\sigma_v$, where σ_+ denotes a bang arc with $u = +1$, σ_h denotes a singular arc along the horizontal singular line, and σ_v denotes a singular arc along the vertical singular line.

The horizontal singular line cannot be followed to its intersection with the vertical singular line due to the control bound, necessitating the bang arc joining σ_h and σ_v . This must be chosen appropriately to ensure that the maximum principle is satisfied, leading to the following definition [10].

Definition 11. A *bridge* between the horizontal and singular vertical lines is a bang arc such that the singular-bang-singular concatenation is an optimal extremal.

This synthesis is qualitatively shown in Figure 2.3.

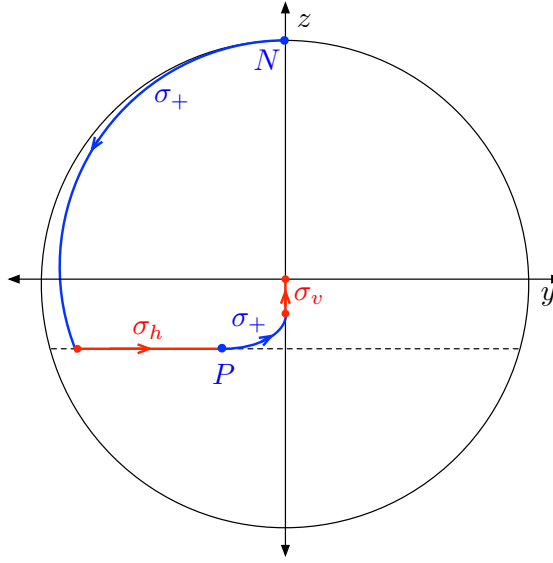


Figure 2.3: Synthesis of single-spin transfer to origin. From the initial point N , a bang arc σ_+ is followed to the intersection with the horizontal singular line, where the control becomes singular. The trajectory follows the singular arc σ_h to the point P , one endpoint of the bridge connecting the two singular arcs. A bang arc σ_+ is used to reach the vertical singular arc σ_v which is followed to the origin.

2.2.1 Experimental result

The previously-used heuristic method for the transfer from N to O , known as *inversion recovery*, was simply to apply a bang control to reach a point on the negative z -axis, followed by a zero control to reach the origin, a bang-singular (BS) control structure. The above-described optimal control, with a BSBS structure, gives a significant time decrease. This improvement depends on a set of parameter values; for instance a decrease of 58% was achieved for a solution of H_2O , D_2O , and deuterated glycerol saturated with CuSO_4 (for which $T_1 = 740$ ms and $T_2 = 60$ ms) in experiments performed by Lapert, et al. [37], which is illustrated versus the heuristic inversion recovery in Figure 2.4.

2.3 Optimality conditions

In this section we give the first- and second-order optimality conditions as they apply to this type of problem (control-affine, Mayer) in general, and give the conjugate point tests as they apply to the single-input contrast problem.

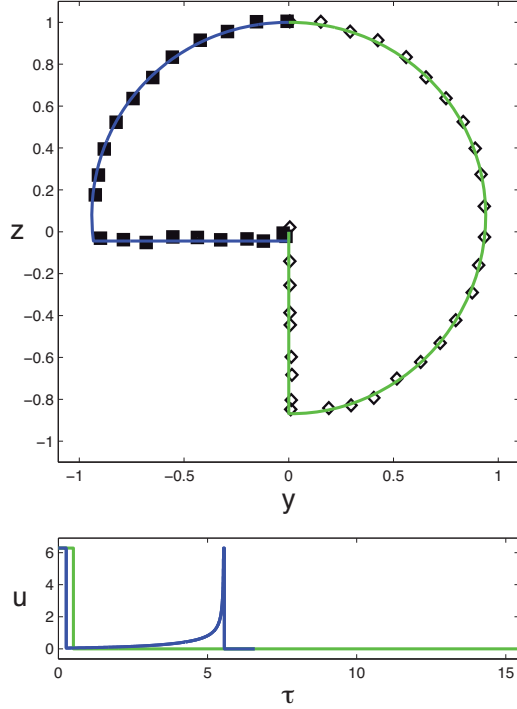


Figure 2.4: Top: Plot of the locally-optimal BSBS sequence, left half-plane (blue), and the inversion recovery sequence, right half-plane (green) [37]. The numerically-calculated trajectories are shown as a solid line with the experimentally-measured trajectories shown as markers. Bottom: controls corresponding to the BSBS sequence (blue) and inversion recovery sequence (green).

2.3.1 Geometric interpretation

Consider a general Mayer problem with terminal manifold $M = \{x : \Psi(x) = 0\}$, cost $J(u) = \varphi(t_f, x(t_f))$, and denote a trajectory from initial point x_0 associated to the control u by $x(\cdot, x_0, u)$, defined on $[t_0, t_f]$. The accessibility set at time t from x_0 is defined as $A(x_0, t) = \bigcup_{u \in \mathcal{U}} x(t, x_0, u)$. For a fixed cost k , we define the set $M_k := \{x : \Psi(x) = 0 \text{ and } \varphi(x) = k\}$ to be a level set of the cost in the terminal manifold.

By the maximum principle, if a control u^* with associated trajectory x^* is optimal, then $x^*(t_f)$ belongs to the boundary of the accessibility set $A(x_0, t_f)$ and lies in the terminal manifold M_k such that k is minimal. This is shown in Figure 2.5.

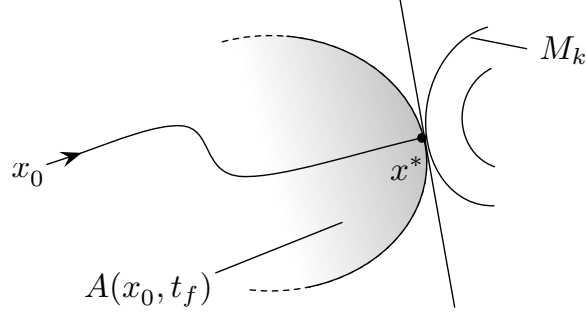


Figure 2.5: Optimal solution in a Mayer problem: x^* lies on the boundary of the accessibility set $A(x_0, t_f)$ and terminal manifold M_k with a minimal cost.

2.3.2 Classification of extremals

Denoting the canonical variable $z = (x, p)$ and the switching surface Σ , we are interested in the classification of extremals near the set Σ .

Single-input case

Here we have $\Sigma := \{z : H_G(z) = 0\}$ with the switching function $\Phi(t) = H_G(z(t))$, where $H_G = \langle p, G \rangle$. Define $\Sigma' := \{z : H_G(z) = \{H_F, H_G\} = 0\}$ as the set containing singular extremals. As in §2.2 we denote σ_+ and σ_- as bang arcs and σ_s as a singular arc; a sequence $\sigma_1\sigma_2$ denotes a concatenation of arcs (which can be bang or singular).

At an *ordinary switching point* a bang arc intersects, at time t , the set $\Sigma \setminus \Sigma'$, and such an extremal is of the form $\sigma_+\sigma_-$ if $\dot{\Phi}(t) < 0$ and $\sigma_-\sigma_+$ if $\dot{\Phi}(t) > 0$. On the other hand, the *fold case* is characterized by a contact of order two of a bang arc with Σ . Recall that

$$\ddot{\Phi}(t) = \{H_F, \{H_F, H_G\}\} + u \{H_G, \{H_F, H_G\}\}$$

and so we define

$$\ddot{\Phi}_\pm(t) = \{H_F, \{H_F, H_G\}\} \pm \{H_G, \{H_F, H_G\}\},$$

with $\ddot{\Phi}_+$ corresponding to $u = +1$ and $\ddot{\Phi}_-$ corresponding to $u = -1$.

Assuming that both $\ddot{\Phi}_\pm(t) \neq 0$, there are three cases [7, 35].

- (i) Hyperbolic: $\ddot{\Phi}_+(t) > 0$ and $\ddot{\Phi}_-(t) < 0$. In this case a connection with a singular arc satisfying the strong generalized Legendre–Clebsch condition is possible, and extremal trajectories are of the form $\sigma_\pm\sigma_s\sigma_\pm$ (where some arcs may be empty).

- (ii) Elliptic: $\ddot{\Phi}_+(t) < 0$ and $\ddot{\Phi}_-(t) > 0$. Every extremal curve has a finite number of switchings and a connection with a singular extremal is not possible, therefore every extremal is bang-bang, although there is no uniform bound on the number of switchings for all extremals.
- (iii) Parabolic: $\ddot{\Phi}_+(t) \cdot \ddot{\Phi}_-(t) > 0$. In this case singular extremals do not satisfy the control bound, and therefore the behavior near the switching point is bang-bang with at most two switchings. The sequence is $\sigma_+\sigma_-\sigma_+$ if $\ddot{\Phi}_+(t) > 0$ and $\sigma_-\sigma_+\sigma_-$ if $\ddot{\Phi}_+(t) < 0$ (where some arcs may be empty).

These three cases are illustrated in Figure 2.6.

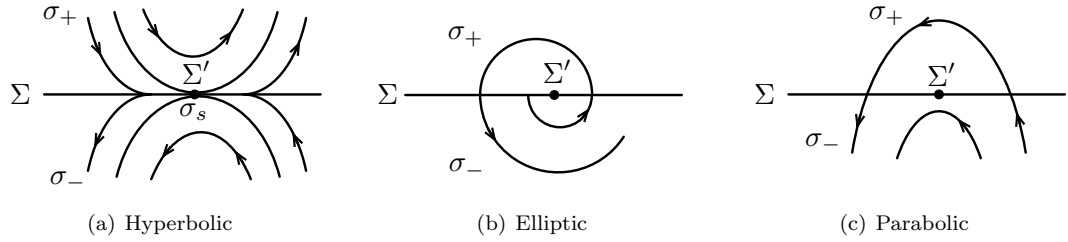


Figure 2.6: Behaviors of extremals in the fold case.

Bi-input case

The switching surface is the set $\Sigma := \{z : H_1(z) = H_2(z) = 0\}$. Differentiating these relations, we have

$$\begin{aligned}\dot{H}_1 &= \{H_0, H_1\} - u_2 \{H_1, H_2\} \\ \dot{H}_2 &= \{H_0, H_2\} + u_1 \{H_1, H_2\}.\end{aligned}$$

At an ordinary switching point, at most one of \dot{H}_1 and \dot{H}_2 are zero. Recalling the parameterization of the control $u_i = H_i / \sqrt{H_1^2 + H_2^2}$ from §B.4, we use polar coordinates $H_1 = r \cos \theta$ and $H_2 = r \sin \theta$.

Then we can find the differential equation for r by differentiating $r^2 = H_1^2 + H_2^2$,

$$2r\dot{r} = 2H_1\dot{H}_1 + 2H_2\dot{H}_2$$

$$r\dot{r} = r \cos \theta (\{H_0, H_1\} - u_2 \{H_1, H_2\}) + r \sin \theta (\{H_0, H_2\} + u_1 \{H_1, H_2\})$$

$$\dot{r} = \{H_0, H_1\} \cos \theta + \{H_0, H_2\} \sin \theta - \frac{H_2}{\sqrt{H_1^2 + H_2^2}} \{H_1, H_2\} \cos \theta + \frac{H_1}{\sqrt{H_1^2 + H_2^2}} \{H_1, H_2\} \sin \theta$$

$$\dot{r} = \{H_0, H_1\} \cos \theta + \{H_0, H_2\} \sin \theta - \{H_1, H_2\} \sin \theta \cos \theta + \{H_1, H_2\} \sin \theta \cos \theta$$

$$\dot{r} = \{H_0, H_1\} \cos \theta + \{H_0, H_2\} \sin \theta.$$

Similarly, we find the differential equation for θ by noticing that

$$\dot{H}_1 H_2 = \widehat{r \cos \theta} r \sin \theta = r \dot{r} \sin \theta \cos \theta - r^2 \dot{\theta} \sin^2 \theta$$

$$H_1 \dot{H}_2 = r \cos \theta \widehat{r \sin \theta} = r \dot{r} \sin \theta \cos \theta + r^2 \dot{\theta} \cos^2 \theta$$

and so $H_1 \dot{H}_2 - \dot{H}_1 H_2 = r^2 \dot{\theta}$, giving

$$\begin{aligned} \dot{\theta} &= \frac{H_1 \dot{H}_2 - \dot{H}_1 H_2}{r^2} \\ &= \frac{r \cos \theta (\{H_0, H_2\} + u_1 \{H_1, H_2\}) - r \sin \theta (\{H_0, H_1\} - u_2 \{H_1, H_2\})}{r^2} \\ &= \frac{\cos \theta (\{H_0, H_2\} + \cos \theta \{H_1, H_2\}) - \sin \theta (\{H_0, H_1\} - \sin \theta \{H_1, H_2\})}{r} \\ &= \frac{\cos \theta \{H_0, H_2\} - \sin \theta \{H_0, H_1\} + \{H_1, H_2\}}{r}. \end{aligned}$$

With these we can evaluate the behavior of extremals intersecting Σ , i.e., such that $r = \theta = 0$. A non-smooth extremal consisting of a concatenation of two order zero extremal arcs meeting at Σ can be constructed if

- (i) $\cos \theta \{H_0, H_2\} - \sin \theta \{H_0, H_1\} + \{H_1, H_2\} = 0$ has two distinct solutions, θ_0 and θ_1 , and
- (ii) $\dot{r} = \{H_0, H_1\} \cos \theta + \{H_0, H_2\} \sin \theta = 0$ has opposite sign for θ_0 and θ_1 .

A subcase, called a π -singularity, occurs when $\{H_1, H_2\} = 0$ and the first condition results in $\tan \theta = \{H_0, H_2\} / \{H_0, H_1\}$ so that $\theta_1 = \theta_0 + \pi$. The generic case and this special case are illustrated in Figure 2.7.

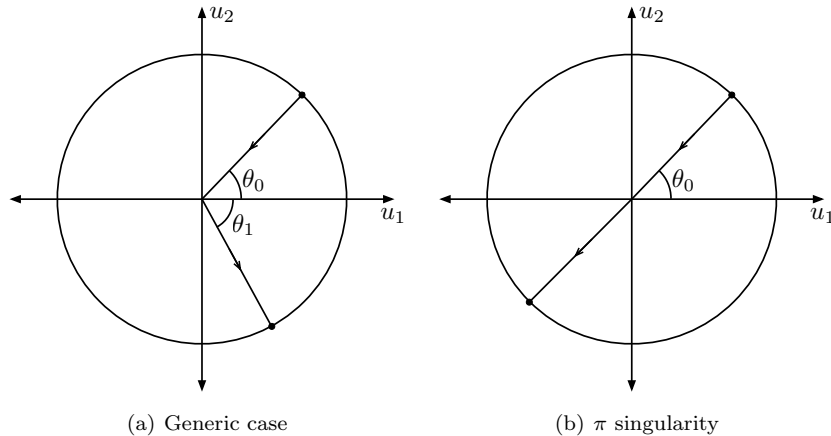


Figure 2.7: Non-smooth extremal of order zero extremal arcs.

2.3.3 Conjugate point algorithms

Here we present the concept of a conjugate point in the control setting in local coordinates (more detail is given in §B.5), and give conjugate point tests used for singular extremals of this problem corresponding to the various sub-cases which depend on the number of inputs, whether the final time is fixed, and whether the extremal is normal (conveniently collected by Bonnard, Caillaud, and Trélat [6]). In each case, conjugate point detection reduces to checking the rank of a particular test matrix and so the calculation of conjugate points is well-suited to numerical methods, and is enabled by the HAMPATH software package [18].

Definition 12. Let $z = (x, p)$ be a reference trajectory of a Hamiltonian vector field \vec{H} defined on $[0, T]$. The variational equation

$$\delta \dot{z} = d\vec{H}(z(t))\delta z$$

is called the Jacobi equation. A Jacobi field $J(t)$, a nontrivial solution $\delta z = (\delta x, \delta p)$, is said to be vertical at time t if $\delta x(t) = 0$.

Definition 13. We define the exponential mapping for fixed $x(0) = x_0$ as the mapping $\exp_{x_0} : (t, p_0) \mapsto \pi(z(t, z_0))$ where $z(\cdot)$ is the solution of \hat{H} with initial condition $z_0 = (x_0, p_0)$, and π is the projection $(x, p) \mapsto x$. A time $t_c > 0$ is said to be geometrically conjugate to zero if the exponential mapping is not an immersion at $t = t_c$ and the associated point $x(t_c)$ is said to be geometrically conjugate to x_0 .

Theorem 14. Assume that the strong Legendre condition holds along $z(\cdot)$, and assume strong

regularity: that u is of corank one along every subinterval $[t_1, t_2] \subseteq [0, T]$. Then the first geometric conjugate time is the first conjugate time along $z(\cdot)$, denoted t_c . Therefore $x(\cdot)$ is locally optimal on $[0, t_c)$, and if $t > t_c$, $x(\cdot)$ is not locally optimal on $[0, t]$ in the L^∞ topology.

In particular, in the contrast problem a necessary optimality condition is the nonexistence of conjugate points on each extremal subarc of order zero.

Bi-input case

The conjugate point test in this case is as follows. Consider the Jacobi fields $\delta z_i = (\delta q_i, \delta p_i)$, $i = 1, \dots, n-1$ such that each $\delta q_i(t_0) = 0$ and such that each $\delta p_i(t_0)$ is orthogonal to $p(t_0)$. At a conjugate time t_c , $\text{rank}\{\delta q_1(t_c), \dots, \delta q_{n-1}(t_c)\} < n-1$.

Single-input, non-exceptional case

The conjugate point test in this case is to consider $(\delta q_i, \delta p_i)$, $i = 1, 2$ a dimension two basis of the vector space formed by the Jacobi fields such that each $\delta q_i(t_0) \in \text{span}\{G(q(t_0))\}$ and such that each $\delta p_i(t_0)$ is orthogonal to $p(t_0)$. At a conjugate time t_c , $\text{rank}\{\delta q_1(t_c), \delta q_2(t_c), G(q(t_c))\} < 3$, or equivalently that the matrix

$$(\delta q_1(t_c), \delta q_2(t_c), F(q(t_c)), G(q(t_c)), [G, [G, F]](q(t_c)))$$

is not of full rank.

Single-input, exceptional case In this case, the variational equation is reduced to $\frac{d\delta q}{dt} = \frac{\partial X_s^e}{\partial q}(q(t))\delta q$, where X_s^e is the flow in the exceptional case. A single Jacobi field $\delta q(\cdot)$ is computed with initial condition $\delta q(0) = G(q(0))$. The conjugate point test is $\delta q(t) \in \text{span}\{F(q(t)), G(q(t))\}$ or equivalently that the matrix

$$(\delta q(t), F(q(t)), G(q(t)), [G, [G, F]](q(t)))$$

is not of full rank.

The result for a sample trajectory initiated at the point $(-1, 0, -1, 0)$ for the four sets of experimental parameters is shown in Figures 2.8–2.11, along with the corresponding smallest singular value along the given reference curve.

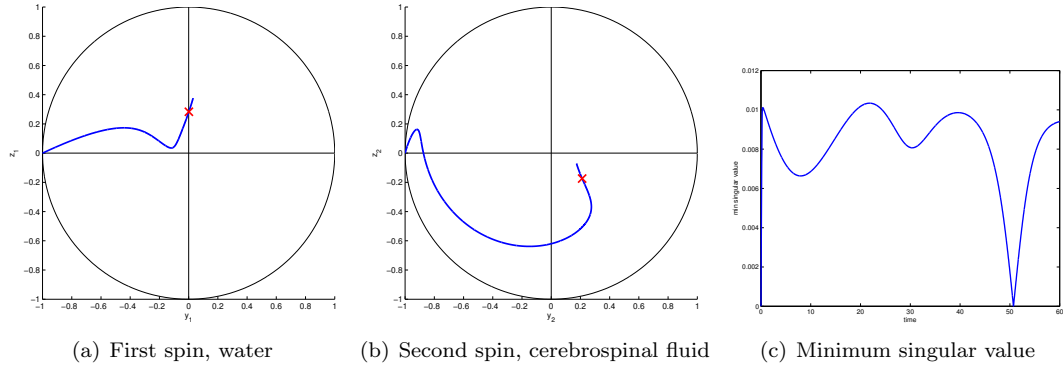


Figure 2.8: The exceptional singular trajectory for parameter set Λ_{wc} initiated at $(-1, 0, -1, 0)$ and the minimum singular value of the conjugate point test matrix along this trajectory. The conjugate point is marked with a red \times .

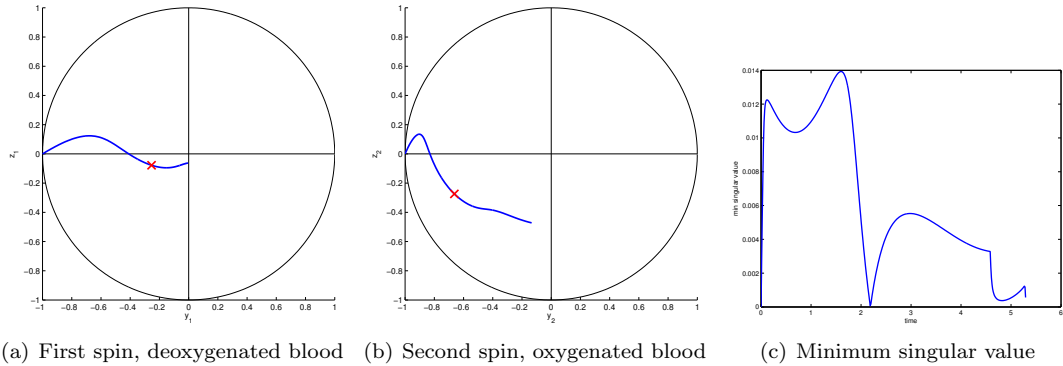


Figure 2.9: The exceptional singular trajectory for parameter set Λ_{do} initiated at $(-1, 0, -1, 0)$ and the minimum singular value of the conjugate point test matrix along this trajectory. The conjugate point is marked with a red \times .

2.4 Symmetry of revolution

We present two results that intuitively follow from the construction of the physical model. First, due to the arbitrary alignment of the xy -plane, trajectories can be rotated about the z -axis to produce an equivalent trajectory, and second, that while we can “mod out” one control for one spin due to this symmetry, it is not generally possible to do this for the pair of spins. Let us make these notions more precise.

The symmetry of revolution about the vertical axis can be directly seen by a change of coordinates

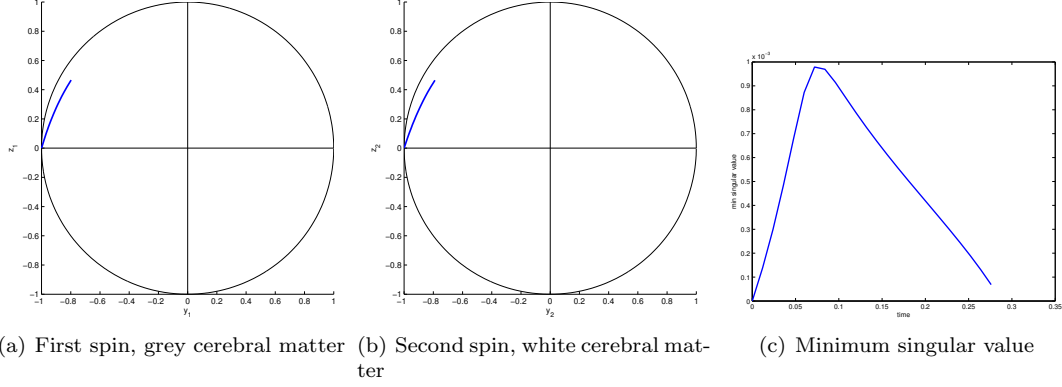


Figure 2.10: The exceptional singular trajectory for parameter set Λ_{gw} initiated at $(-1, 0, -1, 0)$ and the minimum singular value of the conjugate point test matrix along this trajectory. The trajectory encounters the set $D = 0 \cap D' \neq 0$ before a conjugate point is reached, however the minimum singular value is approaching zero as the control explodes.

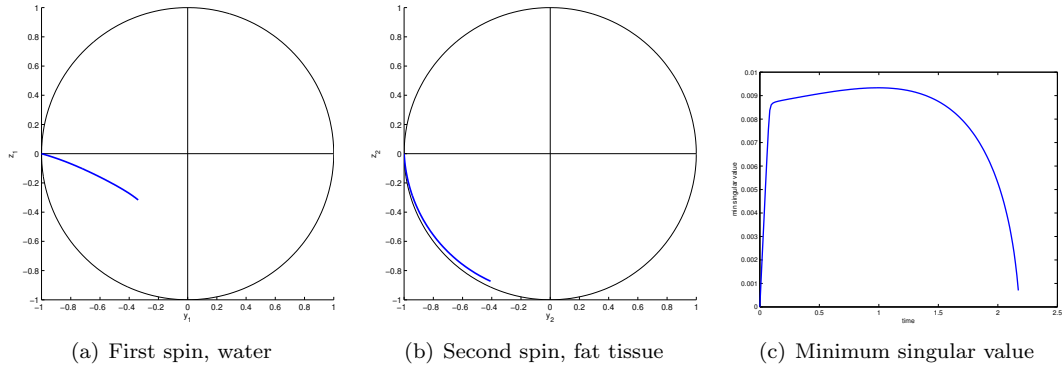


Figure 2.11: The exceptional singular trajectory for parameter set Λ_{wf} initiated at $(-1, 0, -1, 0)$ and the minimum singular value of the conjugate point test matrix along this trajectory. The trajectory encounters the set $D = 0 \cap D' \neq 0$ before a conjugate point is reached, however the minimum singular value is approaching zero as the control explodes.

$(X_i, Y_i, Z_i) = R_\theta(x_i, y_i, z_i)$, for $i = 1, 2$, where R_θ is a rotation

$$\begin{cases} X_i = x_i \cos \theta - y_i \sin \theta \\ Y_i = x_i \sin \theta + y_i \cos \theta \\ Z_i = z_i. \end{cases} \quad (2.7)$$

Lemma 15. *Under the change of coordinates (2.7), the dynamics of the (X_i, Y_i, Z_i) , $i = 1, 2$, system*

is equivalent to the q -dynamics (2.1) under the rotation of the control

$$v_1 = u_1 \cos \theta - u_2 \sin \theta, \quad v_2 = u_1 \sin \theta + u_2 \cos \theta. \quad (2.8)$$

Proof. We will show that \dot{x}_i and \dot{X}_i are equivalent, the others follow similarly.

$$\begin{aligned} \dot{X}_i &= \dot{x}_i \cos \theta - \dot{y}_i \sin \theta \\ &= (-\Gamma_i x_i + u_2 z_i) \cos \theta - (-\Gamma_i y_i - u_1 z_i) \sin \theta \\ &= (-\Gamma_i X_i \cos \theta - \Gamma_i Y_i \sin \theta - v_1 Z_i \sin \theta + v_2 Z_i \cos \theta) \cos \theta \\ &\quad - (\Gamma_i X_i \sin \theta - \Gamma_i Y_i \cos \theta - v_1 Z_i \cos \theta - v_2 Z_i \sin \theta) \sin \theta \\ &= -\Gamma_i X_i + v_2 Z_i \end{aligned}$$

□

Proposition 16.

- (i) The Hamiltonian lift $H_R(q, p) = \langle p, R_\theta(q) \rangle$ is a first integral along the optimal solutions.
- (ii) There is a one-parameter family of optimal solutions, characterized by the rotations (2.7) and (2.8) on the state and control.

Proof. As in §B.4, denote the true Hamiltonian by H_n . The first claim is due to Noether's Theorem in Hamiltonian form, which states that every continuous symmetry of a Hamiltonian system has a corresponding conserved quantity. In particular, if $\{H_n, H_R\} = 0$ then H_R is a first integral along solutions of \vec{H}_n . It can be verified by calculation that

$$\{H_n, H_R\} = \frac{\partial H_R}{\partial p} \frac{\partial H_n}{\partial q} - \frac{\partial H_R}{\partial q} \frac{\partial H_n}{\partial p} = 0.$$

The second statement follows from Lemma 15. □

This symmetry can be further explored with the use of spherical coordinates. Consider the parameterization, for $i = 1, 2$,

$$\begin{cases} x_i = \rho_i \sin \varphi_i \cos \theta_i \\ y_i = \rho_i \sin \varphi_i \sin \theta_i \\ z_i = \rho_i \cos \varphi_i. \end{cases} \quad (2.9)$$

The dynamics for the $(\rho_i, \varphi_i, \theta_i)$ system is computed in a straightforward manner, for instance

$$\begin{aligned}
\dot{\rho}_i &= \frac{1}{2}(x_i^2 + y_i^2 + z_i^2)^{-1/2}(2x_i\dot{x}_i + 2y_i\dot{y}_i + 2z_i\dot{z}_i) \\
&= \frac{-\Gamma_i(x_i^2 + y_i^2) + \gamma_i z_i - \gamma_i z_i^2}{\sqrt{x_i^2 + y_i^2 + z_i^2}} \\
&= \frac{-\Gamma_i(\rho_i^2 \sin^2 \varphi_i \cos^2 \theta_i + \rho_i^2 \sin^2 \varphi_i \sin^2 \theta_i) + \gamma_i \rho_i \cos \varphi_i - \gamma_i \rho_i^2 \cos^2 \varphi_i}{\rho_i} \\
&= \gamma_i \cos \varphi_i - \rho_i(\delta_i \cos^2 \varphi_i + \Gamma_i).
\end{aligned}$$

Proceeding in this manner, we have

$$\begin{cases} \dot{\rho}_i = \gamma_i \cos \varphi_i - \rho_i(\Gamma_i + \delta_i \cos^2 \varphi_i) \\ \dot{\varphi}_i = \delta_i \sin \varphi_i \cos \varphi_i - \frac{\gamma_i \sin \varphi_i}{\rho_i} - u_1 \sin \theta_i + u_2 \cos \theta_i \\ \dot{\theta}_i = -\cot \varphi_i(u_1 \cos \theta_i + u_2 \sin \theta_i). \end{cases} \quad (2.10)$$

Notice here that, writing $x = ((\rho_1, \varphi_1, \theta_1), (\rho_2, \varphi_2, \theta_2))$ and $\dot{x} = G_0 + u_1 G_1 + u_2 G_2$, θ_1 and θ_2 appear only in the control vector fields G_1 and G_2 . Denoting the true Hamiltonian $H_n = H_0 + (H_1^2 + H_2^2)^{1/2}$, $H_i = \langle p, G_i \rangle$, we calculate

$$\begin{aligned}
H_1^2 + H_2^2 &= p_{\varphi_1}^2 + p_{\varphi_2}^2 + p_{\theta_1}^2 \cot^2 \varphi_1 + p_{\theta_2}^2 \cot^2 \varphi_2 \\
&\quad + 2p_{\theta_1} p_{\theta_2} \cot \varphi_1 \cot \varphi_2 (\cos \theta_1 \cos \theta_2 + \sin \theta_1 \sin \theta_2) \\
&\quad + 2p_{\theta_1} p_{\varphi_2} \cot \varphi_1 (\cos \theta_1 \sin \theta_2 - \sin \theta_1 \cos \theta_2) \\
&\quad + 2p_{\varphi_1} p_{\theta_2} \cot \varphi_2 (\sin \theta_1 \cos \theta_2 - \cos \theta_1 \sin \theta_2) \\
&\quad + 2p_{\varphi_1} p_{\varphi_2} (\cos \theta_1 \cos \theta_2 + \sin \theta_1 \sin \theta_2) \\
&= p_{\varphi_1}^2 + p_{\varphi_2}^2 + p_{\theta_1}^2 \cot^2 \varphi_1 + p_{\theta_2}^2 \cot^2 \varphi_2 \\
&\quad + 2(p_{\varphi_1} p_{\varphi_2} + p_{\theta_1} p_{\theta_2} \cot \varphi_1 \cot \varphi_2) \cos(\theta_1 - \theta_2) \\
&\quad + 2(p_{\varphi_1} p_{\theta_2} \cot \varphi_2 - p_{\varphi_2} p_{\theta_1} \cot \varphi_1) \sin(\theta_1 - \theta_2)
\end{aligned} \quad (2.11)$$

which, in terms of the θ_i , clearly only depends on the difference $\theta_1 - \theta_2$. This gives the idea for the following proposition.

Proposition 17. *Define $\theta'_1 = \theta_1$ and $\theta'_2 = \theta_1 - \theta_2$. Then θ'_1 is a cyclic variable, i.e., $p_{\theta'_1}$ is a first integral of the extremal motion defined by \vec{H}_n .*

Proof. Making this substitution, we see that (2.11) does not depend θ'_1 and therefore $\dot{p}_{\theta'_1} = -\frac{\partial H_n}{\partial \theta'_1} = 0$. □

Hence, loosely speaking, we can “mod out” the angle in the x_1y_1 -plane, θ_1 , and maintain only the difference $\theta_1 - \theta_2$, but we cannot eliminate θ_2 as well. We can, however make the following observation concerning the single-input case (which we prove in rectangular coordinates).

Proposition 18. *Extremals of the single-input case are extremals of the bi-input case.*

Proof. Let $((y_1, z_1, y_2, z_2), (p_{y_1}, p_{z_1}, p_{y_2}, p_{z_2}))$ be an extremal of the single-input case with control $u_1(\cdot)$. Adjoining $x_i \equiv 0, p_{x_i} \equiv 0, i = 1, 2$, to this extremal and $u_2 \equiv 0$ to the control, the resulting extremal lift is a solution of the dynamics

$$\dot{x}_i = -\Gamma_i x_i + u_2 z_i, \quad \dot{p}_{x_i} = \Gamma_i p_{x_i} + u_2 p_{z_i},$$

and therefore is an extremal lift of the bi-input system. □

2.5 Generated Lie algebra

Here we identify the Lie algebra generated by the set of vector fields $\{F_0, F_1, F_2\}$. To enable this, we lift the system onto the product $G \times G$, where G is the semi-direct product of Lie groups $\text{GL}(3, \mathbb{R}) \times \mathbb{R}^3 = \text{Aff}(3)$, acting on the state space with the action $(A, a)(q) = Aq + a$. The Lie bracket is computed by $[(A, a), (B, b)] = ([A, B], Ab - Ba)$, where $[A, B] = AB - BA$. We will first determine the Lie algebra generated by these vector fields as restricted to a single spin.

2.5.1 Restriction to a single spin

Since we are dealing with a single spin, we omit subscripts on the state and parameter variables for this subsection. The i and j subscripts are valued in $\{1, 2, 3\}$.

Definition 19. Let $\{e_i\}_{i=1,2,3}$ be the standard ordered basis of \mathbb{R}^3 . Define $E_{ij} \in \mathbb{R}^{3 \times 3}$ to be the matrix with the entry 1 at row i , column j and 0 elsewhere, i.e., $E_{ij} = e_i^T e_j$. Further, for $i \neq j$ define $C_{ij} := E_{ij} - E_{ji}$, $H_{ij} := E_{ij} + E_{ji}$, and $T_{ij} := E_{ii} - E_{jj}$.

Recall the following Lie brackets from §2.1.1, written as elements of $\text{Aff}(3)$ as

$$\begin{aligned} F_0 &= \left(\text{diag}(-\Gamma, -\Gamma, -\gamma), (0, 0, \gamma)^T \right) & [F_0, [F_1, F_0]] &= (-\delta^2 C_{32}, (0, \gamma\eta, 0)^T) \\ F_1 &= (C_{32}, 0_{3 \times 1}) & [F_0, [F_2, F_0]] &= (-\delta^2 C_{13}, (-\gamma\eta, 0, 0)^T) \\ F_2 &= (C_{13}, 0_{3 \times 1}) & [F_1, [F_0, [F_1, F_0]]] &= (0_{3 \times 3}, (0, 0, \gamma\eta)^T) \end{aligned}$$

and denote $F_0 = (A, a)$, so $A = (a_{ij}) = \text{diag}(-\Gamma, -\Gamma, -\gamma)$.

Remark 20. Observe that

$$\begin{aligned} \delta^2 F_1 + [F_0, [F_1, F_0]] &= (0_{3 \times 3}, (0, \gamma\eta, 0)^T) \\ \delta^2 F_2 + [F_0, [F_2, F_0]] &= (0_{3 \times 3}, (-\gamma\eta, 0, 0)^T) \end{aligned}$$

and therefore $\{[F_1, [F_0, [F_1, F_0]]], \delta^2 F_1 + [F_0, [F_1, F_0]], \delta^2 F_2 + [F_0, [F_2, F_0]]\}$ forms a basis for \mathbb{R}^3 since $\gamma, \eta \neq 0$. Therefore the Lie algebra generated by $\{F_0, F_1, F_2\}$ is the semi-direct product $\mathfrak{g} \ltimes \mathbb{R}^3$ where \mathfrak{g} is the Lie algebra generated by $\{A, C_{32}, C_{13}\}$, and our discussion is now reduced to determining this \mathfrak{g} .

Lemma 21. *The nontrivial spectrum of $\text{ad } A$ is $\{0, 0, \delta, \delta, -\delta, -\delta\}$.*

Proof. Generally, $[\text{diag}(\alpha_1, \dots, \alpha_n), E_{ij}] = \alpha_i E_{ij} - \alpha_j E_{ij} = (\alpha_i - \alpha_j) E_{ij}$, so $[A, E_{ij}] = (a_{ii} - a_{jj}) E_{ij}$, where the $(a_{ii} - a_{jj})$ take values in the set $\{0, \delta, -\delta\}$. We have $[A, E_{32}] = -\delta E_{32}$, $[A, E_{23}] = \delta E_{23}$, $[A, E_{13}] = \delta E_{13}$, $[A, E_{31}] = -\delta E_{31}$, and $[A, E_{21}] = [A, E_{12}] = 0$. \square

This lemma gives a direct method to compute $\text{ad } A$ on the E_{ij} , H_{ij} , and T_{ij} defined above, e.g. $[A, C_{ij}] = [A, E_{ij}] - [A, E_{ji}]$, which is because since we immediately see that the H_{ij} and T_{ij} appear in bracket computations. Indeed, we have that $(\text{ad}^k A)E_{ij} = (a_{ii} - a_{jj})^k E_{ij}$ so it is clear that repeatedly applying $\text{ad } A$ to C_{ij} will toggle between (a multiple of) C_{ij} and H_{ij} . Since A and the T_{ij} are diagonal, their brackets are zero. In Table 2.1 we give the brackets of A and the C_{ij} , H_{ij} , and T_{ij} .

Proposition 22. *The Lie algebra \mathfrak{g} generated by $\{A, C_{32}, C_{13}\}$ is $\mathfrak{gl}(3, \mathbb{R})$ if $\delta \neq 0$, and $\mathbb{R}I \oplus \mathfrak{so}(3)$ if $\delta = 0$.*

Proof. This is essentially “proof by Table 2.1.”

Table 2.1: Brackets of A , C_{ij} , H_{ij} , and T_{ij} computed in row, column order.

$[\cdot, \cdot]$	A	C_{32}	C_{13}	C_{21}	H_{32}	H_{13}	H_{21}	T_{32}	T_{13}	T_{21}
A		$-\delta H_{32}$	δH_{13}	0	$-\delta C_{32}$	δC_{13}	0	0	0	0
C_{32}	δH_{32}		C_{21}	$-C_{13}$	$2T_{32}$	$-H_{21}$	H_{13}	$-H_{32}$	H_{32}	$2H_{32}$
C_{13}	$-\delta H_{13}$	$-C_{21}$		C_{32}	H_{21}	$2T_{13}$	$-H_{32}$	$-H_{13}$	$-2H_{13}$	$-H_{13}$
C_{21}	0	C_{13}	$-C_{32}$		$-H_{13}$	H_{32}	$2T_{21}$	$2H_{21}$	H_{21}	$-H_{21}$
H_{32}	δC_{32}	$-2T_{32}$	$-H_{21}$	H_{13}		C_{21}	$-C_{13}$	$-C_{32}$	C_{32}	$2C_{32}$
H_{13}	$-\delta C_{13}$	H_{21}	$-2T_{13}$	$-H_{32}$	$-C_{21}$		C_{32}	$-C_{13}$	$-2C_{13}$	$-C_{13}$
H_{21}	0	$-H_{13}$	H_{32}	$-2T_{21}$	C_{13}	$-C_{32}$		$2C_{21}$	C_{21}	$-C_{21}$
T_{32}	0	H_{32}	H_{13}	$-2H_{21}$	C_{32}	C_{13}	$-2C_{21}$		0	0
T_{13}	0	$-H_{32}$	$2H_{13}$	$-H_{21}$	$-C_{32}$	$2C_{13}$	$-C_{21}$	0		0
T_{21}	0	$-2H_{32}$	H_{13}	H_{21}	$-2C_{32}$	C_{13}	C_{21}	0	0	

First suppose that $\delta = 0$, so that $A = \gamma I$, implying that $[A, B] = 0$ for all $B \in M(3, \mathbb{R})$. Notice that $[C_{32}, C_{13}] = C_{21}$, and in fact that the bracket of any two of these three C_{ij} is (plus or minus) the third one. We have that $\text{span}\{C_{32}, C_{13}, C_{21}\} = \mathfrak{so}(3)$, the set of skew-symmetric matrices. Therefore the Lie algebra generated by $\{A, C_{32}, C_{13}\}$ is exactly $\text{span}\{A, C_{32}, C_{13}, C_{21}\} = \mathbb{R}I \oplus \mathfrak{so}(3)$. Intuitively, since $\delta = 0$ the brackets never escape the first 4×4 block of Table 2.1.

Now suppose that $\delta \neq 0$. It is clear from Table 2.1 that $\mathfrak{gl}(3, \mathbb{R}) \supseteq \mathfrak{g} \supseteq \text{span}\{A, C_{32}, C_{13}, C_{21}, H_{32}, H_{13}, H_{21}, T_{32}, T_{13}, T_{21}\}$. We will show that this span is in fact $\mathfrak{gl}(3, \mathbb{R})$ by showing that each E_{ij} lies in the span.

For $i \neq j$, $E_{ij} = C_{ij} + H_{ij}$. For the E_{ii} , since A , T_{32} , and T_{13} form a basis for diagonal matrices we can form the E_{ii} from these. In particular,

$$\begin{aligned} -(2\Gamma + \gamma)E_{11} &= A - \Gamma T_{32} - (\gamma + \Gamma)T_{13} \\ -(2\Gamma + \gamma)E_{22} &= A + (\gamma + \Gamma)T_{32} + \Gamma T_{13} \\ -(2\Gamma + \gamma)E_{33} &= A - \Gamma T_{32} + \Gamma T_{13}. \end{aligned}$$

□

In conclusion, by Remark 20 and Proposition 22 the Lie algebra generated by $\{F_0, F_1, F_2\}$ is $\mathfrak{gl}(3, \mathbb{R}) \ltimes \mathbb{R}^3$ if $\delta \neq 0$ and $(\mathbb{R}I \oplus \mathfrak{so}(3)) \ltimes \mathbb{R}^3$ if $\delta = 0$.

2.5.2 Lie algebra of the coupled system

In the coupled system, the crux of the matter is whether or not the actions of the two spins can be decoupled or not. The F_i are written as

$$\begin{aligned} F_0 &= \left(\text{diag}(A_1, A_2), (0, 0, \gamma_1, 0, 0, \gamma_2)^T \right) \\ F_1 &= (\text{diag}(C_{32}, C_{32}), 0_{6 \times 1}) \\ F_2 &= (\text{diag}(C_{13}, C_{13}), 0_{6 \times 1}) \end{aligned}$$

where $A_1 = \text{diag}(-\Gamma_1, -\Gamma_1, -\gamma_1)$ and $A_2 = \text{diag}(-\Gamma_2, -\Gamma_2, -\gamma_2)$.

As in the previous case, it can be shown that the basis elements of $(0_{3 \times 3}, 0_{3 \times 3}) \times \mathbb{R}^6$ can each be found in the Lie algebra generated by $\{F_0, F_1, F_2\}$ for arbitrary physical parameters. For example, a multiple of $((0_{3 \times 3}, 0_{3 \times 3}), e_6)$ is

$$\gamma_1 [F_0, [F_1, [F_1, F_0]]] + [F_0, [F_0, [F_1, [F_1, F_0]]]] = ((0_{3 \times 3}, 0_{3 \times 3}), (\gamma_2 - \gamma_1)\gamma_2\eta_2 e_6)$$

if $\gamma_1 \neq \gamma_2$, and is otherwise given by

$$\eta_1 [F_2, [F_2, [F_1, [F_1, F_0]]]] + 2\eta_1 [F_2, [F_2, F_0]] - [F_0, [F_1, [F_1, F_0]]] = ((0_{3 \times 3}, 0_{3 \times 3}), \gamma_2(\eta_1 + \eta_2)\eta_2 e_6).$$

The others are found in a similar manner. Therefore the classification is again reduced to determining the Lie algebra \mathfrak{g} generated by $\{\text{diag}(A_1, A_2), \text{diag}(C_{32}, C_{32}), \text{diag}(C_{13}, C_{13})\}$.

Notice that

$$[\text{diag}(C_{32}, C_{32}), \text{diag}(C_{13}, C_{13})] = \text{diag}(C_{21}, C_{21})$$

so we will always have at least $\mathfrak{g} \supset \text{span}\{\text{diag}(A_1, A_2), \text{diag}(C_{32}, C_{32}), \text{diag}(C_{13}, C_{13}), \text{diag}(C_{21}, C_{21})\}$.

We also have

$$[\text{diag}(A_1, A_2), [\text{diag}(A_1, A_2), \text{diag}(C_{32}, C_{32})]] = \text{diag}(\delta_1^2 C_{32}, \delta_2^2 C_{32}) \quad (2.12)$$

and with this in mind we make the following observations.

Remark 23. We have the following by Table 2.1 and (2.12).

- If $\delta_1^2 \neq \delta_2^2$, we can construct $\text{diag}(C_{32}, 0_{3 \times 3})$ and $\text{diag}(0_{3 \times 3}, C_{32})$ and similarly each of the

$\text{diag}(C_{ij}, 0_{3 \times 3})$ and $\text{diag}(0_{3 \times 3}, C_{ij})$. Otherwise the two spins cannot be decoupled.

- If $\delta_1 \neq 0$, each of the H_{ij} and T_{ij} can be generated for the first block matrix, and the C_{ij} , H_{ij} , and T_{ij} generate $\mathfrak{sl}(3, \mathbb{R})$ in this block, otherwise we have only the C_{ij} generating $\mathfrak{so}(3)$ in this block. The same holds for δ_2 and the second block.

It is therefore clear that the determination of this Lie algebra depends on whether $\delta_1^2 = \delta_2^2$ or not, and whether δ_1 and δ_2 are zero or not.

Proposition 24. *The Lie algebra generated by $\{\text{diag}(A_1, A_2), \text{diag}(C_{32}, C_{32}), \text{diag}(C_{13}, C_{13})\}$ is isomorphic to*

- (i) $\mathbb{R}A \oplus \mathfrak{so}(3)$ (dimension 3) if $\delta_1 = \delta_2 = 0$,
- (ii) $\mathbb{R}A \oplus \mathfrak{sl}(3, \mathbb{R})$ (dimension 9) if $|\delta_1| = |\delta_2| \neq 0$,
- (iii) $\mathbb{R}A \oplus (\mathfrak{sl}(3, \mathbb{R}) \oplus \mathfrak{so}(3))$ (dimension 11) if $\delta_1 \neq 0, \delta_2 = 0$ (or $\delta_1 = 0$ and $\delta_2 \neq 0$), or
- (iv) $\mathbb{R}A \oplus (\mathfrak{sl}(3, \mathbb{R}) \oplus \mathfrak{sl}(3, \mathbb{R}))$ (dimension 17) if $|\delta_1|$ and $|\delta_2|$ are nonzero and distinct.

In particular the generated Lie algebra is never $\mathfrak{gl}(3, \mathbb{R}) \times \mathfrak{gl}(3, \mathbb{R})$.

Proof. The four cases are deduced from Remark 23.

- (i) Suppose that $\delta_1 = \delta_2 = 0$. Since $\delta_1 = \delta_2$, the two blocks are dependent and since $\delta_1 = \delta_2 = 0$, no elements with an H_{ij} or T_{ij} block can be constructed. Therefore the algebra is spanned by A and the $\text{diag}(C_{ij}, C_{ij})$, i.e., it is isomorphic to $\mathbb{R}A \oplus \mathfrak{so}(3)$.
- (ii) Suppose that $|\delta_1| = |\delta_2| \neq 0$. Since $\delta_1 = \delta_2$, the two blocks are dependent and $\delta_1 \neq 0$, each of $\text{diag}(H_{ij}, H_{ij})$ and $\text{diag}(T_{ij}, T_{ij})$ can be constructed. Therefore the algebra is spanned by A and the $\text{diag}(C_{ij}, C_{ij})$, $\text{diag}(H_{ij}, H_{ij})$ and $\text{diag}(T_{ij}, T_{ij})$ elements, yielding $\mathbb{R}A \oplus \mathfrak{sl}(3, \mathbb{R})$.
- (iii) Suppose that $\delta_1 \neq 0, \delta_2 = 0$. The two blocks are decoupled but since $\delta_2 = 0$, only the C_{ij} appear in the second block. Therefore the Lie algebra is spanned by A and each of the $\text{diag}(C_{ij}, 0_{3 \times 3})$, $\text{diag}(H_{ij}, 0_{3 \times 3})$, $\text{diag}(T_{ij}, 0_{3 \times 3})$ and $\text{diag}(0_{3 \times 3}, C_{ij})$, giving an algebra isomorphic to $\mathbb{R}A \oplus (\mathfrak{sl}(3, \mathbb{R}) \oplus \mathfrak{so}(3))$.
- (iv) Suppose that $|\delta_1|$ and $|\delta_2|$ are nonzero and distinct. Then each of $\text{diag}(C_{ij}, 0_{3 \times 3})$, $\text{diag}(0_{3 \times 3}, C_{ij})$, $\text{diag}(H_{ij}, 0_{3 \times 3})$, $\text{diag}(0_{3 \times 3}, H_{ij})$, $\text{diag}(T_{ij}, 0_{3 \times 3})$, and $\text{diag}(0_{3 \times 3}, T_{ij})$ can be

generated. The Lie algebra generated is spanned by these elements and A , and is therefore isomorphic to $\mathbb{R}A \oplus (\mathfrak{sl}(3, \mathbb{R}) \oplus \mathfrak{sl}(3, \mathbb{R}))$.

□

CHAPTER 3

CLASSIFICATION OF THE SINGULAR FLOW: THE EXCEPTIONAL CASE

In this chapter we examine the exceptional case in detail. Recall from its introduction in §1 that in this case we have $u_s^e = -D'(q)/D(q)$ where

$$D = \det(F, G, [F, G], [G, [F, G]]) \quad \text{and} \quad D' = \det(F, G, [F, G], [F, [F, G]]),$$

which defines the singular control X_s^e by $\dot{q} = F(q) - \frac{D'(q)}{D(q)}G(q)$ off of the set $S \setminus S'$, where we recall that $S := \{q : D(q) = 0\}$ and $S' := \{q : D(q) = D'(q) = 0\}$. It can be reparameterized to give the vector field X_r^e , defined as

$$\dot{q} = D(q)F(q) - D'(q)G(q). \tag{3.1}$$

Notably, the exceptional case reduces the control system to a time-invariant, ordinary differential equation.

Remark 25. The objective of the classification is to distinguish properties of the flow with respect to given physical parameters, e.g., equilibrium points and their attractivity. A particular object of interest are the sets S and S' .

In this chapter we first investigate the equilibria of the exceptional flow, and in particular see that this flow and its equilibria are nontrivial to classify. We then recall results of geometric invariant theory, feedback classification of control systems, quadratic differential equations. These concepts are then applied to the exceptional case of the contrast problem to identify invariants, used to distinguish sets of physical parameters, and to identify other features of the system. Finally, we introduce Gröbner bases and use this tool to make an algebraic-geometric determination and classification of the sets S and S' .

3.1 The exceptional flow—equilibria and attractivity

Given the complexity of the flow, we use numerical simulations to identify equilibria and their attractivity. The numerical method, implemented in HAMPATH, is as follows: each point in a discretization of the state space $B_1 \times B_2$ is taken as an initial point of the exceptional flow X_s^e .

The flow is integrated until either an equilibrium point is reached or the integration fails due to contact with the set $S \setminus S'$. Equilibrium points are detected by checking $\log_{10}(|q_n - q_{n-1}|)$ along the trajectory (the q_n being the state values given by the numerical integration), and for our purposes we define such a point as when this value falls below -10 , corresponding to the default state tolerance of the software.

Through this simulation, it is seen that three of the four set of experimental parameters, Λ_{wc} , Λ_{do} , and Λ_{wf} , exhibit the same qualitative behavior—the exceptional flow is attracted to N . Let us first discuss these three cases.

For parameter case Λ_{wc} , 40401 points in $B_1 \times B_2$ are taken as initial points. Of the resulting trajectories, 19011 (about 47%) do not encounter a failure in integration (due to contact with $S \setminus S'$) and reach the point N . A small sample of these trajectories is presented in Figure 3.1. Of the remaining trajectories, the integration fails and it is verified in each case that this is due to intersection with the set $S \setminus S'$. Clearly the sets S and S' play an important role in the exceptional flow, and they will be examined in particular in §3.5.

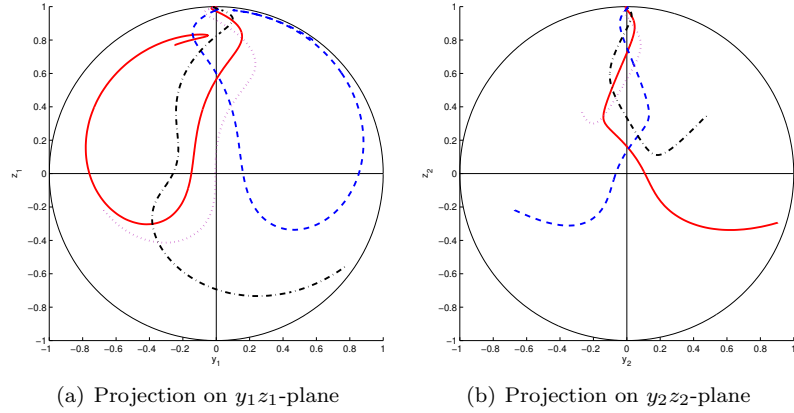


Figure 3.1: Exceptional trajectories reaching the equilibrium for parameters Λ_{wc} . Matching line styles and colors correspond to the same trajectory.

For parameter cases Λ_{do} and Λ_{wf} the situation is qualitatively identical, so we briefly present the quantitative differences. For Λ_{do} , 17969 of the 40401 trajectories (about 44%) reach N , shown in Figure 3.2. For Λ_{wf} , 25714 of the 40401 trajectories (about 64%) reach N , shown in Figure 3.3.

Remark 26. Another aspect of the overall imaging process is that the image is typically captured several times to filter experimental noise, so after the contrast-producing control is applied the system must be reset to the initial point of the next trial. This is currently achieved by simply allowing the

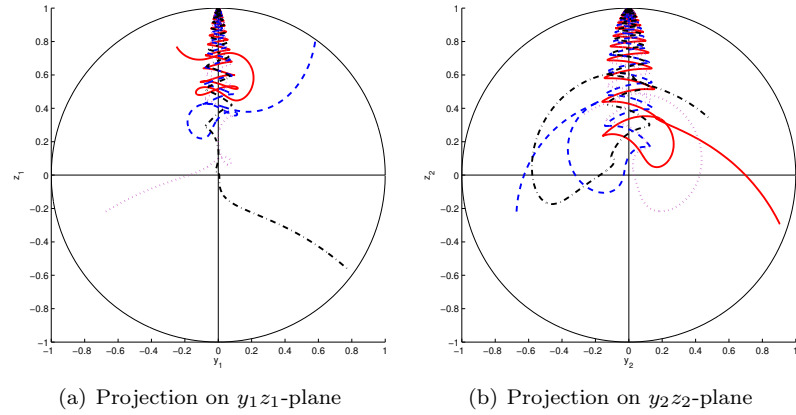


Figure 3.2: Exceptional trajectories reaching the equilibrium for parameters Λ_{do} . Matching line styles and colors correspond to the same trajectory.

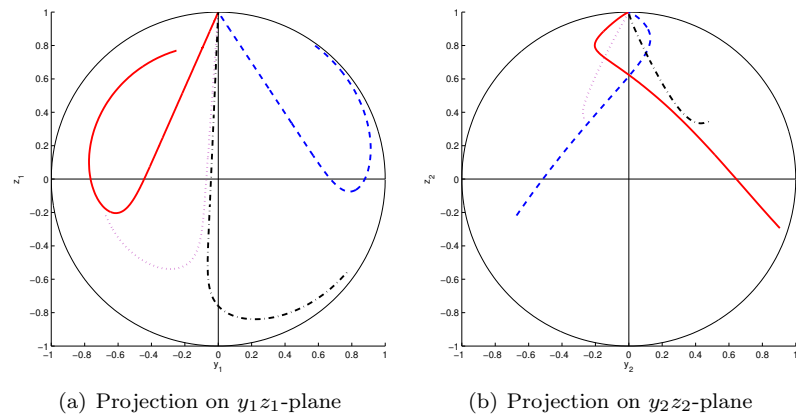


Figure 3.3: Exceptional trajectories reaching the equilibrium for parameters Λ_{wf} . Matching line styles and colors correspond to the same trajectory.

uncontrolled system to relax to the equilibrium, and an interesting problem is to identify the optimal control to return the system to its initial point. Since in the three cases seen here the exceptional flow is attracted to N , an obvious question is whether the exceptional control could play a role in this problem. However, it can be observed that the exceptional flow reaches a neighborhood of N more slowly than under the control $u = 0$, and so a strategy employing the exceptional singular control would use it only up to a first conjugate point.

As mentioned, the situation differs for parameters Λ_{gw} . In this case the simulations indicate that there are two unstable attractors, which are symmetric about the z_i -axes. These points are $(0.1648, 0.4947, 0.1685, 0.5620)$ and $(-0.1648, 0.4947, -0.1685, 0.5620)$. Trajectories are attracted to one of these points and may remain in a neighborhood for some duration, but eventually depart and

then approach either the same or the other attractor. In particular, the trajectories only reach a numerically-detected equilibrium point in 27 of the 40401 cases, and in these cases further numerical tests (performed by initiating new trajectories at these endpoints with higher state tolerance, and by initiating new trajectories at neighboring points) show that these are not genuine equilibria of the system (they simply toggle between the two attractors as other trajectories do). The vast majority of the cases are instead terminated by intersection with $S \setminus S'$. Two sample trajectories are shown in Figures 3.4 and 3.5. These are representative of the general qualitative behavior of the trajectories.

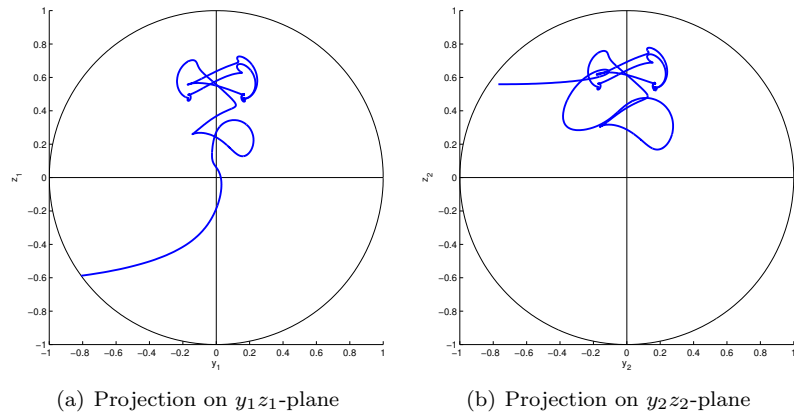


Figure 3.4: Exceptional trajectory for Λ_{gw} . Trajectory is drawn between two unstable attractors.

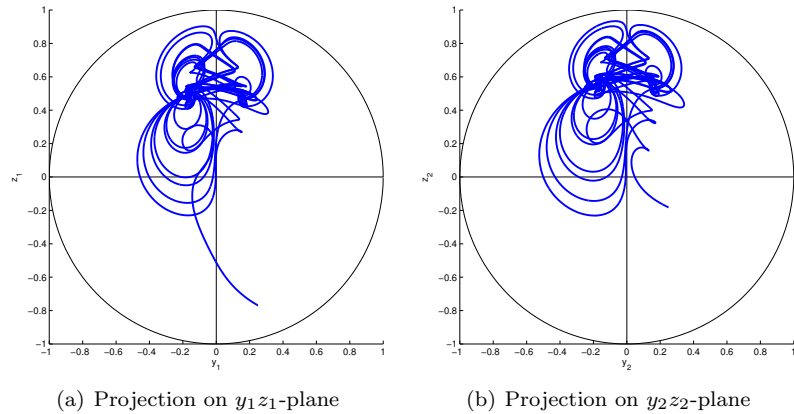


Figure 3.5: Exceptional trajectory for Λ_{gw} . Trajectory is drawn between two unstable attractors.

A continuation on parameter values

Clearly the behavior of the exceptional flow with respect to equilibrium points varies depending on the given parameters. A natural question is how this property changes with respect changes in parameter values. A straightforward numerical examination of this is to use a simple continuation between parameters Λ_{gw} and a parameter set with the “usual” (attracted to N) behavior. For this, we perform the above simulations for a system with parameters $(1 - \alpha)\Lambda_{\text{gw}} + \alpha\Lambda$ where $\Lambda \in \{\Lambda_{\text{wc}}, \Lambda_{\text{do}}, \Lambda_{\text{wf}}\}$ and $\alpha \in [0, 1]$. In such a continuation, we see the same qualitative behavior for each $\Lambda \in \{\Lambda_{\text{wc}}, \Lambda_{\text{do}}, \Lambda_{\text{wf}}\}$: as the parameters move from Λ_{gw} , a pair of unstable attractors exists, which move in location toward N (non-monotonically). At a particular step in the continuation, we have that N is numerically identified as a stable attractor.

Let us illustrate this in greater detail with the continuation from Λ_{gw} to Λ_{wf} . As stated above, the pair of unstable attractors in case Λ_{gw} move non-monotonically in position to N , which then behaves as a stable attractor. These values are given in Table 3.1 and are illustrated in Figure 3.6.

Table 3.1: Attractors in continuation of Λ_{gw} to Λ_{wf} . For $\alpha \in [0, .65]$ a pair of unstable attractors are identified, as listed. For $\alpha \in [0.66, 1]$, $N = (0, 1, 0, 1)$ is a stable attractor.

α	attractive point(s)
0	$(\pm 0.1648, 0.4947, \pm 0.1685, 0.5620)$
0.1	$(\pm 0.1646, 0.4031, \pm 0.1919, 0.5716)$
0.2	$(\pm 0.1671, 0.3890, \pm 0.2062, 0.6467)$
0.3	$(\pm 0.1718, 0.3931, \pm 0.2100, 0.7274)$
0.4	$(\pm 0.1789, 0.4150, \pm 0.2010, 0.8072)$
0.5	$(\pm 0.1888, 0.4725, \pm 0.1741, 0.8848)$
0.6	$(\pm 0.1901, 0.6516, \pm 0.1137, 0.9600)$
0.61	$(\pm 0.1859, 0.6889, \pm 0.1037, 0.9674)$
0.62	$(\pm 0.1786, 0.7340, \pm 0.0921, 0.9747)$
0.63	$(\pm 0.1659, 0.7894, \pm 0.0783, 0.9820)$
0.64	$(\pm 0.1426, 0.8591, \pm 0.0609, 0.9894)$
0.65	$(\pm 0.0907, 0.9491, \pm 0.0345, 0.9967)$
0.66	$(0, 1, 0, 1)$
\vdots	\vdots
1	$(0, 1, 0, 1)$

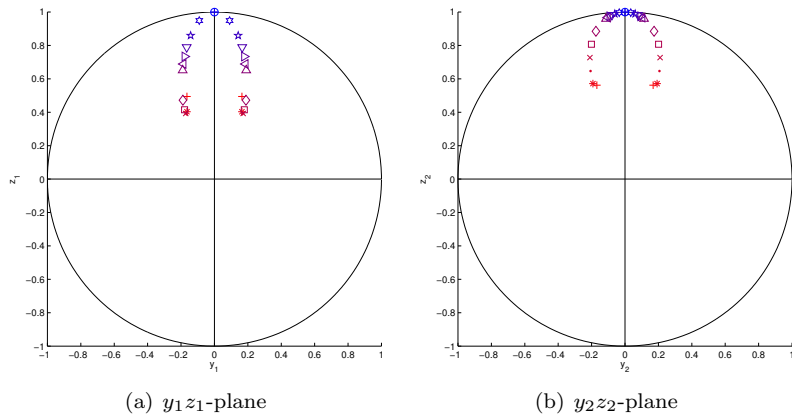


Figure 3.6: Attractors in continuation of Λ_{gw} to Λ_{wf} , given in Table 3.1. Matching colors and marker styles correspond to the same point. As the continuation value α goes from 0 to 1, the marker colors vary from red to blue. The pair of attractors converge to N .

3.2 Feedback classification

We first recall standard definitions of geometric invariant theory [22, 46] and of feedback classification for single-input, control-affine systems [3], then see the application of these concepts to the exceptional case.

3.2.1 Definitions

Definition 27. Given a diffeomorphism φ and a vector field X , the *pull-back* of X , φ^*X , and the *push-forward* of X , φ_*X , are vector fields defined as

$$\varphi^*X = T\varphi^{-1} \circ X \circ \varphi \quad \text{and} \quad \varphi_*X = T\varphi \circ X \circ \varphi^{-1}$$

where T is the tangent map.

Lemma 28 (Pull-back and push-forward property of the Lie bracket [40, 52]). *The pull-back and push-forward commute with the Lie bracket, i.e.,*

$$\varphi_*[X, Y] = [\varphi_*X, \varphi_*Y] \quad \text{and} \quad \varphi^*[X, Y] = [\varphi^*X, \varphi^*Y]$$

for vector fields X and Y .

Definition 29. Let E and F be real vector spaces, and let \mathcal{G} be a group acting linearly on E and

F. A homomorphism $\chi : \mathcal{G} \rightarrow \mathbb{R} \setminus \{0\}$ is called a *character*.

- A *semi-invariant* of weight χ is a map $\lambda : E \rightarrow \mathbb{R}$ such that for all $g \in \mathcal{G}$ and $x \in E$,
 $\lambda(g \cdot x) = \chi(g)\lambda(x)$.
- A semi-invariant is an *invariant* if $\chi = 1$.
- A *semi-covariant* of weight χ is a map $\lambda : E \rightarrow F$ such that for all $g \in \mathcal{G}$ and $x \in E$,
 $\lambda(g \cdot x) = \chi(g)g \cdot \lambda(x)$.
- A semi-covariant is a *covariant* if $\chi = 1$.

Let the pair of vector fields (X, Y) be associated to the system $\dot{x} = X(x) + Y(x)u$ with $x \in \mathbb{R}^n$ and $u \in \mathbb{R}^m$.

Definition 30. Two affine control systems (X, Y) and (X', Y') are called *feedback equivalent* if there exists a \mathcal{C}^∞ diffeomorphism ψ of \mathbb{R}^n and a feedback $u = \alpha(x) + \beta(x)u'$, where α and β are \mathcal{C}^∞ and β is invertible such that $X' = \psi^*X + \psi^*Y \cdot \alpha$ and $Y' = \psi^*Y \cdot \beta$.

The *orbit* of (X, Y) is the set of all affine control systems which are feedback equivalent to (X, Y) .

We can see that if the above definition is satisfied, we have

$$\dot{x}' = X' + Y'u' = \psi^*X + \psi^*Y \cdot \alpha + \psi^*Y \cdot \beta\beta^{-1}(u - \alpha) = \psi^*X + \psi^*Yu,$$

and that (X, Y) and (X', Y') are equivalent under a change of coordinates.

For linear, controllable systems the classification is given by the Brunovský canonical form [16]. In the nonlinear case there are no such general results, however we find the following theorem useful.

Theorem 31 (B. Bonnard [3]). *Let λ be the map associating a system (X, Y) to the constrained Hamiltonian differential equation \vec{H}_s defined by*

$$\dot{x} = \frac{\partial H_s}{\partial p}, \quad \dot{p} = -\frac{\partial H_s}{\partial x}, \quad (x, p) \in \Sigma' \setminus S$$

where $\Sigma' := \{z : H_Y = \{H_X, H_Y\} = 0\}$ and $S := \{z : \{H_Y, \{H_X, H_Y\}\} = 0\}$. Define the action of $(\alpha, \beta, \psi) \in \mathcal{Y}$ on (\vec{H}_s, Σ') to be the symplectic change of coordinates

$$x' = \psi(x), \quad p' = p \frac{\partial \psi^{-1}}{\partial x}$$

and in particular the feedback acts trivially as a symplectic change of coordinates.

The following diagram is commutative:

$$\begin{array}{ccc} \mathcal{A} & \xrightarrow{\lambda} & \lambda(\mathcal{A}) \\ \mathcal{G} \downarrow & & \downarrow \mathcal{G} \\ \mathcal{A} & \xrightarrow{\lambda} & \lambda(\mathcal{A}) \end{array}$$

where \mathcal{A} is the set of pairs (X, Y) (with some nonsingularity assumptions). In other words, λ is a covariant.

3.2.2 Application to the exceptional case

Let ψ be a diffeomorphism of \mathbb{R}^n which acts on a mapping $\alpha : \mathbb{R}^n \rightarrow \mathbb{R}$ by $\psi\alpha = \alpha \circ \psi$ and on a vector field X as $\psi X = \psi^* X$. We have the following lemma concerning the action of a feedback (ψ, α, β) on the exceptional dynamics.

Lemma 32. Let $D^{(F,G)} := \det(F, G, [F, G], [G, [F, G]])$ and $D'^{(F,G)} := \det(F, G, [F, G], [F, [F, G]])$, and let ψ, α , and β be as in Definition 30. We have that

- (i) $D^{(F+\alpha G, \beta G)} = \beta^4 D^{(F,G)}$,
- (ii) $D'^{(F+\alpha G, \beta G)} = \beta^3 (D'^{(F,G)} + \alpha D^{(F,G)})$,
- (iii) $D^{(\psi^* F, \psi^* G)}(q) = \det\left(\frac{\partial \psi^{-1}}{\partial q}\right) D^{(F,G)}(\psi(q))$, and
- (iv) $D'^{(\psi^* F, \psi^* G)}(q) = \det\left(\frac{\partial \psi^{-1}}{\partial q}\right) D'^{(F,G)}(\psi(q))$.

Proof. These are shown directly. Recall that $[fX, gY] = fg[X, Y] + f(Xg)Y - g(Yf)X$.

- (i) To show that $D^{(F+\alpha G, \beta G)} = \beta^4 D^{(F,G)}$, we first notice that $[F + \alpha G, \beta G] = [F, \beta G] +$

$[\alpha G, \beta G] = [F, \beta G]$, and that $\det(\alpha G, \beta G, \cdot, \cdot) = 0$. Hence

$$\begin{aligned}
D^{(F+\alpha G, \beta G)} &= \det(F + \alpha G, \beta G, [F + \alpha G, \beta G], [\beta G, [F + \alpha G, \beta G]]) \\
&= \det(F, \beta G, [F, \beta G], [\beta G, [F, \beta G]]) \\
&= \det(F, \beta G, \beta [F, G] + (F\beta)G, [\beta G, [F, \beta G]]) \\
&= \det(F, \beta G, \beta [F, G], [\beta G, [F, \beta G]]) \\
&= \det(F, \beta G, \beta [F, G], [\beta G, \beta [F, G] + (F\beta)G]) \\
&= \det(F, \beta G, \beta [F, G], [\beta G, \beta [F, G]]) \\
&= \det(F, \beta G, \beta [F, G], \beta^2 [G, [F, G]] + \beta(G\beta) [F, G] - \beta([F, G] \beta)G) \\
&= \det(F, \beta G, \beta [F, G], \beta^2 [G, [F, G]]) \\
&= \beta^4 \det(F, G, [F, G], [G, [F, G]]).
\end{aligned}$$

(ii) The demonstration that $D^{(F+\alpha G, \beta G)} = \beta^3(D^{(F, G)} + \alpha D^{(F, G)})$ follows similarly,

$$\begin{aligned}
D^{F+\alpha G, \beta G} &= \det(F + \alpha G, \beta G, [F + \alpha G, \beta G], [F + \alpha G, [F + \alpha G, \beta G]]) \\
&= \det(F, \beta G, \beta [F, G], [F + \alpha G, [F, \beta G]]) \\
&= \det(F, \beta G, \beta [F, G], [F, [F, \beta G]]) + \det(F, \beta G, \beta [F, G], [\alpha G, [F, \beta G]]) \\
&= \beta^3 \det(F, G, [F, G], [F, [F, G]]) + \alpha \beta^3 \det(F, G, [F, G], [G, [F, G]]).
\end{aligned}$$

The final two points follow directly from the pull-back property of the Lie bracket (Lemma 28), which also shows that a similar statement can be made by replacing ψ^* with ψ_* and ψ with ψ^{-1} . We have that

$$\begin{aligned}
D^{(\psi^* F, \psi^* G)} &= \det(\psi^* F, \psi^* G, [\psi^* F, \psi^* G], [\psi^* G, [\psi^* F, \psi^* G]]) \\
&= \det(\psi^* F, \psi^* G, \psi^* [F, G], \psi^* [G, [F, G]]) \\
&= \det\left(\frac{\partial \psi^{-1}}{\partial q} F \psi, \frac{\partial \psi^{-1}}{\partial q} G \psi, \frac{\partial \psi^{-1}}{\partial q} [F, G] \psi, \frac{\partial \psi^{-1}}{\partial q} [G, [F, G]] \psi\right) \\
&= \det\left(\frac{\partial \psi^{-1}}{\partial q} (F \psi, G \psi, [F, G] \psi, [G, [F, G]] \psi)\right) \\
&= \det\left(\frac{\partial \psi^{-1}}{\partial q}\right) \det(F \psi, G \psi, [F, G] \psi, [G, [F, G]] \psi)
\end{aligned}$$

and identical steps show the statement for D' . \square

From this, we deduce the following proposition, where the weights are associated to β and $\det\left(\frac{\partial\psi^{-1}}{\partial q}\right)$.

Proposition 33. *We have the following covariants.*

- (i) *The mapping $(F, G) \mapsto X_s^e$ is a covariant.*
- (ii) *The mapping $(F, G) \mapsto X_r^e$ is a semi-covariant.*
- (iii) *The mapping $(F, G) \mapsto D$ is a semi-covariant.*
- (iv) *The mapping $(F, G) \mapsto D'$ is a semi-covariant on the set $\{q : D(q) = D'(q)\}$.*

Proof. The first claim is due to Theorem 31, and the second claim follows from this since X_r^e is a multiple of X_s^e . The next assertion is by definition of a semi-covariant: in the notation as given in Definition 29 the map λ is D , the weight χ is β^4 , and g is the feedback element (ψ, α, β) . Finally, (iv) is a consequence of (iii). \square

Geometric interpretation

The action of diffeomorphisms on X_s^e can be used to classify the pairs (F, G) by the sets of physical parameters, and by doing so we find invariants related to the properties of an optimal solution. In particular the geometric interpretation of the invariants in connection with the above covariants is the following.

- Invariant properties of the dynamical system X_s^e : equilibrium points, stability analysis, and integrability of solutions.
- The set $S = \{q : D(q) = 0\}$ contains the points where the singular control is undefined, while $S' = \{q : D(q) = D'(q) = 0\}$ is the set where the singular control can cross the set S , which also characterizes the equilibria of X_r^e .

To study the invariants we will examine two physical invariants of the problem: the origin O and the north pole N of the Bloch balls. The point O physically corresponds to saturation, and $N = ((0, 1), (0, 1))$ is the globally attractive, stable equilibrium of the uncontrolled system.

Lemma 34. *The points O and N are equilibrium points of X_r^e , and the z_i -axes are line solutions along which the singular control u_s^e is zero, connecting the points $O \rightarrow N$.*

Proof. The first claim is since at O the vector field G is zero (and so the matrix in the definition of D and D' has a zero column) so $D(O) = D'(O) = 0$, and likewise at N the vector field F is zero.

For the second part, consider a point $((0, z_1), (0, z_2))$ with each $z_i \in (0, 1)$. Then D' is zero since F , $[F, G]$, and $[F, [F, G]]$ are linearly dependent, and it can be checked that D is almost everywhere zero. Therefore u_s^e is zero and the uncontrolled system is attracted to N along the z_i -axes. \square

The analysis of the dynamical system X_r^e at these two points is nontrivial, and to simplify the calculations we take the *quadratic approximations* of X_r^e at these points. Let us first recall results on such systems.

3.2.3 Quadratic differential equations

Consider a quadratic differential equation in \mathbb{R}^n ,

$$\frac{dx_i}{dt} = \sum_{j,k=1}^n a_{jk}^i x_j x_k, \quad i = 1, \dots, n \quad (3.2)$$

such that $a_{jk}^i = a_{kj}^i$, written as $\dot{x} = Q(x)$.

We have the following results [4]. The linear classification of such a $Q(x)$ is analyzed by introducing the following.

Definition 35. Let (e_i) be the canonical basis of \mathbb{R}^n and endow \mathbb{R}^n with the multiplication defined by $e_j \cdot e_k = \sum_{i=1}^n a_{jk}^i e_i$. The associated commutative algebra (in general non-associative) is denoted by \mathcal{Q} .

Two quadratic differential equations are (linearly) isomorphic if and only if their associated algebras are isomorphic and the classification relies on the following.

Proposition 36. *An algebra \mathcal{E} is a subalgebra of \mathcal{Q} if and only if \mathcal{E} is an invariant vector space for the solutions of $\dot{x} = Q(x)$ and one can define the restriction of the equation to \mathcal{E} . A subalgebra I of \mathcal{Q} is an ideal if and only if $\dot{x} = Q(x)$ can be projected on the quotient \mathcal{Q}/I .*

Ray solutions

One-dimensional subalgebras are called *ray solutions* of $\dot{x} = Q(x)$ [43]. They correspond to lines $\mathbb{R}v$ such that for all $v_0 \in \mathbb{R}v$ there exists $\rho \in \mathbb{R}$ with $Q(v_0) = \rho v_0$, i.e., the velocity and state are always collinear; the line is invariant under the dynamics. Each line contains two ray solutions, to

or from the origin. Geometrically, they correspond either to a line of non-isolated equilibrium points if $\rho \equiv 0$, or otherwise to nontrivial ray solutions in which $\mathbb{R}v$ is a solution along which the dynamics are reduced to $\dot{y}_0 = y_0^2$ and $\dot{y}_i = 0$ for $i = 1, \dots, n-1$ under some linear change of coordinates.

We introduce the differential equation on the sphere S^{n-1} with dynamics $\dot{v} = Q(v) - \langle v, Q(v) \rangle \cdot v$. Ray solutions correspond to equilibrium points of this system, and eigenvalues and eigenspaces of the linearization at an equilibrium point are obtained as follows, giving the role of ray solutions in the classification problem.

Proposition 37. *Let $(y_0, y_1, \dots, y_{n-1})$ be a linear change of coordinates such that a quadratic system $\dot{x} = Q(x)$ takes the form*

$$\begin{cases} \dot{y}_0 = \lambda_0 y_0^2 + y_0 O(y) + O(y^2) \\ \dot{y} = y_0 B y + O(y^2) \end{cases} \quad (3.3)$$

where $\mathbb{R}y_0$ is a ray, $y = (y_1, \dots, y_{n-1})$, and $O(y)$ and $O(y^2)$ denote combinations of terms linear and quadratic in y , respectively.

The eigenvalues of the linearization of Q^π , the projection defined by $u_i = y_i/y_0$, $i = 1, \dots, n-1$, evaluated at the equilibrium point y_0 are $\lambda_1 - \lambda_0, \dots, \lambda_{n-1} - \lambda_0$ where $\{\lambda_1, \dots, \lambda_{n-1}\}$ is the spectrum of B .

Proof. Let (y_0, y) be as in the form (3.3), which exists [43, Theorem 2], and without loss of generality assume that $B = (b_{ij})$ is in Jordan form and that the indices are such that $b_{ii} = \lambda_i$, $i = 1, \dots, n-1$.

Let u_1, \dots, u_{n-1} be coordinates of the projection $u_i = y_i/u_0$, $i = 1, \dots, n-1$. Then

$$\begin{aligned} \dot{u}_i &= \frac{\dot{y}_i y_0 - \dot{y}_0 y_i}{y_0^2} \\ &= \frac{\left(\left(\sum_{j=1}^{n-1} b_{ij} y_0 y_j \right) + O(y^2) \right) y_0 - (\lambda_0 y_0^2 + y_0 O(y) + O(y^2)) y_i}{y_0^2} \\ &= \sum_{j=1}^{n-1} b_{ij} y_j - \lambda_0 y_i - \frac{y_0 O(y^2) + O(y^3)}{y_0^2} \end{aligned}$$

and so in row i of the Jacobian evaluated at y_0 (i.e., $y_i = 0$ for $i = 1, \dots, n-1$), $b_{ii} - \lambda_0 = \lambda_i - \lambda_0$ at column i , and is b_{ij} elsewhere in the row.

Therefore $\frac{\partial Q^\pi}{\partial y}(y_0)$ is a matrix in Jordan form with diagonal entries $\lambda_i - \lambda_0$, so these are its eigenvalues. \square

The following lemma will be useful in later calculation.

Lemma 38. *Let $\dot{x} = Q(x)$ be a quadratic differential equation of the form (3.2). Then for the coordinate reparameterization $v_i = x_i/x_1$, $i = 2, \dots, n$, and time reparameterization $ds = x_1 dt$, the v -dynamics are*

$$\frac{dv_i}{ds} = \sum_{j,k=1}^n (a_{jk}^i - a_{jk}^1 v_i) v_j v_k.$$

Proof. Computing,

$$\begin{aligned} \dot{v}_i &= \frac{\dot{x}_i x_1 - \dot{x}_1 x_i}{x_1^2} \\ &= \frac{\sum_{j,k=1}^n (a_{jk}^i x_j x_k x_1) - \sum_{j,k=1}^n (a_{jk}^1 x_j x_k x_i)}{x_1^2} \\ &= \frac{\sum_{j,k=1}^n (a_{jk}^i v_j v_k x_1^3) - \sum_{j,k=1}^n (a_{jk}^1 v_j v_k v_i x_1^3)}{x_1^2} \\ &= \sum_{j,k=1}^n (a_{jk}^i v_j v_k - a_{jk}^1 v_j v_k v_i) x_1 \end{aligned}$$

and by the time reparameterization, we have the result. □

In order to apply this discussion, we define quadratic approximations at the points N and O .

Quadratic approximation at the north pole

We make a translation so that N is the origin of the coordinate system ($z_i \rightarrow z_i - 1$). At N , the lowest-order terms of X_r^e are quadratic. Writing D and D' as

$$\begin{aligned} D(q) &= D_0(q) + D_1(q) + D_2(q) + D_3(q) + D_4(q) \\ D'(q) &= D'_0(q) + D'_1(q) + D'_2(q) + D'_3(q) + D'_4(q), \end{aligned}$$

where D_k contains the terms of D of order k (likewise for D'). These are fully written in §3.3; for now we note that $D_0(q) = D'_0(q) = D'_1(q) = 0$. We define the homogeneous quadratic vector field

$$Q_N(q) := D_1(q)F(q) - D'_2(q)G'(q)$$

where

$$D_1 = (\Gamma_1 - \Gamma_2)[\gamma_2\eta_1z_2 - \gamma_1\eta_2z_1]$$

$$D'_2 = (\Gamma_1 - \Gamma_2)[\gamma_2\eta_1(\Gamma_2 - \delta_1)y_1z_2 - \gamma_1\eta_2(\Gamma_1 - \delta_2)z_1y_2],$$

and $F = (-\Gamma_1y_1, -\gamma_1z_1, -\Gamma_2y_1, -\gamma_2z_2)^T$ is unaltered and $G' = (0, -1, 0, -1)^T$ is a constant approximation of G near N .

Clearly if $\Gamma_1 = \Gamma_2$ or if $\eta_1 = \eta_2 = 0$ this system is trivial, so assume that these are not the case. We further assume that each η_i are positive, which is the case for the physical parameters (Table 1.1) and simplifies the discussion.

Quadratic approximation at the origin

We define the D_k and D'_k as in the preceding case, and again the lowest-order terms of X_r^e at O are quadratic, leading us to define the homogeneous quadratic vector field

$$Q_O(q) := D_2(q)F'(q) - D'_1(q)G(q)$$

where

$$D_2 = \gamma_2^2\mu_1y_1^2 - \gamma_1\gamma_2(\mu_1 + \mu_2)y_1y_2 + \gamma_1^2\mu_2y_2^2 + \gamma_2^2\eta_1z_1^2 - \gamma_1\gamma_2(\eta_1 + \eta_2)z_1z_2 + \gamma_1^2\eta_2z_2^2$$

and

$$D'_1 = \gamma_1\gamma_2^2(\eta_2 - \eta_1)y_1 + \gamma_1^2\gamma_2(\eta_1 - \eta_2)y_2$$

(each of the D_k and D'_k will be given in §3.4). The vector $F' = (0, \gamma_1, 0, \gamma_2)^T$ is a constant approximation of F near O , and $G = (-z_1, y_1, -z_2, y_2)^T$ is unaltered.

Note that if $\eta_1 = \eta_2$ we have $D'_1 = 0$, a degenerate case. Therefore when working with this system we assume that $\eta_1 \neq \eta_2$, and as before we assume $\eta_1, \eta_2 > 0$.

Observe that in the quadratic approximations at N and O the roles of F and G are exchanged in terms of which is taken as constant, but the analysis cannot be similarly interchanged: F is a stable vector field while G is a rotation, and D and D' are approximated distinctly by linear or quadratic forms in the two cases.

Let us now examine these two quadratic systems in detail, in particular to identify invariants of the quadratic systems.

Remark 39. Since parameter sets $\Lambda = (\gamma_1, \Gamma_1, \gamma_2, \Gamma_2)$ are unique only up to a scalar multiple, only the ratios of eigenvalues calculated in Proposition 37 have invariant meaning.

3.3 Quadratic approximation at the north pole

In this section we investigate the quadratic system Q_N with the translated coordinates where N is set to the origin, $z_i \rightarrow z_i - 1$. Since this translation is uniform throughout this section, we do not use a special mark for the translated coordinates, and recall from the introduction of Q_N that we assume $\Gamma_1 \neq \Gamma_2$ and that $\eta_1, \eta_2 > 0$.

The full expansions of D and D' in these coordinates are now listed.

$$\begin{aligned}
D &= \det(F, G, [F, G], [G, [F, G]]) \\
&= \begin{vmatrix} -\Gamma_1 y_1 & -(z_1 + 1) & \Gamma_1 - \delta_1 z_1 & 2 - \delta_1 y_1 \\ -\gamma_1 z_1 & y_1 & -\delta_1 y_1 & 2\delta_1 z_1 - \eta_1 \\ -\Gamma_2 y_2 & -(z_2 + 1) & \Gamma_2 - \delta_2 z_2 & 2 - \delta_2 y_2 \\ -\gamma_2 z_2 & y_2 & -\delta_2 y_2 & 2\delta_2 z_2 - \eta_2 \end{vmatrix} \\
&= D_1(q) + D_2(q) + D_3(q) + D_4(q)
\end{aligned}$$

The D_k are the homogeneous terms of order k of D :

$$D_1(q) = (\Gamma_2 - \Gamma_1)[\gamma_1 \eta_2 z_1 + \gamma_2 \eta_1 z_2]$$

$$\begin{aligned}
D_2(q) &= \Gamma_1 \eta_2 (\Gamma_2 - \delta_1) y_1^2 - \eta_1 \eta_2 (\Gamma_1 + \Gamma_2) y_1 y_2 + \Gamma_2 \eta_1 (\Gamma_1 - \delta_2) y_2^2 \\
&\quad + [\gamma_1 \gamma_2^2 + \gamma_1^2 \gamma_2 + 4\Gamma_1 \gamma_2 (\Gamma_1 - \Gamma_2) + \gamma_1 (2\Gamma_2 \eta_2 - 2\Gamma_1 (\gamma_2 + 2\Gamma_2))] z_1 z_2 \\
&\quad + \gamma_1 \eta_2 (\delta_1 + \Gamma_2) z_1^2 + \gamma_2 \eta_1 (\delta_2 + \Gamma_1) z_2^2
\end{aligned}$$

$$\begin{aligned}
D_3(q) &= 2\delta_1\eta_2(\gamma_1 + \Gamma_1 + \Gamma_2)y_1z_1y_2 + 2\delta_2\eta_1(\gamma_2 + \Gamma_2 + \Gamma_1)y_1y_2z_2 \\
&+ (\gamma_2^2\Gamma_1 - \gamma_2\Gamma_1^2 + \gamma_1\gamma_2(\mu_1 - 2\Gamma_2) - 3\gamma_2\Gamma_1\Gamma_2 + 4\Gamma_1\Gamma_2(\Gamma_2 - \delta_1))y_1^2z_2 \\
&+ (\gamma_1^2\Gamma_2 - \gamma_1\Gamma_2^2 + \gamma_2\gamma_1(\mu_2 - 2\Gamma_1) - 3\gamma_1\Gamma_2\Gamma_1 + 4\Gamma_2\Gamma_1(\Gamma_1 - \delta_2))z_1y_2^2 \\
&+ (\gamma_1\gamma_2^2 - \gamma_2\gamma_1^2 - \gamma_1\gamma_2(\Gamma_1 + 3\Gamma_2) + 2\gamma_2\Gamma_1(\Gamma_1 - \Gamma_2) + 4\gamma_1\Gamma_2(\delta_1 + \Gamma_2))z_1^2z_2 \\
&+ (\gamma_2\gamma_1^2 - \gamma_1\gamma_2^2 - \gamma_2\gamma_1(\Gamma_2 + 3\Gamma_1) + 2\gamma_1\Gamma_2(\Gamma_2 - \Gamma_1) + 4\gamma_2\Gamma_1(\delta_2 + \Gamma_1))z_1z_2^2
\end{aligned}$$

$$\begin{aligned}
D_4(q) &= 2\left[(\gamma_1\Gamma_2^2 + \gamma_1^2\Gamma_2 + \gamma_2\Gamma_1^2 + \gamma_2^2\Gamma_1 - \gamma_1\gamma_2(\Gamma_1 + \Gamma_2) - \Gamma_1\Gamma_2(\gamma_1 + \gamma_2)) (y_1^2y_2^2 + z_1^2z_2^2) \right. \\
&+ (\gamma_1^2\gamma_2 + \gamma_1\gamma_2^2 - \gamma_1\gamma_2(\Gamma_1 + \Gamma_2) - \Gamma_1\Gamma_2(\delta_1 + \delta_2)) (y_1^2z_2^2 + y_2^2z_1^2) \\
&\quad \left. + 2((\Gamma_1^2 - \gamma_1^2)\delta_2 + (\Gamma_2^2 - \gamma_2^2)\delta_1) y_1y_2z_1z_2 \right]
\end{aligned}$$

$$\begin{aligned}
D' &= \det(F, G, [F, G], [F, [F, G]]) \\
&= \begin{vmatrix} -\Gamma_1y_1 & -(z_1 + 1) & \Gamma_1 - \delta_1z_1 & -\Gamma_1^2 - \delta_1^2z_1 \\ -\gamma_1z_1 & y_1 & -\delta_1y_1 & \delta_1^2y_1 \\ -\Gamma_2y_2 & -(z_2 + 1) & \Gamma_2 - \delta_2z_2 & -\Gamma_2^2 - \delta_2^2z_2 \\ -\gamma_2z_2 & y_2 & -\delta_2y_2 & \delta_2^2y_2 \end{vmatrix} \\
&= D'_1(q) + D'_2(q) + D'_3(q) + D'_4(q)
\end{aligned}$$

Likewise, D'_k are the homogeneous terms of order k of D' :

$$D'_1(q) = 0$$

$$D'_2(q) = (\Gamma_1 - \Gamma_2)[\gamma_2\eta_1(\Gamma_2 - \delta_1)y_1z_2 - \gamma_1\eta_2(\Gamma_1 - \delta_2)z_1y_2]$$

$$\begin{aligned}
D'_3(q) &= \Gamma_1 \eta_2 (\delta_1 - \delta_2) (\Gamma_2 - \delta_1) y_1^2 y_2 - \Gamma_2 \eta_1 (\delta_1 - \delta_2) (\Gamma_1 - \delta_2) y_1 y_2^2 \\
&\quad + 2\gamma_2 (\delta_1) (\Gamma_2^2 - \delta_1^2) y_1 z_1 z_2 + 2\gamma_1 \delta_2 (\Gamma_1^2 - \delta_2^2) y_2 z_1 z_2 \\
&\quad + \gamma_1 (\gamma_2 - 2\Gamma_2) (\delta_1 + \delta_2) (\delta_1 + \Gamma_2) y_2 z_1^2 - \gamma_2 \eta_1 (\delta_1 + \delta_2) (\delta_2 + \Gamma_1) y_1 z_2^2
\end{aligned}$$

$$D'_4(q) = 2 (\delta_1^2 - \delta_2^2) \left[\Gamma_1 \delta_2 y_1^2 y_2 z_2 - \Gamma_2 \delta_1 y_1 y_2^2 z_1 - \gamma_2 \delta_1 y_1 z_1 z_2^2 + \gamma_1 \delta_2 y_2 z_1^2 z_2 \right]$$

The quadratic approximation at N is

$$Q_N(q) := D_1(q)F(q) - D'_2(q)G'$$

where these components are

$$\begin{aligned}
D_1 &= (\Gamma_1 - \Gamma_2) [\gamma_2 \eta_1 z_2 - \gamma_1 \eta_2 z_1] \\
D'_2 &= (\Gamma_1 - \Gamma_2) [\gamma_2 \eta_1 (\Gamma_2 - \delta_1) y_1 z_2 - \gamma_1 \eta_2 (\Gamma_1 - \delta_2) z_1 y_2] \\
F &= (-\Gamma_1 y_1, -\gamma_1 z_1, -\Gamma_2 y_1, -\gamma_2 z_2)^T \\
G' &= (0, -1, 0, -1)^T,
\end{aligned}$$

giving

$$Q_N(q) = (\Gamma_1 - \Gamma_2) \begin{pmatrix} \gamma_1 \eta_2 [\Gamma_1 y_1 + (\delta_2 - \Gamma_1) y_2] z_1 + \gamma_2 \eta_1 (\Gamma_2 - \gamma_1) y_1 z_2 \\ \gamma_1 (z_1 \gamma_1 \eta_2 - z_2 \gamma_2 \eta_1) z_1 \\ \gamma_1 \eta_2 (\gamma_2 - \Gamma_1) z_1 y_2 + \gamma_2 \eta_1 [(\Gamma_2 - \delta_1) y_1 - \Gamma_2 y_2] z_2 \\ \gamma_2 (z_1 \gamma_1 \eta_2 - z_2 \gamma_2 \eta_1) z_2 \end{pmatrix}. \quad (3.4)$$

3.3.1 Non-isolated equilibria

Lemma 40. *The set of equilibrium points of (3.4) is the union of two planes E_1 and E_2 ,*

$$\begin{aligned}
E_1 &:= \{q : z_1 = z_2 = 0\} \\
E_2 &:= \{q : (\Gamma_2 - \delta_1) y_1 = (\Gamma_1 - \delta_2) y_2 \text{ and } \gamma_1 \eta_2 z_1 = \gamma_2 \eta_1 z_2\}.
\end{aligned}$$

Proof. Computing the equilibria of (3.4) amounts to solving

$$\gamma_1\eta_2[\Gamma_1y_1 + (\delta_2 - \Gamma_1)y_2]z_1 + \gamma_2\eta_1(\Gamma_2 - \gamma_1)y_1z_2 = 0 \quad (3.5a)$$

$$z_1\gamma_1(z_1\gamma_1\eta_2 - z_2\gamma_2\eta_1) = 0 \quad (3.5b)$$

$$\gamma_1\eta_2(\gamma_2 - \Gamma_1)z_1y_2 + \gamma_2\eta_1[(\Gamma_2 - \delta_1)y_1 - \Gamma_2y_2]z_2 = 0 \quad (3.5c)$$

$$z_2\gamma_2(z_1\gamma_1\eta_2 - z_2\gamma_2\eta_1) = 0. \quad (3.5d)$$

Clearly (3.5b) and (3.5d) imply that either $z_1 = z_2 = 0$ or $D_1 = 0$.

If $z_1 = z_2 = 0$, $Q_N(q) = 0$, showing that E_1 is a set of equilibrium points.

Otherwise, we necessarily have $D_1 = 0$ which is characterized by $\gamma_1\eta_2z_1 = \gamma_2\eta_1z_2$. Substituting this relation into (3.5a) and (3.5c), these both become

$$\gamma_1\eta_2z_1 [(\Gamma_2 - \delta_1)y_1 - (\Gamma_1 - \delta_2)y_2] = 0$$

which is satisfied by $z_1 = 0$ (falling under the previous case) or $(\Gamma_2 - \delta_1)y_1 = (\Gamma_1 - \delta_2)y_2$. \square

To employ Proposition 37, we find the eigenvalues of Q_N^x (the projection of Q_N on S^3) at E_1 and E_2 . At a point of E_1 ,

$$\frac{\partial Q}{\partial q} \Big|_{z_1=z_2=0} = (\Gamma_1 - \Gamma_2) \begin{pmatrix} 0 & \gamma_1\eta_2(\Gamma_1y_1 + (\delta_2 - \Gamma_1)y_2) & 0 & \eta_1\gamma_2(\Gamma_2 - \gamma_1)y_1 \\ 0 & 0 & 0 & 0 \\ 0 & \gamma_1\eta_2(\gamma_2 - \Gamma_1)y_2 & 0 & \eta_1\gamma_2((\Gamma_2 - \delta_1)y_1 - \Gamma_2y_2) \\ 0 & 0 & 0 & 0 \end{pmatrix}$$

which has all zero eigenvalues. At a point of E_2 the situation is less degenerate. Consider the change of coordinates $q = Px$, where

$$P = \begin{pmatrix} \Gamma_1 - \delta_2 & 0 & 0 & 0 \\ 0 & \gamma_2\eta_1 & 0 & 0 \\ \Gamma_2 - \delta_1 & 0 & 1 & 0 \\ 0 & \gamma_1\eta_2 & 0 & 1 \end{pmatrix}$$

so that E_2 is identified to the plane $x_3 = x_4 = 0$. Under this change of coordinates we have

$$\dot{x} = D_1(Px)P^{-1}FPx - D'_2(Px)P^{-1}G'$$

and the linearization on E_2 , $L := \frac{\partial P^{-1}Q_{N \circ P}}{\partial x} \Big|_{x_3=x_4=0}$, is

$$L = (\Gamma_1 - \Gamma_2) \begin{pmatrix} 0 & 0 & -\gamma_1\gamma_2\eta_1\eta_2x_2 & -\eta_1\gamma_2(\gamma_1 - \Gamma_2)x_1 \\ 0 & 0 & 0 & -\gamma_1\gamma_2\eta_1x_2 \\ 0 & 0 & -\gamma_1\gamma_2\eta_1\eta_2(\gamma_1 - \gamma_2)x_2 & -\eta_1\gamma_2(\delta_1 - \Gamma_2)(\gamma_1 + \Gamma_1 - \gamma_2 - \Gamma_2)x_1 \\ 0 & 0 & 0 & \gamma_1\gamma_2\eta_1\eta_2(\gamma_1 - \gamma_2)x_2 \end{pmatrix}$$

and the eigenvalues of L are $(0, 0, \beta, -\beta)$, where

$$\beta = \gamma_1\gamma_2\eta_1\eta_2(\Gamma_1 - \Gamma_2)(\gamma_1 - \gamma_2)x_2. \quad (3.6)$$

By construction, lines in the x_1x_2 -plane are lines of non-isolated equilibria, so we can use the x_2 -axis for the parameterization on S^3 , $u_i = x_i/x_2$ with $i = 1, 3, 4$, and the resulting system, with the time reparameterization $ds = x_2dt$, is

$$\begin{aligned} \dot{u}_1 &= (\Gamma_1 - \Gamma_2)\gamma_2\eta_1u_4 \left[\left(\frac{\Gamma_1(\Gamma_1 - \delta_2) - \Gamma_2(\Gamma_2 - \delta_1)}{\gamma_2 - \gamma_1} + \gamma_1 \right) u_1 + \frac{(\Gamma_1 - \Gamma_2)}{\gamma_2 - \gamma_1} u_3 \right] \\ \dot{u}_3 &= (\Gamma_1 - \Gamma_2)\gamma_2\eta_1 \left[\gamma_1\eta_2(\gamma_2 - \gamma_1)u_3 + u_3u_4 \left(\frac{\Gamma_2(\Gamma_1 - \delta_2) - \Gamma_1(\Gamma_2 - \delta_1)}{\gamma_2 - \gamma_1} + \Gamma_1 + \Gamma_2 \right) \right. \\ &\quad \left. + u_1u_4 \left[(\Gamma_1 - \delta_2)(\Gamma_2 - \delta_1) \left(\frac{\Gamma_2 - \Gamma_1 + \gamma_2 - \gamma_1}{\gamma_2 - \gamma_1} \right) \right] \right] \\ \dot{u}_4 &= (\Gamma_1 - \Gamma_2)\gamma_2\eta_1u_4 [\gamma_1\eta_2(\gamma_1 - \gamma_2) + (\gamma_1 - \gamma_2)u_4] \end{aligned} \quad (3.7)$$

(unless $\gamma_1 = \gamma_2$, which will be addressed below).

Remark 41. The work of Remizov [48] analyzes non-isolated equilibria, in particular giving a theorem to find an invariant two-dimensional foliation for systems of this form. In the case of (3.7), it can be checked that the coefficients do not meet the assumptions of the relevant theorem, and therefore it cannot be applied. The analysis of the integrability of the system is nontrivial.

Theorem 42 (A. O. Remizov [48, Theorem 2]). *Consider a system of the form*

$$\begin{aligned} \dot{x} &= \lambda x + a_1x^2 + a_2xy + a_3y^2 + a_4xz + a_5yz + \dots \\ \dot{y} &= -\lambda y + b_1x^2 + b_2xy + b_3y^2 + b_4xz + b_5yz + \dots \\ \dot{z} &= \gamma_1x^2 + \gamma_2xy + \gamma_3y^2 + \gamma_4xz + \gamma_5yz + \dots \end{aligned}$$

If $a_4 + b_5 \neq 0$ and $\gamma_2 \neq 0$ then the system is foliated by a family of invariant surfaces $U = \text{const}$, where U is diffeomorphic to $xy - z^2$.

Although we cannot apply this result, we note that u_4 can be integrated in (3.7), hence the analysis in the general case amounts to integrating a time-dependent, two-dimensional system. In the special case $\gamma_1 = \gamma_2$, which is the case for parameter set Λ_{do} (the blood case), the system can be fully integrated and so this merits additional attention.

Special case $\gamma_1 = \gamma_2$

In the case $\gamma_1 = \gamma_2$, all eigenvalues are zero (β in (3.6) is zero) and (3.7) is simply

$$\begin{aligned}\dot{u}_1 &= (\Gamma_1 - \Gamma_2)\gamma_1\eta_1 [(\delta_2 - \Gamma_1)\eta_2 u_3 + \Gamma_2 u_1 u_4] \\ \dot{u}_3 &= (\Gamma_1 - \Gamma_2)\gamma_1\eta_1 [(\Gamma_1 - \Gamma_2)u_1 u_4 + (\gamma_1 - \Gamma_2)u_3 u_4] \\ \dot{u}_4 &= 0\end{aligned}\tag{3.8}$$

and so u_4 is constant and the first two equations form a linear system which can be directly solved.

The behavior depends on the constant value of u_4 , call it c .

Inserting the physical parameters Λ_{do} , (3.8) is

$$\begin{pmatrix} \dot{u}_1 \\ \dot{u}_3 \end{pmatrix} = 10^{-3} \begin{pmatrix} 2.00c & -2.79 \\ 6.01c & -1.71c \end{pmatrix} \begin{pmatrix} u_1 \\ u_3 \end{pmatrix}\tag{3.9}$$

which has eigenvalues $\sqrt{0.000148c} \pm \sqrt{(3.44c^2 - 16.7c)10^{-6}}$. Since $z_1, z_2 \in [-2, 0]$ and $c = \frac{z_2}{z_1}\eta_1 - \eta_2$, $c \in [-0.287, \infty)$. Thus the classification of the phase portraits of (3.8) depends on values of c in this range, and this classification is given in Lemma 43 and is illustrated in Figure 3.7.

Lemma 43. *In the system (3.9) with eigenvalues λ_+ and λ_- , the value of c produces the following behaviors.*

- (i) For $c \in [-0.287, 0) \cup (4.89, \infty)$, λ_+ and λ_- have opposite sign. The origin is a saddle.
- (ii) For $c \in (0, 4.87)$, the eigenvalues are complex with a positive real part. The origin is an unstable focus.
- (iii) For $c \in [4.87, 4.89)$, both eigenvalues are positive $\lambda_+ > \lambda_- > 0$. The origin is an unstable node.

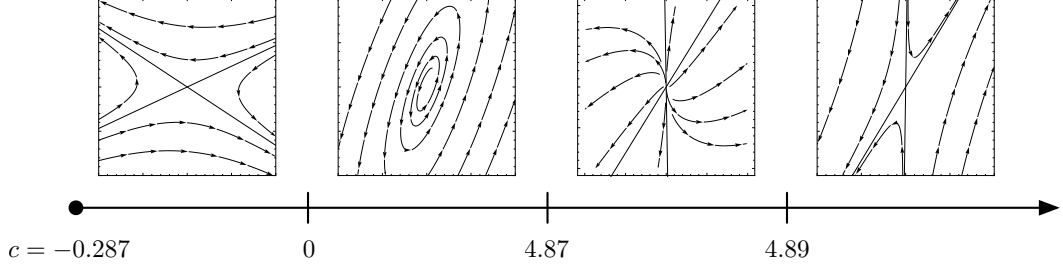


Figure 3.7: Classification of the flow of Q_N^π for the blood parameters (Lemma 43).

3.3.2 Ray solutions

To compute the ray solutions of Q_N , we first make the following observations.

Lemma 44. *There are no nontrivial ray solutions contained in the set $\{q : D_1(q) = 0\}$.*

Proof. Suppose that $D_1(q) = 0$. Then a ray solution satisfies

$$D'_2(1, 0, 1, 0)^T = \rho(y_1, z_1, y_2, z_2)^T,$$

by which we have $0 = \rho z_1 = \rho z_2$. Since $\rho \neq 0$, we must have $z_1 = z_2 = 0$. Then $D'_2 = (\Gamma_1 - \Gamma_2)[\gamma_2 \eta_1 (\Gamma_2 - \delta_1) y_1 z_2 - \gamma_1 \eta_2 (\Gamma_1 - \delta_2) z_1 y_2] = 0$ as well, and similarly $0 = \rho y_1 = \rho y_2 \implies y_1 = y_2 = 0$. So there are no nontrivial ray solutions contained in this set. \square

Corollary 45. *There are no nontrivial ray solutions on which $z_1 = z_2 = 0$.*

With the above facts in mind, we search for nontrivial ray solutions. By definition, a ray solution of the quadratic system satisfies

$$D'_2 - \Gamma_1 D_1 y_1 = \rho y_1 \tag{3.10a}$$

$$-\gamma_1 D_1 z_1 = \rho z_1 \tag{3.10b}$$

$$D'_2 - \Gamma_2 D_1 y_2 = \rho y_2 \tag{3.10c}$$

$$-\gamma_2 D_1 z_2 = \rho z_2 \tag{3.10d}$$

Since for a nontrivial ray solution at least one z_i is nonzero, we consider the cases where one is nonzero or not separately.

Case 1. If $z_1 = 0$ and $z_2 \neq 0$, then by (3.10d), $-D_1 \gamma_2 z_2 = \rho z_2$, so $\rho = -D_1 \gamma_2$.

The remaining relations are found in (3.10a) and (3.10c), which with this ρ are

$$D_1 y_1 (\gamma_2 - \Gamma_1) + D_2' = 0 \quad (3.11a)$$

$$D_1 y_2 (\gamma_2 - \Gamma_2) + D_2' = 0 \quad (3.11b)$$

which first gives that

$$y_2 (\gamma_2 - \Gamma_2) = y_1 (\gamma_2 - \Gamma_1). \quad (3.12)$$

Now there are several sub-cases.

(1a) If $\gamma_2 - \Gamma_2 \neq 0 \neq \gamma_2 - \Gamma_1$ (i.e., these are both nonzero) and one of $y_i = 0$, then $y_1 = y_2 = z_1 = 0$ and z_2 is free.

(1b) If $\gamma_2 - \Gamma_2 \neq 0 \neq \gamma_2 - \Gamma_1$ and the y_i are nonzero, then by (3.11a) we have a relation on the parameters: $\Gamma_2 = \gamma_1 - \gamma_2$.

(1c) If $\gamma_2 - \Gamma_2 = 0$ (for instance with water), then $y_1 = 0$ and y_2 is free.

(1d) If $\gamma_2 - \Gamma_1 = 0$, then $y_2 = 0$ and by (3.11b), $D_2' = 0$. Then since $z_2 \neq 0$, $y_1 = 0$, falling under case (1a).

(1e) If both $\gamma_2 - \Gamma_1 = \gamma_2 - \Gamma_2 = 0$, then $\Gamma_1 = \Gamma_2$, a contradiction.

Case 1'. If $z_1 \neq 0$ and $z_2 = 0$, the result is symmetric to the previous case.

Case 2. If $z_1 \neq 0 \neq z_2$, (3.10b) and (3.10d) are $-D_1 \gamma_1 z_1 = \rho z_1$ and $-D_1 \gamma_2 z_2 = \rho z_2$. Therefore, necessarily $\gamma_1 = \gamma_2$ (which is the case for the blood parameters), and then $\rho = -D_1 \gamma$, where $\gamma = \gamma_1 = \gamma_2$.

Using this, (3.10a) and (3.10c) are

$$D_1 y_1 (\gamma - \Gamma_1) + D_2' = 0 \quad (3.13)$$

$$D_1 y_2 (\gamma - \Gamma_2) + D_2' = 0$$

yielding $y_1 (\gamma - \Gamma_1) = y_2 (\gamma - \Gamma_2)$. Again, there are sub-cases.

(2a) If $\gamma - \Gamma_1 \neq 0 \neq \gamma - \Gamma_2$ and one of the y_i is zero, then $y_1 = y_2 = 0$ and the z_i are free.

(2b) If $\gamma - \Gamma_1 \neq 0 \neq \gamma - \Gamma_2$ and the y_i are nonzero, substituting $y_1 (\gamma - \Gamma_1) = y_2 (\gamma - \Gamma_2)$ into (3.13), we have a relation between z_1 and z_2 which simplifies to $\Gamma_1 \delta_1 \eta_2 z_1 = \Gamma_2 \delta_2 \eta_1 z_2$.

(2c) If $\gamma - \Gamma_1 = 0$ and $\gamma - \Gamma_2 \neq 0$ then $y_2 = 0$ and the remaining variables are free. A symmetric statement can be made with the indices swapped.

(2d) If $\gamma - \Gamma_1 = \gamma - \Gamma_2 = 0$ the parameters are degenerate.

These results are summarized in the following proposition.

Proposition 46. *There are ten classes of ray solutions of Q_N .*

(1a) *The z_2 -axis is a ray solution (for any set of parameters).*

(1b) *With the parameter relation $\Gamma_2 = \gamma_1 - \gamma_2$, there exist ray solutions in the set $\{q : z_1 = 0, y_2(\gamma_2 - \Gamma_2) = y_1(\gamma_2 - \Gamma_1)\}$.*

(1c) *With the parameter relation $\gamma_2 = \Gamma_2$, there exist ray solutions in the y_2z_2 -plane.*

(1a') *The z_1 -axis is a ray solution.*

(1b') *With the parameter relation $\Gamma_1 = \gamma_2 - \gamma_1$, there exist ray solutions in the set $\{q : z_2 = 0, y_1(\gamma_1 - \Gamma_1) = y_2(\gamma_1 - \Gamma_2)\}$.*

(1c') *With the parameter relation $\gamma_1 = \Gamma_1$, there exist ray solutions in the y_1z_1 -plane.*

(2a) *With the parameter relation $\gamma_1 = \gamma_2$, there exist ray solutions in the z_1z_2 -plane.*

(2b) *With the parameter relation $\gamma_1 = \gamma_2$, there exist ray solutions in the plane $\{q : y_1(\gamma - \Gamma_1) = y_2(\gamma - \Gamma_2), z_1\Gamma_1\delta_1\eta_2 = z_2\Gamma_2\delta_2\eta_1\}$.*

(2c) *With the parameter relation $\gamma_1 = \Gamma_1 = \gamma_2$, there exist ray solutions in the set $\{q : y_2 = 0\}$.*

(2c') *With the parameter relation $\gamma_1 = \gamma_2 = \Gamma_2$, there exist ray solutions in the set $\{q : y_1 = 0\}$.*

Several of these rays rely on specific configurations of parameters, some experimentally relevant and some not. For example, solutions (1c) and (2a) occur in the given parameter sets (water and blood, respectively) while (2c) is rather restrictive and is not interesting from the physical standpoint.

The z_2 -axis ray

Investigating the ray (1a), we use coordinates $(x_0, x_1, x_2, x_3) = (z_2, y_1, z_1, y_2)$ and the system in these coordinates in the form of Proposition 37 is

$$\dot{x}_0 = \lambda_0 x_0^2 + \dots$$

$$\dot{x} = x_0 Bx + \dots$$

where $x = (x_1, x_2, x_3)$. The values are $\lambda_0 = -\gamma_2^2 \eta_1 (\Gamma_1 - \Gamma_2)$ and

$$B = (\Gamma_1 - \Gamma_2) \begin{pmatrix} \gamma_2 \eta_1 (\Gamma_2 - \gamma_1) & 0 & 0 \\ 0 & -\gamma_1 \gamma_2 \eta_1 & 0 \\ \gamma_2 \eta_1 (\Gamma_2 - \delta_1) & 0 & -\gamma_2 \Gamma_2 \eta_1 \end{pmatrix}$$

where the eigenvalues of B are

$$\lambda_1 = \gamma_2 \eta_1 (\Gamma_2 - \gamma_1) (\Gamma_1 - \Gamma_2), \quad \lambda_2 = -\gamma_1 \gamma_2 \eta_1 (\Gamma_1 - \Gamma_2), \quad \lambda_3 = -\gamma_2 \Gamma_2 \eta_1 (\Gamma_1 - \Gamma_2).$$

In light of Proposition 37, the differences $\sigma_i = \lambda_i - \lambda_0$, $i = 1, 2, 3$, are

$$\sigma_1 = \gamma_2 \eta_1 (\gamma_2 + \Gamma_2 - \gamma_1) (\Gamma_1 - \Gamma_2), \quad \sigma_2 = \gamma_2 \eta_1 (\gamma_2 - \gamma_1) (\Gamma_1 - \Gamma_2), \quad \sigma_3 = \gamma_2 \eta_1 \delta_2 (\Gamma_1 - \Gamma_2), \quad (3.14)$$

and recalling Remark 39, we calculate the ratios of these, $I_i = \sigma_i / \sigma_1$, $i = 2, 3$, which are

$$I_1 = \frac{\gamma_2 - \gamma_1}{\gamma_2 + \Gamma_2 - \gamma_1}, \quad I_2 = \frac{\gamma_2 - \Gamma_2}{\gamma_2 + \Gamma_2 - \gamma_1}. \quad (3.15)$$

In the four sets of parameters these invariants, shown in Table 3.2, are distinct, giving the following result.

Theorem 47. *We have the following results related to the invariant values.*

- (i) *The eigenvalues of the linearized system correspond to the z_2 -axis ray solution projected on S^3 are σ_1 , σ_2 , and σ_3 , given in (3.14).*
- (ii) *I_1 and I_2 are two independent, rational invariants, given in (3.15).*
- (iii) *Computing along the z_1 -axis amounts to an exchange of indices (giving values I'_1 and I'_2), and allows us to define four rational invariants. A choice of three of them separates the generic flows in the feedback classification problem.*

Proof. The only claim not justified above is that a choice of three of the invariants separates generic orbits in the feedback classification. This is due to the fact that each orbit contains an element (F, G) which is determined by the set of parameters $\Lambda = (\gamma_1, \Gamma_1, \gamma_2, \Gamma_2)$. Therefore an orbit can be identified to such a set Λ , which, as previously stated, is unique only up to a scalar factor and is therefore characterized by three invariants. \square

Table 3.2: Invariant values for the four sets of parameters.

	Λ_{wc}	Λ_{do}	Λ_{gw}	Λ_{wf}
λ_0	2.70×10^{-7}	-2.96×10^{-4}	3.17×10^{-5}	8.82×10^{-5}
λ_1	-1.58×10^{-6}	1.71×10^{-3}	-2.48×10^{-4}	-1.69×10^{-4}
λ_2	2.16×10^{-7}	-2.97×10^{-4}	2.69×10^{-5}	7.06×10^{-6}
λ_3	1.80×10^{-6}	-2.00×10^{-3}	2.75×10^{-4}	1.76×10^{-4}
σ_1	-1.85×10^{-6}	2.00×10^{-3}	-2.80×10^{-4}	-2.58×10^{-4}
σ_2	-5.39×10^{-8}	0	-4.83×10^{-6}	-8.11×10^{-5}
σ_3	1.53×10^{-6}	-1.71×10^{-3}	2.43×10^{-4}	8.82×10^{-5}
I_1	0.0291	0	0.0173	0.315
I_2	-0.825	-0.852	-0.869	-0.342
I'_1	-1/3	0	-0.020	1.095
I'_2	0	-0.963	-0.909	0

Remark 48. Here we have computed a set of invariants corresponding to the quadratic terms of the dynamics. We therefore have a set of partial invariants of the exceptional dynamics since it is a necessary condition that for two systems to be feedback equivalent, their quadratic terms must be equivalent.

3.4 Quadratic approximation at the origin

In this section we investigate the quadratic system Q_O . Recall from its introduction that in this case we assume that $\eta_1 \neq \eta_2$ and $\eta_1, \eta_2 > 0$.

We now list the full expansions of D and D' .

$$\begin{aligned}
 D &= \det(F, G, [F, G], [G, [F, G]]) \\
 &= \begin{vmatrix} -\Gamma_1 y_1 & -z_1 & \gamma_1 - \delta_1 z_1 & 2\delta_1 y_1 \\ \gamma_1(1 - z_1) & y_1 & -\delta_1 y_1 & \gamma_1 - 2\delta_1 z_1 \\ -\Gamma_2 y_2 & -z_2 & \gamma_2 - \delta_2 z_2 & 2\delta_2 y_2 \\ \gamma_2(1 - z_2) & y_2 & -\delta_2 y_2 & \gamma_2 - 2\delta_2 z_2 \end{vmatrix} \\
 &= D_1(q) + D_2(q) + D_3(q) + D_4(q)
 \end{aligned}$$

The D_k are the homogeneous terms of order k of D :

$$D_1(q) = 0$$

$$D_2(q) = \gamma_2^2 \mu_1 y_1^2 - \gamma_1 \gamma_2 (\mu_1 + \mu_2) y_1 y_2 + \gamma_1^2 \mu_2 y_2^2 + \gamma_2^2 \eta_1 z_1^2 - \gamma_1 \gamma_2 (\eta_1 + \eta_2) z_1 z_2 + \gamma_1^2 \eta_2 z_2^2$$

$$\begin{aligned} D_3(q) &= 2\delta_1 \gamma_2 (\gamma_1 + \Gamma_1 + \mu_2) y_1 y_2 z_1 + 2\gamma_1 \delta_2 (\mu_1 + \gamma_2 + \Gamma_2) y_1 y_2 z_2 \\ &\quad + \gamma_1 (3\gamma_2 \Gamma_2 - 2\gamma_2^2 - \Gamma_2^2 + \gamma_1 (\Gamma_2 - 4\gamma_2) + \Gamma_1 (2\gamma_2 + \Gamma_2)) y_2^2 z_1 \\ &\quad + \gamma_2 (\Gamma_1 (\gamma_2 - \Gamma_1 + \Gamma_2) - 2\gamma_1^2 + \gamma_1 (3\Gamma_1 - 4\gamma_2 + 2\Gamma_2)) y_1^2 z_2 \\ &\quad + \gamma_2 (\gamma_1 (3\Gamma_1 + \gamma_2 + \Gamma_2) - \gamma_1^2 - 2\Gamma_1 (\Gamma_1 + \mu_2)) z_1^2 z_2 \\ &\quad + \gamma_1 (\gamma_1 (\gamma_2 - 4\Gamma_2) - \gamma_2^2 + 3\gamma_2 \Gamma_2 - 2\Gamma_2^2 + \Gamma_1 (\gamma_2 + 2\Gamma_2)) z_1 z_2^2 \end{aligned}$$

$$\begin{aligned} D_4(q) &= 2[(\Gamma_1 \gamma_2 (\Gamma_1 + \delta_2) + \gamma_1^2 \Gamma_2 - \gamma_1 (\delta_2 \Gamma_2 + \Gamma_1 (\gamma_2 + \Gamma_2))) y_1^2 y_2^2 \\ &\quad + (\gamma_1^2 \gamma_2 + \Gamma_1 \Gamma_2 (\Gamma_1 - \delta_2) + \gamma_1 (\gamma_2 \delta_2 - \Gamma_1 (\gamma_2 + \Gamma_2))) y_2^2 z_1^2 \\ &\quad + (\gamma_1^2 \gamma_2 + \Gamma_1 \Gamma_2 (\Gamma_1 - \delta_2) + \gamma_1 (\gamma_2 \delta_2 - \Gamma_1 (\gamma_2 + \Gamma_2))) y_1^2 z_2^2 \\ &\quad + (\Gamma_1 \gamma_2 (\Gamma_1 + \delta_2) + \gamma_1^2 \Gamma_2 - \gamma_1 (\delta_2 \Gamma_2 + \Gamma_1 (\gamma_2 + \Gamma_2))) z_1^2 z_2^2 \\ &\quad - 2\delta_1 \delta_2 (\gamma_1 + \Gamma_1 + \gamma_2 + \Gamma_2) y_1 y_2 z_1 z_2] \end{aligned}$$

$$D' = \det(F, G, [F, G], [F, [F, G]])$$

$$\begin{aligned} &= \begin{vmatrix} -\Gamma_1 y_1 & -z_1 & \gamma_1 - \delta_1 z_1 & -\gamma_1 \eta_1 - \delta_1^2 z_1 \\ \gamma_1 (1 - z_1) & y_1 & -\delta_1 y_1 & \delta_1^2 y_1 \\ -\Gamma_2 y_2 & -z_2 & \gamma_2 - \delta_2 z_2 & -\gamma_2 \eta_2 - \delta_2^2 z_2 \\ \gamma_2 (1 - z_2) & y_2 & -\delta_2 y_2 & \delta_2^2 y_2 \end{vmatrix} \\ &= D'_1(q) + D'_2(q) + D'_3(q) + D'_4(q) \end{aligned}$$

Likewise, D'_k are the homogeneous terms of order k of D' :

$$D'_1(q) = \gamma_1\gamma_2^2(\eta_2 - \eta_1)y_1 + \gamma_1^2\gamma_2(\eta_1 - \eta_2)y_2$$

$$\begin{aligned} D'_2(q) &= \gamma_1\gamma_2(2\gamma_2^2 - 2\gamma_2(2\Gamma_2 + \mu_1) + (\Gamma_2 + 2\gamma_1 - 3\Gamma_1)(\Gamma_2 - \delta_1))y_1z_2 \\ &\quad + \gamma_1\gamma_2(2\gamma_1^2 - 2\gamma_1(2\Gamma_1 + \mu_2) + (\Gamma_1 + 2\gamma_2 - 3\Gamma_2)(\Gamma_1 - \delta_2))z_1y_2 \end{aligned}$$

$$\begin{aligned} D'_3(q) &= \gamma_1\gamma_2(2\gamma_1^2 + 3\Gamma_1^2 - 2\Gamma_1\delta_2 - \delta_2^2 + \gamma_1(\gamma_2 - 5\Gamma_1 - \Gamma_2))y_1z_2^2 \\ &\quad - \Gamma_1\gamma_2(\gamma_1^2 + \Gamma_1^2 - \Gamma_1\gamma_2 - 2\gamma_2^2 - \gamma_1(2\Gamma_1 + \eta_2) + 2\Gamma_1\Gamma_2 + 5\gamma_2\Gamma_2 - 3\Gamma_2^2)y_1^2y_2 \\ &\quad - \gamma_1\gamma_2(\gamma_1^2 + \Gamma_1^2 - 2\gamma_2^2 - \Gamma_1\eta_2 - \gamma_1(2\Gamma_1 - \eta_2) + 5\gamma_2\Gamma_2 - 3\Gamma_2^2)y_2z_1^2 \\ &\quad + \gamma_1\Gamma_2(2\gamma_1^2 + 3\Gamma_1^2 + 2\Gamma_1\delta_2 - \delta_2^2 - \gamma_1(5\Gamma_1 + \delta_2))y_1y_2^2 \\ &\quad + 2\delta_1\gamma_2(\delta_1^2 - 2\gamma_2^2 + 4\gamma_2\Gamma_2 - \Gamma_2^2)y_1z_1z_2 + 2\gamma_1\delta_2(4\gamma_1\Gamma_1 - 2\gamma_1^2 - \Gamma_1^2 + \delta_2^2)y_2z_1z_2 \end{aligned}$$

$$D'_4(q) = 2(\delta_1^2 - \delta_2^2)[\Gamma_1\delta_2y_1^2y_2z_2 - \delta_1\Gamma_2y_1y_2^2z_1 + \gamma_1\delta_2y_2z_1^2z_2 - \delta_1\gamma_2y_1z_1z_2^2]$$

Thus Q_O is

$$Q_O(q) := D_2(q)F'(q) - D'_1(q)G(q)$$

where

$$D_2 = \gamma_2^2\mu_1y_1^2 - \gamma_1\gamma_2(\mu_1 + \mu_2)y_1y_2 + \gamma_1^2\mu_2y_2^2 + \gamma_2^2\eta_1z_1^2 - \gamma_1\gamma_2(\eta_1 + \eta_2)z_1z_2 + \gamma_1^2\eta_2z_2^2$$

$$D'_1 = \gamma_1\gamma_2^2(\eta_2 - \eta_1)y_1 + \gamma_1^2\gamma_2(\eta_1 - \eta_2)y_2$$

$$F' = (0, \gamma_1, 0, \gamma_2)^T$$

$$G = (-z_1, y_1, -z_2, y_2)^T.$$

As in §3.3 we assume that $\eta_1, \eta_2 > 0$ and $\eta_1 \neq \eta_2$. Note that the μ_i may have any sign (and each occurs in the given physical parameters—for water it is positive, for fat tissue it is zero, and it is negative for the remaining substances).

3.4.1 Non-isolated equilibria

Calculating the set $\{q : Q_O(q) = 0\}$ amounts to solving

$$\begin{cases} \gamma_1 D_2 - D'_1 y_1 = 0 & (3.16a) \\ D'_1 z_2 = 0 & (3.16b) \\ \gamma_2 D_2 - D'_1 y_2 = 0 & (3.16c) \\ D'_1 z_1 = 0. & (3.16d) \end{cases}$$

Lemma 49. *There are no equilibria with $D'_1 \neq 0$.*

Proof. Suppose that $D'_1(q) \neq 0$ for some $q = (y_1, z_1, y_2, z_2)$. Then by (3.16b) and (3.16d) we have that $z_1 = z_2 = 0$. With this, (3.16a) is

$$\gamma_1(\gamma_2^2 \mu_1 y_1^2 - \gamma_1 \gamma_2 (\mu_1 + \mu_2) y_1 y_2 + \gamma_1^2 \mu_2 y_2^2) - (\gamma_1 \gamma_2^2 (\eta_2 - \eta_1) y_1 + \gamma_1^2 \gamma_2 (\eta_1 - \eta_2) y_2) y_1 = 0$$

which can be solved for y_1 in terms of y_2 . Doing the same for (3.16c), we have another pair of solutions for y_1 in terms of y_2 , and the only values satisfying both pairs of solutions are $y_1 = y_2 = 0$, which would imply that $D'_1 = 0$. \square

Define the linear change of coordinates

$$\begin{cases} x_1 = \gamma_1 \gamma_2 (\eta_2 - \eta_1) (\gamma_2 y_1 - \gamma_1 y_2) \\ x_2 = \frac{1}{\gamma_1 \gamma_2 (\eta_2 - \eta_1)} (\gamma_2 \mu_1 y_1 - \gamma_1 \mu_2 y_2) \\ x_3 = \gamma_2 z_1 - \gamma_1 z_2 \\ x_4 = \gamma_2 \eta_1 z_1 - \gamma_1 \eta_2 z_2. \end{cases} \quad (3.17)$$

In these coordinates, D'_1 and D_2 have the normal forms $D'_1 = x_1$ and $D_2 = x_1 x_2 + x_3 x_4$.

Proposition 50. *In coordinates (3.17), the set of equilibria of Q_O is the set*

$$\{x : x_1 = 0 \text{ and } (x_3 = 0 \text{ or } x_4 = 0)\}.$$

Proof. Let $x_0 \in \{x : Q_O(x) = 0\}$. By Lemma 49, $x_1 = 0$. It then remains to satisfy $\gamma_1 D_2(x_0) = \gamma_2 D_2(x_0) = 0$, therefore $D_2(x_0) = 0$, which gives that $x_3 = 0$ or $x_4 = 0$. \square

We therefore have that non-isolated equilibria of Q_O lie in two planes, $E_1 := \{x : x_1 = x_3 = 0\}$ and $E_2 := \{x : x_1 = x_4 = 0\}$.

Theorem 51. *The eigenvalues of the linearized system on the planes E_1 and E_2 are as follows.*

(i) *On E_1 the eigenvalues are zero.*

(ii) *On E_2 the eigenvalues are given by $\{0, 0, \lambda, -\lambda\}$ where $\lambda = \gamma_1\gamma_2(\eta_1 - \eta_2)x_3$.*

Proof. We have

$$Q_O(x) = \begin{pmatrix} \gamma_1\gamma_2(\eta_2 - \eta_1)x_1x_3 \\ \frac{((\mu_1\eta_2 - \mu_2\eta_1)x_3 + (\mu_2 - \mu_1)x_4)x_1}{\gamma_1\gamma_2(\eta_1 - \eta_2)^2} \\ \frac{x_1^2}{\gamma_1\gamma_2(\eta_1 - \eta_2)^2} \\ \frac{f(x)}{\gamma_1\gamma_2^2(\mu_1 - \mu_2)^2(\eta_1 - \eta_2)} \end{pmatrix}$$

where $f(x)$ is a rather long polynomial.

By calculation, the eigenvalues of $\frac{\partial Q_O}{\partial x}|_{x_1=x_3=0}$ are $\{0, 0, 0, 0\}$ and the eigenvalues of $\frac{\partial Q_O}{\partial x}|_{x_1=x_4=0}$ are $\{0, 0, \gamma_1\gamma_2(\eta_1 - \eta_2)x_3, -\gamma_1\gamma_2(\eta_1 - \eta_2)x_3\}$. \square

3.4.2 Ray solutions

Proposition 52. *There are no nontrivial ray solutions of Q_O .*

Proof. A nontrivial ray is a solution of

$$\begin{cases} D'_1 z_1 = \rho y_1 & (3.18a) \\ \gamma_1 D_2 - D'_1 y_1 = \rho z_1 & (3.18b) \\ D'_1 z_2 = \rho y_2 & (3.18c) \\ \gamma_2 D_2 - D'_1 y_2 = \rho z_2 & (3.18d) \end{cases}$$

with $\rho \neq 0$.

First assume that $y_1 \neq 0$. Then by (3.18a), D'_1 and z_1 are both nonzero, giving the value $\rho = D'_1 z_1 / y_1$. Using this value in (3.18c), we have

$$D'_1 z_2 = \frac{D'_1 z_1}{y_1} y_2 \implies y_1 z_2 = z_2 y_2. \quad (3.19)$$

Substituting this ρ into (3.18b) gives

$$\gamma_1 D_2 - D'_1 y_1 = \frac{D'_1 z_1}{y_1} z_1, \quad (3.20)$$

and notice that if $D_2 = 0$ then $-y_1^2 = z_1^2$, a contradiction, so D_2 is nonzero as well. Also from (3.20), since z_1 is nonzero we have

$$\frac{D'_1 z_1}{y_1} = \frac{\gamma_1 D_2 - D'_1 y_1}{z_1}. \quad (3.21)$$

Substituting ρ into (3.18d) gives $\gamma_2 D_2 - D'_1 y_2 = (D'_1 z_1 / y_1) z_2$, and with (3.21) this gives

$$\gamma_2 D_2 z_1 - D'_1 y_2 z_1 = \gamma_1 D_2 z_2 - D'_1 y_1 z_2$$

and using $y_1 z_2 = z_2 y_2$ from (3.19), this is $\gamma_2 D_2 z_1 = \gamma_1 D_2 z_2 \implies \gamma_2 z_1 = \gamma_1 z_2$ (again using $D'_1 \neq 0$ and $D_2 \neq 0$). However the relations $\gamma_2 z_1 = \gamma_1 z_2$ and $y_1 z_2 = z_1 y_2$ together imply that $D'_1 = 0$, a contradiction.

Next assume that $y_1 = 0$. Then from (3.18a), $D'_1 = 0$ or $z_1 = 0$. If $D'_1 = 0$ and $z_1 \neq 0$, then first note that $D_2 \neq 0$, otherwise $D'_1 = D_2 = 0$ would give $\rho = 0$. Now, (3.18b) gives the value $\rho = \gamma_1 D_2 / z_1$. Substituting this into (3.18d), we have

$$\gamma_1 z_2 D_2 = \gamma_2 z_1 D_2 \implies \gamma_1 z_2 = \gamma_2 z_1.$$

However, $D'_1 = 0$ and $\gamma_1 z_2 = \gamma_2 z_1$ give that $D_2 = 0$, a contradiction. In the case $z_1 = 0$, (3.18b) is simply $\gamma_1 D_2 = 0$, so $D_2 = 0$. Then multiplying (3.18c) by z_2 and (3.18d) by y_2 , we have $-D'_1 y_2^2 = \rho y_2 z_2 = D'_1 z_2^2$. Since $D'_1 \neq 0$ (again, this would be $D'_1 = D_2 = 0$), $-y_2^2 = z_2^2$, a contradiction. \square

3.5 Algebraic geometric classification

Gröbner bases are an effective tool for determining properties of ideals of polynomial rings, and in particular can assist in computing the zero locus of such an ideal. We will introduce Gröbner bases and employ them to make the algebraic-geometric classification of the surfaces $S := \{q : D(q) = 0\}$ and $S' := \{q : D(q) = D'(q) = 0\}$, which as stated in §3.2.2, contain respectively the points where the singular control explodes and where the singular control can cross S .

In this section we use the coordinate translation of §3.3 where N is set to the origin.

3.5.1 Gröbner bases

We recall the following standard material [21, 23, 24]. We will, just below, define \mathcal{F} to be a given set of polynomials, I to be the ideal generated by \mathcal{F} , and \mathcal{G} to be the Gröbner basis of I . To avoid restatement, we let these meanings of \mathcal{F} , I , and \mathcal{G} persist for the remainder of this subsection.

Definition 53. Let R denote the ring of polynomials in n variables x_1, \dots, x_n with real coefficients, $R = \mathbb{R}[x_1, \dots, x_n]$. Let $\mathcal{F} = \{f_1, \dots, f_m\}$ be a set of polynomials, $f_i \in R$. The ideal I generated by \mathcal{F} , $I = (f_1, \dots, f_m)$ is

$$I = \left\{ \sum_{i=1}^n p_i f_i : p_i \in R \right\}.$$

Definition 54. Denote a term of a polynomial by $a \prod x_i^{r_i}$, $a \in \mathbb{R}$. The *multidegree* of this term is (r_1, r_2, \dots, r_n) , i.e., an ordered list of the powers of x_i in the term. Given a lexicographic ordering $x_{k_1} \succ x_{k_2} \succ \dots \succ x_{k_n}$ of x_1, \dots, x_n , the leading term of $f \in R$, $\text{LT}(f)$, is the term of highest degree with respect to the ordering.

As an example, let $f(x, y) = x^3 + 5xy$. The multidegree of the term x^3 is $(3, 0)$ and the multidegree of xy is $(1, 1)$. With the lexicographic ordering $x \succ y$, $\text{LT}(f) = x^3$, while with the ordering $y \succ x$, $\text{LT}(f) = xy$.

Definition 55. Given a lexicographic ordering of x_1, \dots, x_n , the Gröbner basis for an ideal $I \subseteq R$ is a finite set of generators $\{g_1, \dots, g_k\}$ for I whose leading terms generate the ideal of all leading terms in I . That is, $\{g_1, \dots, g_k\}$ is such that $I = (g_1, \dots, g_k)$ and $\text{LT}(I) = (\text{LT}(g_1), \dots, \text{LT}(g_k))$.

For an arbitrary ideal in R , its Gröbner basis exists and can be computed by an algorithm initially given by Bruno Buchberger in his Ph.D. thesis [17]. There have been improvements to the algorithm, and it is a standard tool in modern computer algebra systems. It is important to note that this algorithm (and its improvements) has large upper bounds on space and running time requirements.

Definition 56. The zero locus of a set of polynomials \mathcal{F} , $\mathcal{Z}(\mathcal{F})$, is the set of points on where all functions in \mathcal{F} simultaneously vanish, i.e., $\mathcal{Z}(\mathcal{F}) = \{a \in \mathbb{R}^n : f(a) = 0 \text{ for all } f \in \mathcal{F}\}$. We note that \mathcal{Z} is an algebraic variety.

Lemma 57. *If $(a_1, \dots, a_n) \in \mathcal{Z}(\mathcal{F})$, then we have that for every $f \in I$, $f(a_1, \dots, a_n) = 0$. Furthermore if $\mathcal{G} = \{g_1, \dots, g_k\}$ is any set generating I , $\mathcal{Z}(\mathcal{G}) = \mathcal{Z}(\mathcal{F})$.*

Remark 58. By Hilbert's Nullstellensatz, $\mathcal{Z}(\mathcal{F})$ is empty if and only if $\mathcal{G} = \{1\}$.

Gröbner bases can be employed to find the zero locus of an ideal in the spirit of Gauss-Jordan elimination. The idea is to find some element of I which is a polynomial of only one variable, say, $f_n(x_n)$, then the solution the solution a_n of $f_n(x_n) = 0$ is the last coordinate of a solution $(a_1, \dots, a_n) \in \mathcal{Z}(I)$. The next step is to find an element f_{n-1} which is a polynomial of only x_n and x_{n-1} , and the solution of $f_{n-1}(x_{n-1}, a_n) = 0$ is coordinate a_{n-1} . If this process can be iterated for each x_i , the full solution is constructed. This notion gives rise to elimination theory.

The additional condition concerning leading terms in the definition of the Gröbner basis shows that the choice of lexicographic order determines which basis is given by an algorithm. This allows for flexibility when solving $\mathcal{Z}(I)$ by elimination since the bases corresponding to the different orderings can each be inspected in terms of elimination.

Basis construction algorithm

In the following Gröbner basis calculations, we use a construction and factorization algorithm mentioned in a work of Jacquemard and Teixeira [29] (and elsewhere [25, 28, 45]). The idea of this algorithm is, given a basis \mathcal{G} where some element, say, g_j is a product of squarefree factors, $g_j = p \cdot q$, the basis is split into two, with g_j replaced by each of these factors. That is, we decompose \mathcal{G} into $\mathcal{G}_1 = \{g_1, \dots, g_{j-1}, p, g_{j+1}, \dots, g_k\}$ and $\mathcal{G}_2 = \{g_1, \dots, g_{j-1}, q, g_{j+1}, \dots, g_k\}$. This process is repeated where possible, resulting in a set of polynomial ideals and a Gröbner basis is computed for each ideal of this set. In this way, a large part of the complexity of computing a Gröbner basis can be bypassed, and in particular the basis can be computed in cases where a straightforward attempt to compute a Gröbner basis fails due to machine memory constraints.

3.5.2 Analysis of the set S

Here we determine the set S , and in particular we are interested singularities of this set, i.e., points q such that $D(q) = 0$ and $\nabla D(q) = 0$. To analyze the singularities of S we define I to be the ideal generated by the set of polynomials $\{D, \nabla D\}$, and the singularities are $\mathcal{Z}(I)$. For each set of parameters we compute a Gröbner basis with lexicographic ordering $y_1 \succ y_2 \succ z_1 \succ z_2$. For

the computations, parameter values taken as rational numbers (so that the basis computation is performed with rational coefficients), but we present the resulting bases with coefficients written in decimal for the sake of readability.

Lemma 59. *The functions D and the Gröbner basis \mathcal{G} of the ideal generated by $\{D, \nabla D\}$ are as follows.*

Λ_{wc} : *Water and cerebrospinal fluid.*

$$\begin{aligned} D = & 0.000243995z_1(z_1 + 0.88) + 0.00019058(z_1 + 0.588235)(z_1 + 1.14118)y_2^2 \\ & + 0.000431608(z_1 - 0.0463456)(z_1 + 0.870333)z_2 - (0.000273275 + 0.000284749z_2)y_1y_2 \\ & + (0.00019058y_2^2 + 0.00019058(z_2 + 1.08824)(z_2 + 1.17647))y_1^2 \\ & + 0.00019058(z_1 - 0.0882353)(z_1 + 0.858824)z_2^2 \end{aligned}$$

$$\begin{aligned} \mathcal{G} = \{ & (2737z_2 + 3256)(1751z_2 + 1628)(z_2 + 1), -281911z_2^2 - 295592 + 3390z_1 - 580893z_2, \\ & y_2(1751z_2 + 1628), 1598y_2^2 + (2737z_2 + 3256)(z_2 + 1), 1695y_1 - 4841y_2 \} \end{aligned}$$

Λ_{do} : *Deoxygenated blood and oxygenated blood.*

$$\begin{aligned} D = & 0.138817(z_1 + 0.986897)(z_1 + 1.0315)y_2^2 + 0.00635023(z_1 + 1.05049)(z_1 + 1.94049)z_2 \\ & - (0.269681 + z_1(0.272433 + 0.257851z_2) + 0.255458z_2)y_1y_2 \\ & - 0.00290223(z_1 + 1.05195)z_1 + 0.00989171(z_1 + 1.04938)(z_1 + 1.30864)z_2^2 \\ & + (0.00989171y_2^2 + 0.138817(z_2 + 0.931034)(z_2 + 1.0315))y_1^2 \end{aligned}$$

$$\begin{aligned} \mathcal{G} = \{ & 18824.8 + 93893.2z_2 + 186780.2z_2^2 + 185197.2z_2^3 + 91522.9z_2^4 + 18034.0z_2^5 + 3.67782z_1, \\ & (21z_2 + 25)(z_2 + 1)(507.284 + 2097.44z_2 + 3243.45z_2^2 + 2223.18z_2^3 + 569.89z_2^4), \\ & (569890113z_2^4 + 2223178574z_2^3 + 3243449880z_2^2 + 2097437250z_2 + 507284375)y_2, \\ & 2.882y_2^2 - (21z_2 + 25)(z_2 + 1)(545.998 + 1731.81z_2 + 1820.65z_2^2 + 634.095z_2^3), \\ & 2.73707y_1 + (473.001 + 1404.87z_2 + 1378.94z_2^2 + 448.061z_2^3)y_2 \} \end{aligned}$$

Λ_{gw} : *Gray and white cerebral matter.*

$$\begin{aligned}
D &= 0.00148466z_1(z_1 + 0.505495) + 0.122044(z_1 + 0.957663)(z_1 + 1.058)y_2^2 \\
&\quad + 0.000521754(z_1 - 3.75468)(z_1 + 0.408111)z_2 - 0.0000404056(z_1 - 0.186613)(z_1 + 16.3125)z_2^2 \\
&\quad - (0.248111 + z_1(0.244169z_2 + 0.245892) + 0.247065z_2)y_1y_2 \\
&\quad + (0.122044(z_2 + 0.954276)(z_2 + 1.0684) - 0.0000404056y_2^2)y_1^2
\end{aligned}$$

$$\begin{aligned}
\mathcal{G} &= \{(26029z_2 + 29302)(z_2 + 1)(2.342 + 9.386z_2 + 14.097z_2^2 + 9.403z_2^3 + 2.350z_2^4), \\
&\quad 5702.97 + 1.15687z_1 + 27870.z_2 + 54421.5z_2^2 + 53069.7z_2^3 + 25844.9z_2^4 + 5028.55z_2^5, \\
&\quad 7.484y_2^2 - (26029z_2 + 29302)(z_2 + 1)(2.405 + 6.890z_2 + 6.560z_2^2 + 2.078z_2^3), \\
&\quad 2.061y_1 + (1740.3 + 5193.84z_2 + 5155.61z_2^2 + 1703.81z_2^3)y_2, \\
&\quad (2.342 + 9.386z_2 + 14.097z_2^2 + 9.402z_2^3 + 2.350z_2^4)y_2\}
\end{aligned}$$

Λ_{wf} : *Water and fat tissue.*

$$\begin{aligned}
D &= 0.00207726(z_1 - 0.289688)(z_1 + 0.946831)z_2 - y_1y_2(0.00185173 + 0.00182799z_2) \\
&\quad + 0.00178051z_1(z_1 + 0.96) + 0.000593502y_2^2(z_1 + 1)(z_1 + 1.08) \\
&\quad + 0.000593502 [(z_1 - 0.5)(z_1 + 0.92)z_2^2 + y_1^2(y_2^2 + (z_2 + 1.5)(z_2 + 2))]
\end{aligned}$$

$$\begin{aligned}
\mathcal{G} &= \{(71z_2 + 144)(73z_2 + 72)(z_2 + 1), -15549z_2^2 - 24240 + 1900z_1 - 41689z_2, \\
&\quad y_2(73z_2 + 72), 4y_2^2 + (71z_2 + 144)(z_2 + 1), 475y_1 - 73y_2\}
\end{aligned}$$

With these bases, we can compute the singular points of S .

Lemma 60. *For any set of parameters, $O = (0, -1, 0, -1)$ is a singular point. The remaining roots are given below for each parameter set, where $\epsilon \in \{1, -1\}$ in the conjugate pairs.*

Λ_{wc} : *Water and cerebrospinal fluid.*

$$\begin{aligned}
&(0, 1.035, 0, -1.189) \quad (\text{outside the Bloch ball}) \\
&(\epsilon 0.505i, -0.236, \epsilon 0.177i, -0.930)
\end{aligned}$$

Λ_{do} : *Deoxygenated blood and oxygenated blood.*

$$(0, -1.039, 0, -1.190) \quad (\text{inside the Bloch ball})$$

$$(\epsilon 0.0480i, -0.979, \epsilon 0.232i, 0.870)$$

$$(\epsilon 0.00489i, -1.033, \epsilon 0.0637i, 1.098)$$

$$(\epsilon 0.0371i, -0.981, \epsilon 0.0823i, -0.918)$$

$$(\epsilon 0.0387i, -0.990, \epsilon 0.124i, -1.014)$$

Λ_{gw} : *Gray and white cerebral matter.*

$$(0, -1.117, 0, -1.126) \quad (\text{inside the Bloch ball})$$

$$(\epsilon 0.0309i, -1.081, \epsilon 0.0308i, -1.090)$$

$$(\epsilon 0.0562i, -0.966, \epsilon 0.0640i, -0.963)$$

$$(0.0180 + \epsilon 0.116i, -0.978 - 0.0221i, 0.0177 + \epsilon 0.125i, -0.974 - 0.0219i)$$

$$(-0.0180 + \epsilon 0.116i, -0.978 + 0.0221i, -0.0177 + \epsilon 0.125i, -0.974 + 0.0219i)$$

Λ_{wf} : *Water and fat tissue.*

$$(0, 1.920, 0, -2.028) \quad (\text{outside the Bloch ball})$$

$$(\epsilon 0.077i, -0.922, \epsilon 0.503i, -0.986)$$

These roots are represented in Figure 3.8.

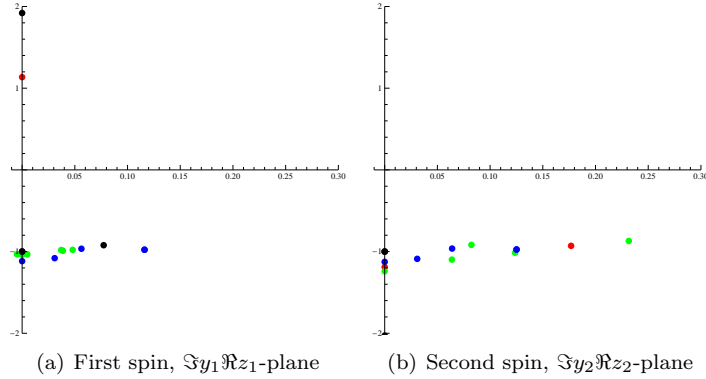


Figure 3.8: The roots of $\{D, \nabla D\}$ in the translated system (see Lemma 60), projected onto the $\Im y_i \Re z_i$ -plane. Since the roots are in conjugate pairs, only the right half-plane is shown. The roots corresponding to parameters Λ_{wc} , Λ_{do} , Λ_{gw} , and Λ_{wf} are respectively shown in red, green, blue, and black.

3.5.3 Analysis of the surface S'

To determine the set S' we employ the algorithm described in §3.5.1. This gives an algorithmic decomposition of algebraic varieties, each of them being described by a Gröbner basis. Observe

that the number of algebraic varieties in this decomposition depends upon the chosen lexicographic order. Furthermore, here we are interested only in surfaces and so we select only those algebraic varieties of Hilbert dimension 2. In each of our parameter cases, we obtain exactly two varieties of dimension 2.

Our discussion proceeds as follows: we examine the singularities of S' with respect to the first set of parameters, Λ_{wc} , and then give general results on the singularities of S' , illustrated by parameters Λ_{wc} , but which apply to each set of parameters. We then restate the results for the other experimental cases.

Case 1, parameter set Λ_{wc} : water and cerebrospinal fluid.

In this case, the decomposition algorithm results in 18 Gröbner bases with lexicographic ordering $y_1 \succ y_2 \succ z_2 \succ z_1$, two of which correspond to varieties of Hilbert dimension 2. We denote these two parameterized surfaces by ξ_1 and ξ_2 , which are rational expressions in terms of y_2, z_2 .

Lemma 61. *The varieties of Hilbert dimension 2 of the set S' for the set of parameters Λ_{wc} are given by the parameterized surfaces ξ_1 and ξ_2 :*

$$\xi_1 = \begin{cases} y_1 = \frac{2}{5} \frac{r_1(y_2, z_2)}{p_1(y_2, z_2)} \\ z_1 = \frac{r_2(y_2, z_2)}{p_1(y_2, z_2)} \end{cases}$$

and

$$\xi_2 = \begin{cases} y_1 = \frac{12(34z_2+37)(1940y_2^2-219z_2^2-264z_2)y_2}{p_2(y_2, z_2)} \\ z_1 = \frac{5(51z_2^2-340y_2^2+60z_2)(1940y_2^2-219z_2^2-264z_2)}{p_2(y_2, z_2)} \end{cases}$$

where

$$r_1(y_2, z_2) = (2698288382z_2y_2^2 - 5536464613z_2^3 - 20627775843z_2^2 + 3667613456y_2^2 - 25369952652z_2 - 10283489920) y_2,$$

$$r_2(y_2, z_2) = 1182824402z_2^2y_2^2 - 157088262z_2^4 + 1849056680y_2^4 - 616517631z_2^3 + 2940213172z_2y_2^2 - 800838720z_2^2 + 1825508960y_2^2 - 343833600z_2,$$

$$p_1(y_2, z_2) = 5678189924z_2y_2^2 + 2317540708z_2^2y_2^2 + 3345625840y_2^2 - 3143396356y_2^4 - 1780333636z_2^4 \\ - 8924621716z_2^3 - 16679889609z_2^2 - 13773791680z_2 - 4240614400,$$

and

$$p_2(y_2, z_2) = 2890000y_2^4 + 65025z_2^4 + 153000z_2^3 + 90000z_2^2 - 700536z_2^2y_2^2 - 657696z_2y_2^2 + 197136y_2^2.$$

The following lemma shows that these two parameterizations are well-defined on the open Bloch ball.

Lemma 62. *Points of S' such that $p_1(y_2, z_2) = 0$ or $p_2(y_2, z_2) = 0$ are outside the open Bloch ball.*

Proof. We first compute a Gröbner basis of the set $\{D, D', p_1\}$ and see that it is a one-dimensional algebraic variety V_1 . To check the intersection of p_1 with the boundary S_1 , we compute the Gröbner basis of $\{D, D', p_2, s_1\}$, where $s_1 := y_1^2 + (1 + z_1)^2 - 1$ is the polynomial of S_1 , with lexicographic order $y_2 \succ z_2 \succ y_1 \succ z_1$, and there are no real solutions in $B_1 \times B_2$. To check the intersection of p_1 with the boundary S_2 , we likewise compute a Gröbner basis of $\{D, D', p_2, s_2\}$ (with s_2 as the polynomial of S_2) with lexicographic order $y_1 \succ z_1 \succ y_2 \succ z_2$, which has no real roots. Therefore, the components of V_1 do not enter the open Bloch ball.

Carrying out the same process for p_2 , we have that again the basis of $\{D, D', p_2\}$ is a one-dimensional variety, V_2 . The only root when adding the boundary polynomials to the basis is $N = ((0, 0), (0, 0))$, on the boundary of $B_1 \times B_2$. This zero of p_2 is isolated p_2 (p_2 has a constant sign around N). Hence, in this case we again have that the components of V_2 do not enter the open Bloch ball. \square

Singularities of the set S' . We denote the singular set of S' by $\Xi = \{q : D(q) = D'(q) = 0, \nabla D(q) = \nabla D'(q) = 0\}$. To compute it, we consider the ideal generated by the set $\{D, D', M_1, \dots, M_6\}$ where $M_i, i = 1, \dots, 6$, are the minors of the matrix $(\nabla D^T, \nabla D'^T)$. The

Gröbner basis of this ideal with lexicographic order $y_1 \succ y_2 \succ z_2 \succ z_1$ is

$$\begin{aligned}
& \{1600.111z_1 - 9.255z_2 + 4912.951z_1^2z_2^2 + 4388.973z_1^2z_2 + 4837.109z_1z_2 + 5458.334z_1z_2^2 + 21.271z_2^2 \\
& + 1453.444z_1^2 + 25.799z_2^4 + 55.437z_2^3 + 516.255z_2^4z_1 + 443.279z_2^4z_1^2 + 2418.896z_1^2z_2^3 + 2734.898z_1z_2^3, \\
& - 54.539z_1 - 10.864z_2 - 49.655z_1^2 - 151.884z_1z_2 - 10.857z_2^2 - 128.538z_1^2z_2 - 125.275z_1z_2^2 \\
& + 63.918y_2^2 - 1.517z_2^3 - 104.044z_1^2z_2^2 + 100.311y_2^2z_1 - 30.367z_1z_2^3 + 38.440z_1^2y_2^2 - 26.075z_1^2z_2^3, \\
& 457.515z_1 - 29.487z_2 + 1454.211z_1z_2 - 22.619z_2^2 + 1763.023z_1z_2^2 + 153.451y_2^2 \\
& + 9.446z_2^3 + 130.454y_2^2z_1 + 953.381z_1z_2^3 + 6.455z_2^4 + 190.930z_2^4z_1 + 139.545y_2^4, \\
& 9.758y_1 - 9.465y_2 - 7638.245y_2z_1 - 2652.303z_2^2y_2z_1 - 9752.321z_1z_2y_2 \\
& + 2909.641z_2y_2 + 2373.072z_2^2y_2 - 16344.017y_2^3 - 10754.129y_2^3z_1, \\
& 29.209z_1 + 1.169z_2 + 75.610z_1z_2 + 61.202z_1z_2^2 - 22.612y_2^2z_1 \\
& - 7.651y_2^2 - 1.016z_2^2 + 15.402z_2y_2^2 - 1.648z_2^3 + 15.338z_1z_2^3\}
\end{aligned}$$

(exact values truncated).

Computing a Gröbner basis with lexicographic ordering $y_2 \succ z_2 \succ y_1 \succ z_1$, the first polynomial of this basis yields a condition on (y_1, z_1) :

$$\begin{aligned}
p_{\Xi_1} = & 3293877500y_1^6 - 2959733405z_1^5 + 3918731625z_1^7 - 4135314282z_1^4 + 1305015625y_1^8 \\
& + 2459541725z_1^6 + 9047296725y_1^4z_1^2 + 8212960950y_1^2z_1^4 + 11756194875y_1^4z_1^3 \\
& + 11756194875y_1^2z_1^5 + 7830093750y_1^4z_1^4 + 5220062500y_1^2z_1^6 + 3918731625y_1^6z_1 \\
& + 5220062500y_1^6z_1^2 - 1329755152z_1^3 + 7519135700y_1^4z_1 + 4559402295y_1^2z_1^3 \\
& + 6286025680y_1^2z_1^2 + 3474152000y_1^2z_1 + 1305015625z_1^8 - 122100000y_1^4.
\end{aligned}$$

The zero set of this relation is shown in Figure 3.9(a). Likewise, by computing a Gröbner basis with lexicographic order on $y_1 \succ z_1 \succ y_2 \succ z_2$ we obtain a relation on (y_2, z_2) :

$$\begin{aligned}
p_{\Xi_2} = & 50949255z_2^4 - 362042438z_2^2y_2^2 + 263510200y_2^4 + 183816495z_2^3 \\
& - 859505788z_2y_2^2 + 218825640z_2^2 - 491434592y_2^2 + 85958400z_2.
\end{aligned}$$

The zero set of this relation is shown in Figure 3.9(b).

Definition 63. In our coordinates, $O = (0, -1, 0, -1)$ and $N = (0, 0, 0, 0)$. We define the point $\Omega \neq O$ such that $D(\Omega) = D'(\Omega) = 0$ and $\nabla D(\Omega) = 0$, and the point $\Omega' \neq N$ such that $D(\Omega') = D'(\Omega') = 0$ and $\nabla D'(\Omega') = 0$.

Lemma 64. *The set Ξ is a dimension-one algebraic variety, invariant by the involution $(y_1, z_1, y_2, z_2) \mapsto (-y_1, z_1, -y_2, z_2)$. Its intersection with $B_1 \times B_2$ is the union of two connected arcs, Ξ_D and $\Xi_{D'}$.*

Proof. By direct computation, the Hilbert dimension of Ξ variety is 1. Moreover, at O (respectively Ω) the degree of the projection $(y_1, y_2, z_1, z_2) \mapsto (y_2, z_2)$ is 1. So there are two arcs (see Figure 3.9) in \mathbb{R}^4 . Let Ξ_D denote the connected component passing by O and by $\Xi_{D'}$ the connected component whose (y_2, z_2) -projection to is the closed component (see Figure 3.9(b)). Observe that it is not possible to algebraically separate Ξ_D and $\Xi_{D'}$. We denote by Ω_-, Ω_+ the points of Ξ crossing the boundary S_2 (see Figure 3.10). The coordinates of Ω' are $(0, -\frac{1606}{2125}, 0, -\frac{1760}{1241})$, which lies in $B_1 \times B_2$. This is the case for all points of the arc $[\Omega', \Omega_+)$ (respectively $[\Omega', \Omega_-)$). Moving away from O on Ξ_D the coordinates (y_2, z_2) remain in B_2 provided (y_1, z_1) remains in B_1 . Thus $\Xi_D \cap B_1 \times \mathbb{R}^2 \subset B_1 \times B_2$. \square

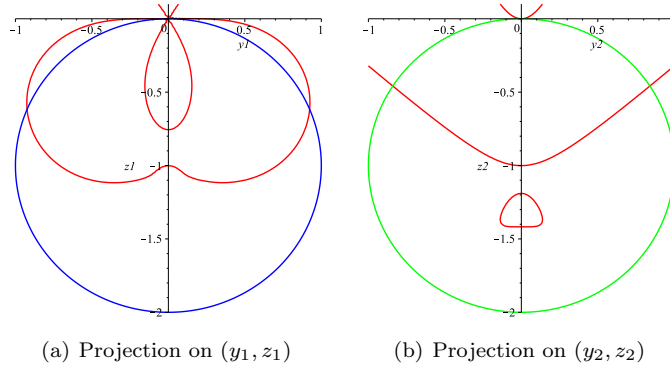


Figure 3.9: Projections of the singular set Ξ of the set S' for parameter set Λ_{wc} , shown in red. The boundary S_1 is shown in blue, and S_2 is shown in green.

General results

As previously noted, the points N and O are such that $D(N) = D'(N) = 0$ and $D(O) = D'(O) = 0$. The singularities of S' of highest complexity are restricted to the plane $y_1 = y_2 = 0$.

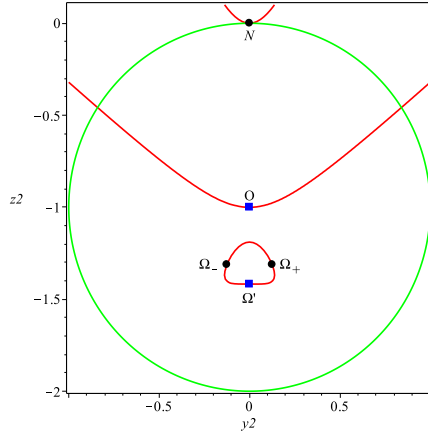


Figure 3.10: Projection on (y_2, z_2) of the singular set Ξ of the set S' for parameter set Λ_{wc} , shown in red, and the points N , Ω_- , and Ω_+ representing the intersection of Ξ and S_1 are shown as a black \circ , as labeled. The boundary S_2 is shown in green. For reference, the points O and Ω' are shown as a blue \square .

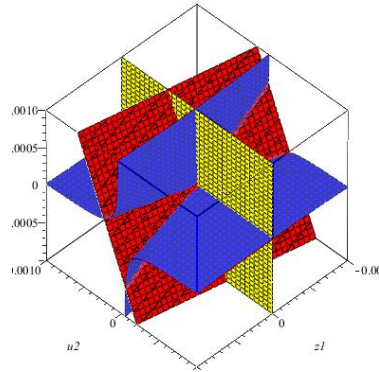


Figure 3.11: Singularity Ω_+ , $D = 0$ in red, $D' = 0$ in blue, S_1 in yellow

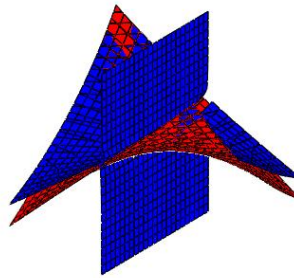


Figure 3.12: Singularity Ω' , projection on $z_2 = -\frac{1760}{1241}$, $D = 0$ in red, $D' = 0$ in blue

Lemma 65. *Assume that*

$$(\Gamma_2 + \delta_1)(\Gamma_1 + \delta_2)(\delta_1 - \delta_2) \neq 0 \quad (3.22)$$

and

$$\begin{aligned} 2\Gamma_1^2 - 2\Gamma_2\Gamma_1 + \gamma_1^2 - \gamma_2\gamma_1 - 3\Gamma_1\gamma_1 + 3\Gamma_2\gamma_1 &\neq 0 \\ \gamma_2\gamma_1 - 2\Gamma_2^2 - 3\gamma_2\Gamma_1 + 3\Gamma_2\gamma_2 + 2\Gamma_2\Gamma_1 - \gamma_2^2 &\neq 0. \end{aligned} \quad (3.23)$$

Then singularities on $y_1 = y_2 = 0$ consist of four points: N , O , Ω , and Ω' , defined by

$$\Omega = \left(\left(0, \frac{\eta_1(\Gamma_2 - \Gamma_1)}{2\Gamma_1^2 - 2\Gamma_2\Gamma_1 + \gamma_1^2 - \gamma_2\gamma_1 - 3\Gamma_1\gamma_1 + 3\Gamma_2\gamma_1} \right), \left(0, \frac{\eta_2(\Gamma_2 - \Gamma_1)}{\gamma_2\gamma_1 - 2\Gamma_2^2 - 3\gamma_2\Gamma_1 + 3\Gamma_2\gamma_2 + 2\Gamma_2\Gamma_1 - \gamma_2^2} \right) \right)$$

and

$$\Omega' = \frac{\Gamma_1 - \Gamma_2}{\delta_2 - \delta_1} \left(\left(0, \frac{\Gamma_1 + \delta_2}{\Gamma_2 + \delta_1} \right), \left(0, \frac{\Gamma_2 + \delta_1}{\Gamma_1 + \delta_2} \right) \right).$$

Moreover, D (and not D') is singular at O and Ω , and D' (and not D) is singular at N and Ω' .

Proof. We consider the system $\mathcal{Z}(D, D', M_1, \dots, M_6)$ where M_i , $i = 1, \dots, 6$, are the minors of the matrix $(\nabla D^T, \nabla D'^T)$, where we substitute $y_1 = y_2 = 0$. We get a system $S_{\text{sing}}^{y_1=y_2=0}$. We factor the polynomials in this system, and construct the set of all the systems corresponding to factors of polynomials in $S_{\text{sing}}^{y_1=y_2=0}$. We then compute a Gröbner basis for each system and cancel redundant bases, resulting in four systems. One is associated to the solution $z_1 = z_2 = 0$, which corresponds to N , at the boundary of the Bloch ball. Provided that (3.22) holds, the second system has a unique solution which corresponds to the point Ω' whose coordinates are given in the statement. The third system has one solution, $z_1 = z_2 = -1$, which corresponds to O . Provided that (3.23) holds, the last system has a unique solution which corresponds to the point Ω whose coordinates are given in the statement. A simple check shows that O and Ω are singular points of $D = 0$ (and not of $D' = 0$), while N and Ω' are singular points of $D' = 0$ (and not of $D = 0$). \square

We have the following local models at these points.

Lemma 66. *At N , D and D' correspond to the local models*

$$D = -(\Gamma_2 - \Gamma_1) [\gamma_1 \eta_2 z_1 - \gamma_2 \eta_1 z_2]$$

$$D' = -(\Gamma_1 - \Gamma_2) \gamma_1 (2\Gamma_2(\Gamma_1 - \gamma_2 + \Gamma_2) - \gamma_2) y_2 z_1 + (\Gamma_1 - \Gamma_2) \gamma_2 (2\Gamma_1(\Gamma_1 - \gamma_1 + \Gamma_2) - \gamma_1) y_1 z_2.$$

Lemma 67. *At O , D and D' correspond to the local models (with $v_i = z_i + 1$):*

$$D = (\gamma_2 v_1 - \gamma_1 v_2) (\gamma_2 v_2 \gamma_1 - 2\gamma_1 v_2 \Gamma_2 - \gamma_1 v_1 \gamma_2 + 2v_1 \gamma_2 \Gamma_1)$$

$$+ (\gamma_2 y_1 - \gamma_1 y_2) (2y_2 \gamma_2 \gamma_1 - y_2 \Gamma_2 \gamma_1 - 2y_1 \gamma_2 \gamma_1 + y_1 \gamma_2 \Gamma_1)$$

$$D' = \gamma_1 \gamma_2 (\gamma_1 y_2 - \gamma_2 y_1) (\eta_1 - \eta_2)$$

For the first set of parameters, projections of the singularity at O are represented in Fig. 3.13.

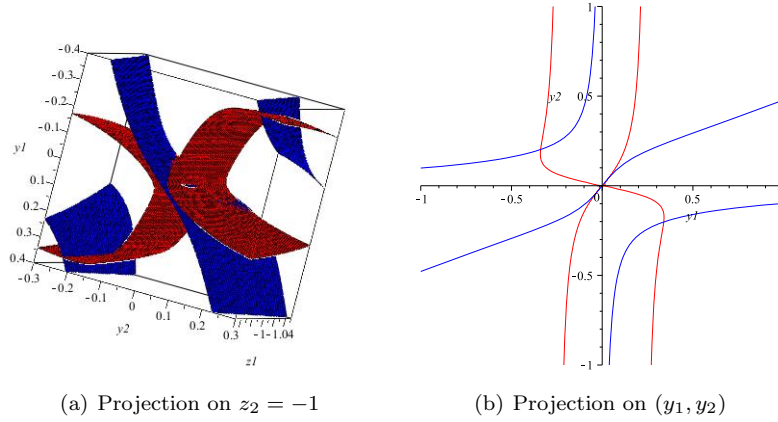


Figure 3.13: Singularity at O for parameter set Λ_{wc} . The set S is in red and $\{q : D'(q) = 0\}$ is in blue.

Lemma 68. *The local models of D and D' at Ω are (with $v_i = z_i - z_i(\Omega)$)*

$$D = dv(v_1, v_2) + dy(y_1, y_2)$$

$$D' = \lambda_y (\alpha_{y_1} y_1 + \alpha_{y_2} y_2)$$

where

$$\begin{aligned}
dv(v_1, v_2) &= \frac{(2\Gamma_1^2 - 2\Gamma_2\Gamma_1 + \gamma_1^2 - \gamma_2\gamma_1 - 3\Gamma_1\gamma_1 + 3\Gamma_2\gamma_1)^2 \eta_2 \gamma_2^2 v_1^2}{(\gamma_2\gamma_1 - 2\Gamma_2^2 - 3\gamma_2\Gamma_1 + 3\Gamma_2\gamma_2 + 2\Gamma_2\Gamma_1 - \gamma_2^2)^2} \\
&\quad + \frac{(\gamma_2\gamma_1 - 2\Gamma_2^2 - 3\gamma_2\Gamma_1 + 3\Gamma_2\gamma_2 + 2\Gamma_2\Gamma_1 - \gamma_2^2)^2 \eta_1 \gamma_1^2 v_2^2}{(2\Gamma_1^2 - 2\Gamma_2\Gamma_1 + \gamma_1^2 - \gamma_2\gamma_1 - 3\Gamma_1\gamma_1 + 3\Gamma_2\gamma_1)^2} \\
&\quad - \gamma_1\gamma_2(\eta_1 - \eta_2)v_2v_1,
\end{aligned}$$

$$\begin{aligned}
dy(y_1, y_2) &= \frac{(3\Gamma_1^2 - 3\Gamma_1\gamma_1 + \gamma_2\Gamma_1 - 3\Gamma_2\Gamma_1 + 2\Gamma_2\gamma_1) \gamma_2^2 \eta_1 \eta_2 (\delta_2 - \delta_1) y_1^2}{(\gamma_2\gamma_1 - 2\Gamma_2^2 - 3\gamma_2\Gamma_1 + 3\Gamma_2\gamma_2 + 2\Gamma_2\Gamma_1 - \gamma_2^2)^2} \\
&\quad - \frac{\eta_1 \eta_2 (\delta_2 - \delta_1) \gamma_2 \gamma_1 (3\Gamma_1^2 - \gamma_2\Gamma_1 - 3\Gamma_1\gamma_1 - 3\Gamma_2^2 + \Gamma_2\gamma_1 + 3\Gamma_2\gamma_2) y_2 y_1}{r} \\
&\quad + \frac{(3\Gamma_2\Gamma_1 - 2\gamma_2\Gamma_1 - 3\Gamma_2^2 + 3\Gamma_2\gamma_2 - \Gamma_2\gamma_1) \gamma_1^2 \eta_1 \eta_2 (\delta_2 - \delta_1) y_2^2}{(2\Gamma_1^2 - 2\Gamma_2\Gamma_1 + \gamma_1^2 - \gamma_2\gamma_1 - 3\Gamma_1\gamma_1 + 3\Gamma_2\gamma_1)^2},
\end{aligned}$$

$$\lambda_y = \frac{\eta_1 \eta_2 (\Gamma_1 - \Gamma_2)^2 (\delta_1 + \delta_2) (\delta_2 - \delta_1) (\gamma_1 - \gamma_2 - 2\Gamma_1 + 2\Gamma_2) \gamma_1 \gamma_2}{r^2},$$

$$r = (2\Gamma_1^2 - 2\Gamma_2\Gamma_1 + \gamma_1^2 - \gamma_2\gamma_1 - 3\Gamma_1\gamma_1 + 3\Gamma_2\gamma_1) (\gamma_2\gamma_1 - 2\Gamma_2^2 - 3\gamma_2\Gamma_1 + 3\Gamma_2\gamma_2 + 2\Gamma_2\Gamma_1 - \gamma_2^2),$$

$$\alpha_{y_1} = \gamma_2 (2\Gamma_1^2 - 2\Gamma_2\Gamma_1 + \gamma_1^2 - \gamma_2\gamma_1 - 3\Gamma_1\gamma_1 + 3\Gamma_2\gamma_1),$$

and

$$\alpha_{y_2} = \gamma_1 (2\Gamma_2^2 - 2\Gamma_1\Gamma_2 + \gamma_2^2 - \gamma_1\gamma_2 - 3\Gamma_2\gamma_2 + 3\Gamma_1\gamma_2).$$

Lemma 69. *The local models of D and D' at Ω' are, with $v_i = z_i - z_i(\Omega')$,*

$$\begin{aligned}
D &= \frac{(\Gamma_2 - \Gamma_1)(\delta_1 + \delta_2)(\eta_1 - \eta_2)^2 \gamma_1 \gamma_2}{(\Gamma_1 + \delta_2)^2 (\delta_2 - \delta_1)^2 (\delta_1 + \Gamma_2)^2} [\gamma_2 v_1 (\delta_1 + \Gamma_2)^2 - \gamma_1 v_2 (\Gamma_1 + \delta_2)^2] \\
D' &= (\Gamma_1 - \Gamma_2) \left[\frac{2\eta_1 \delta_1 \gamma_2^2 (\delta_1 + \Gamma_2)^2 v_1}{(\delta_2 - \delta_1) (\Gamma_1 + \delta_2)^2} + \frac{\gamma_2 \gamma_1 (\delta_1 - \Gamma_2) (\delta_1 + \delta_2) v_2}{\delta_2 - \delta_1} \right] y_1 \\
&\quad + (\Gamma_1 - \Gamma_2) \left[\frac{\gamma_2 \gamma_1 (\delta_2 - \Gamma_1) (\delta_1 + \delta_2) v_1}{\delta_2 - \delta_1} - \frac{2\eta_2 (\Gamma_2 - \gamma_2) (\Gamma_1 + \delta_2)^2 \gamma_1^2 v_2}{(\delta_1 + \Gamma_2)^2 (\delta_2 - \delta_1)} \right] y_2.
\end{aligned}$$

Remark 70. In these results for general sets of parameter values, we have defined the points N , O , Ω , and Ω' , and given local models at each of these points. So in particular the general discussion is lacking the parameterizations ξ_1 and ξ_2 and the characterization of Ξ that were given in the study of parameter set Λ_{wc} . Thus these remain to be determined for the other parameter sets.

Case 2, parameter set Λ_{do} : deoxygenated blood and oxygenated blood.

As in the previous case, we compute two Hilbert dimension 2 components, giving two ideals. One corresponds to a parameterized (rational parameterization) surface. The other one is hybrid: we have a rational parameterization of y_2 and z_2 is a root of a degree-3 polynomial. The parameters are (y_1, z_1) .

The first solution is

$$\xi_1 = \begin{cases} y_2 = 4 \frac{y_1(52z_1+53)(3537y_1^2-77z_1^2-81z_1)}{p_1(y_1, z_1)} \\ z_2 = \frac{(77z_1^2-3537y_1^2+81z_1)(2187y_1^2-127z_1^2-131z_1)}{p_1(y_1, z_1)} \end{cases}$$

where

$$p_1(y_1, z_1) = 303372y_1^2 - 320598y_1^2z_1^2 - 39798y_1^2z_1 + 7499223y_1^4 + 10287z_1^4 + 21406z_1^3 + 11135z_1^2.$$

The second solution, which is implicit, is

$$\xi_2 = \begin{cases} y_2 = \frac{y_1(713z_2+675)(534924z_1z_2+524524z_1+572135z_2+562383)}{p_2(z_1, z_2)} \\ p_3(z_2, y_1, z_1) = 0 \end{cases}$$

where

$$p_2(z_1, z_2) = 379608525 + 709928281z_1z_2 - 38329362y_1^2z_2 + 343071450z_1^2z_2 \\ + 734492475z_1 - 42974550y_1^2 + 354488750z_1^2 + 366486255z_2$$

and

$$\begin{aligned}
p_3(z_2, y_1, z_1) = & (1.990 + 5.865z_1^3 + 9.774z_1^2 + 7.213z_1 + 3.576y_1^2 \\
& + 2.630y_1^2z_1^2 + 1.315z_1^4 + 1.315y_1^4 + 6.145y_1^2z_1)z_2^3 \\
& + (4.122 + 7.774y_1^2 + 18.880z_1^2 + 14.465z_1 + 5.220y_1^2z_1^2 \\
& + 12.815y_1^2z_1 + 10.849z_1^3 + 4.174y_1^4 + 2.312z_1^4)z_2^2 \\
& + (2.135 + 5.010y_1^2 + 3.624z_1^3 + 2.728y_1^2z_1^2 + 7.563y_1^2z_1 \\
& + 7.681z_1^2 + 0.565z_1^4 + 6.757z_1 + 4.398y_1^4)z_2 \\
& - 0.504z_1 + 0.900y_1^2z_1 - 1.368z_1^3 + 1.539y_1^4 \\
& + 0.816y_1^2 - 1.438z_1^2 + 0.141y_1^2z_1^2 - 0.433z_1^4
\end{aligned}$$

(exact values truncated).

We now state a lemma analogous to Lemma 62 for this parameter set, but with a different outcome: in this case the parameterization is not necessarily well-defined everywhere on the interior of the Bloch ball.

Lemma 71. *The parameterizations ξ_1 and ξ_2 are well-defined on the Bloch ball outside of a dimension-two component.*

Proof. It can be calculated that $p_1(y_1, z_1) = 0$ has a dimension one component, call it α in the interior of B_1 , shown in Figure 3.14(a).

Similarly, there exists a dimension two component of $p_2(y_1, z_1, z_2) = 0$, call it β , which contains points in the interior of B . It is shown for $z_2 = -1$ in Figure 3.14(b).

Therefore points outside of the union of α and β , are such that the parameterizations ξ_1 and ξ_2 are well-defined. \square

The singularities of the set S' are shown in Figure 3.15. As in the previous case we can find the projection of Ξ onto the planes (y_1, z_1) and (y_2, z_2) by taking the first polynomial in a Gröbner basis computed with lexicographic ordering $y_2 \succ z_2 \succ y_1 \succ z_1$ and $y_1 \succ z_1 \succ y_2 \succ z_2$, respectively, giving

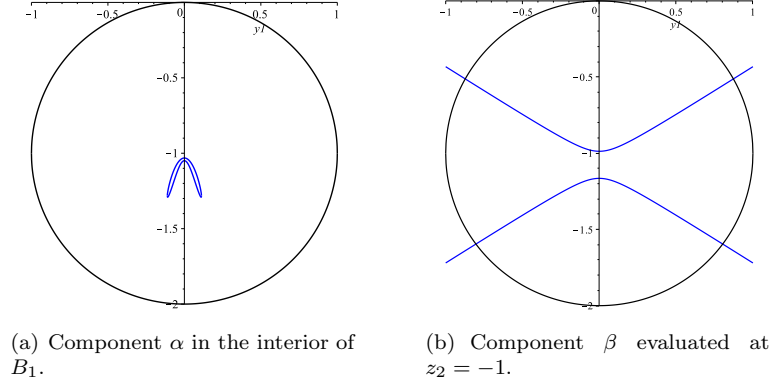


Figure 3.14: Components of $p_1(y_1, z_1) = 0$ and $p_2(y_1, z_1, z_2) = 0$ in the interior of the Bloch ball (see Lemma 71).

p_{Ξ_1} and p_{Ξ_2} , which are

$$\begin{aligned}
p_{\Xi_1} = & 63338583z_1^8 + 18859556388y_1^2z_1^6 - 489162865670y_1^4z_1^4 - 1571527612476y_1^6z_1^2 \\
& + 1514530578375y_1^8 + 329747245z_1^7 + 100848610981y_1^2z_1^5 - 2135046331105y_1^4z_1^3 \\
& - 3161644898481y_1^6z_1 + 686495038z_1^6 + 215677279156y_1^2z_1^4 - 3486867163282y_1^4z_1^2 \\
& - 1585737098064y_1^6 + 714412722z_1^5 + 230575302603y_1^2z_1^3 - 2525538658241y_1^4z_1 \\
& + 371636651z_1^4 + 123215976114y_1^2z_1^2 - 684551333700y_1^4 + 77310305z_1^3 + 26328897450y_1^2z_1
\end{aligned}$$

and

$$\begin{aligned}
p_{\Xi_2} = & -3685153920z_2^8 + 1199340926688y_2^2z_2^6 - 5355374141192y_2^4z_2^4 \\
& - 1293574040982y_2^6z_2^2 + 2689478841123y_2^8 - 19013001344z_2^7 \\
& + 6262846071232y_2^2z_2^5 - 24321413612872y_2^4z_2^3 - 3700202945904y_2^6z_2 \\
& - 39160425728z_2^6 + 13090933982464y_2^2z_2^4 - 41163229421176y_2^4z_2^2 \\
& - 2372013535050y_2^6 - 40250999040z_2^5 + 13690278319680y_2^2z_2^3 \\
& - 30820082607800y_2^4z_2 - 20646891136z_2^4 + 7162536314400y_2^2z_2^2 \\
& - 8623206000000y_2^4 - 4228470400z_2^3 + 1499688000000y_2^2z_2.
\end{aligned}$$

The full Gröbner basis with ordering $y_2 \succ z_2 \succ y_1 \succ z_1$ contains nine polynomials, the first being p_{Ξ_1} . The following four are in variables y_1, z_1 , and z_2 , and the final four are in variables y_1, z_1, y_2 ,

and z_2 .

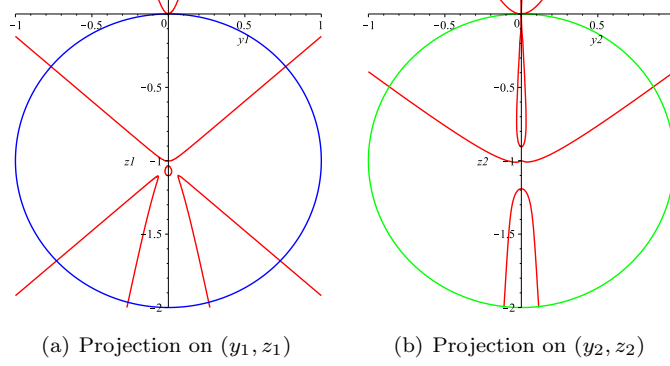


Figure 3.15: Projections of the singular set Ξ of the set S' for parameter set Λ_{do} in the y_2z_2 -plane, shown in red. The boundary S_1 is shown in blue, and S_2 is shown in green.

Case 3, parameter set Λ_{gw} : gray and white cerebral matter.

As in the previous case, we arrive at two solutions, one of which is implicit. The first solution is

$$\xi_1 = \begin{cases} y_2 = \frac{8970y_1(82z_1+87)(455z_1^2+230z_1+38134y_1^2)}{p_1(y_1, z_1)} \\ z_2 = \frac{13(455z_1^2+230z_1+38134y_1^2)(22678y_1^2+50435z_1^2+53360z_1)}{p_1(y_1, z_1)} \end{cases}$$

where

$$p_1(y_1, z_1) = 4286726660y_1^2z_1^2 + 34123906760y_1^2z_1 + 31231207800y_1^2 \\ - 10522637356y_1^4 - 124322275z_1^4 - 108332300z_1^3 + 24545600z_1^2.$$

The second solution is

$$\xi_2 = \begin{cases} y_2 = \frac{2y_1(667z_2+637)(203888531z_2z_1+522716831z_1-40368174z_2+280342101)}{p_2(y_1, z_1, z_2)} \\ p_3(y_1, z_1, z_2) = 0 \end{cases}$$

where

$$p_2(y_1, z_1, z_2) = 353676077664 + 690546205349z_1^2 - 2082719912y_1^2 + 1030622173763z_1 \\ - 1830023888y_1^2z_2 + 205381056542z_2z_1 + 270157276466z_2z_1^2 - 51080375424z_2$$

and

$$\begin{aligned}
p_3(y_1, z_1, z_2) = & (6.021 - 54.338z_1 - 52.613y_1^2 + 9.887z_1^4 + 166.860z_1^3 \\
& + 87.422z_1^2 + 257.076y_1^2z_1 + 9.887y_1^4 + 19.775y_1^2z_1^2)z_2^3 \\
& + (168.582z_1 - 83.381 + 1010.042y_1^2z_1 + 320.758y_1^2 \\
& - 165.409y_1^2z_1^2 - 100.859z_1^4 + 1130.203z_1^2 + 804.825z_1^3 + 31.942y_1^4)z_2^2 \\
& + (288.661 + 34.284y_1^4 + 2052.742z_1^2 - 709.422z_1^4 + 1476.879z_1 \\
& + 407.119y_1^2z_1 - 794.008y_1^2z_1^2 + 361.409y_1^2 + 182.419z_1^3)z_2 \\
& - 270.966z_1 - 2005.471z_1^3 - 989.240z_1^4 + 7.366y_1^2 \\
& - 1296.260z_1^2 - 589.567y_1^2z_1^2 + 12.221y_1^4 - 307.260y_1^2z_1
\end{aligned}$$

(exact values truncated).

We now state a lemma similar to Lemma 71 for this parameter set, with a qualitatively similar result.

Lemma 72. *The parameterizations ξ_1 and ξ_2 are well-defined on the Bloch ball outside of a dimension-two component.*

Proof. As in the previous parameter case, there exists a dimension one component of $p_1(y_1, z_1) = 0$ in the interior of B_1 , let us again denote it α , shown in Figure 3.16(a).

Similarly, there is a dimension two component β of $p_2(y_1, z_1, z_2) = 0$ which contains points in the interior of B , β is shown for $z_2 = -1$ in Figure 3.16(b).

Therefore points outside of the union of α and β , are such that the parameterizations ξ_1 and ξ_2 are well-defined. \square

Although we have shown that the parameterizations ξ_1 and ξ_2 are not well-defined everywhere on B , they are well-defined off of the components α and β as identified here.

The singularities of the set S' are shown in Figure 3.17. Note that in this case the relatively small difference between the pairs of physical parameters yields figures that are very similar visually, but are not identical.

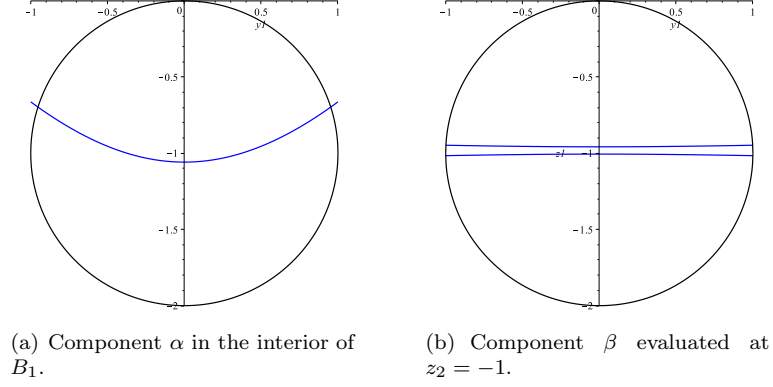


Figure 3.16: Components of $p_1(y_1, z_1) = 0$ and $p_2(y_1, z_1, z_2) = 0$ in the interior of the Bloch ball (see Lemma 72).

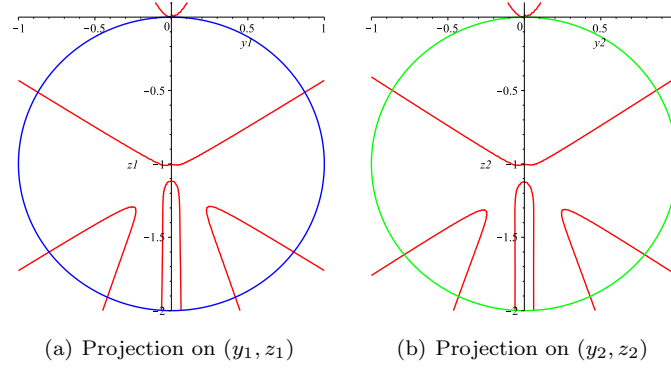


Figure 3.17: Projections of the singular set Ξ of the set S' for parameter set Λ_{gw} , shown in red. The boundary S_1 is shown in blue, and S_2 is shown in green.

Case 4, parameter set Λ_{wf} : water and fat tissue.

As in the previous cases, we compute two Hilbert dimension 2 components, giving solutions ξ_1 and ξ_2 ,

$$\xi_1 = \begin{cases} y_1 = \frac{2(3+2z_2)(23z_2^2+48z_2-54y_2^2)y_2}{2484z_2^2y_2^2+4952z_2y_2^2-2500y_2^4-36y_2^2-625z_2^4-2500z_2^3-2500z_2^2} \\ z_1 = \frac{25(23z_2^2+48z_2-54y_2^2)(z_2^2+2z_2-2y_2^2)}{2484z_2^2y_2^2+4952z_2y_2^2-2500y_2^4-36y_2^2-625z_2^4-2500z_2^3-2500z_2^2} \end{cases}$$

and

$$\xi_2 = \begin{cases} y_2 = \frac{50y_1(25y_1^2+25z_1^2+24z_1)}{1250y_1^2-625y_1^4-1250y_1^2z_1^2-1250y_1^2z_1-625z_1^4-1250z_1^3-621z_1^2} \\ z_2 = \frac{2(25y_1^2+25z_1^2+27z_1)(25y_1^2+25z_1^2+24z_1)}{1250y_1^2-625y_1^4-1250y_1^2z_1^2-1250y_1^2z_1-625z_1^4-1250z_1^3-621z_1^2} \end{cases}.$$

The following lemma shows that these two parameterizations are well-defined on the open Bloch ball.

Lemma 73. *Let p_1 be the denominator in the parameterization ξ_1 , and p_2 be the denominator in ξ_2 . Points of S' such that $p_1(y_2, z_2) = 0$ or $p_2(y_2, z_2) = 0$ are outside the open Bloch ball.*

Proof. We follow the same reasoning as the proof of Lemma 62. For p_1 , the basis of $\{D, D', p_1\}$ is a one-dimensional variety V_1 . When separately adding the boundary polynomials of S_1 and S_2 to the basis, we find no solutions in the Bloch ball.

Next, for p_2 we again see that the basis of $\{D, D', p_2\}$ is a one-dimensional variety V_2 . Separately adding the boundary polynomials of S_1 and S_2 to the basis, we have only the solution $((0, 0), (0, 0))$ in the closed Bloch ball. This zero of p_2 lies on the line $z_2 = 0$ of zeroes of p_2 , so this component is tangent to the Bloch ball. Therefore the components of V_2 do not enter the open Bloch ball. \square

The singularities of the set S' are shown in Figure 3.18.

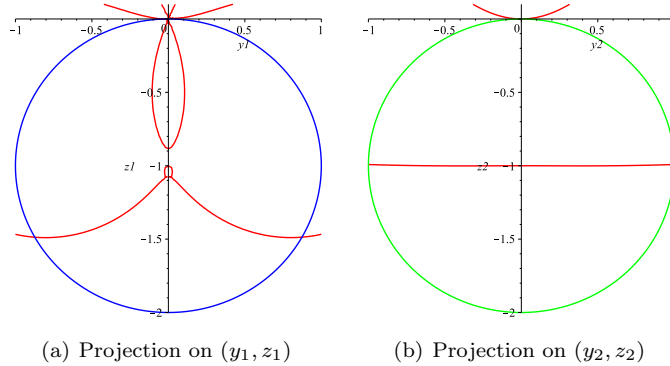


Figure 3.18: Projections of the singular set Ξ of the set S' for parameter set Λ_{wf} , shown in red. The boundary S_1 is shown in blue, and S_2 is shown in green.

3.6 Classification

As a conclusion we present in Figure 3.19 partial results about the phase portrait of the vector field X_r^e . Those results are valid only for the quadratic approximation near the north pole and the origin. A first step in the analysis of the equilibrium points of X_r^e is presented in §3.5 where we analyze the problem of parameterizing this set using Gröbner basis. Additional feedback invariants related to optimality properties of the singular arcs are described in §3.3. Connected work is ongoing on the analysis of the singular flow in the bi-input case where both the amplitude and the phase of the radio-frequency field are controlled.

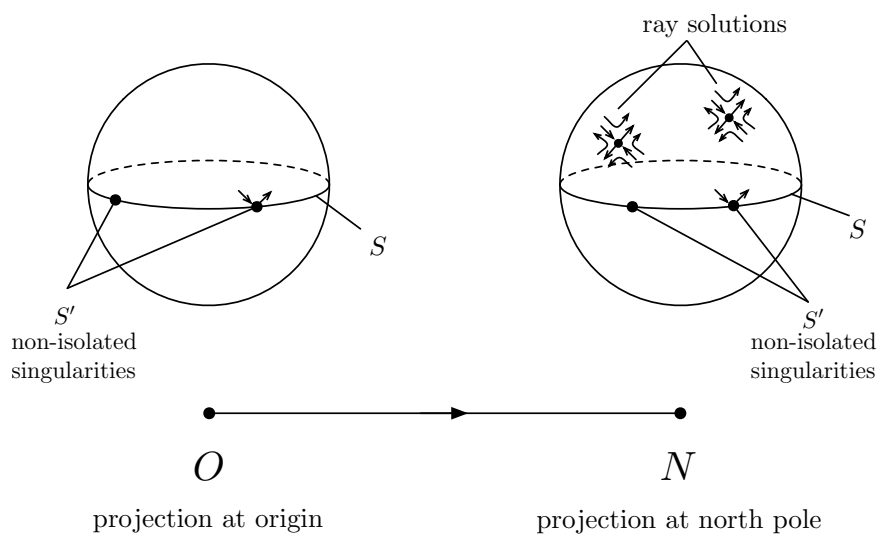


Figure 3.19: Partial phase portrait of the vector field X_r^e .

CHAPTER 4

CONCLUSION

In this work we have primarily dealt with the single-input contrast problem by saturation, in particular studying the exceptional case of the singular dynamics.

In Chapter 2, we identified geometric properties and optimality conditions of the problem, giving an overview of the methods used in the analysis of a problem of this type, and preliminary results on the structure of optimal solutions.

In Chapter 3 we saw a detailed study of the exceptional case: properties of the flow of the dynamics, the calculation of a set of feedback invariants, and an algebraic-geometric classification of the singularities of the sets S and S' . In general, identifying equilibria of nonlinear system is nontrivial, and this classification was completed for the four cases of physical parameters.

Future work on the contrast problem can proceed in several directions.

- The bi-input case, where singular extremals are as described in §2.3.2. It is a natural conjecture that improved contrast can be achieved in this more general case, but even numerical simulations become more complex.
- The contrast problem, not necessarily by saturation, can be examined with similar tools, although without the convenient boundary conditions of saturation. For numerical work on this case, extremals of the contrast problem by saturation can be used to initialize the optimization schemes. Notably, the exceptional singular extremals are extremals of such a system.
- The classification of the singular extremals in the general (not necessarily exceptional) case.
- As mentioned in §3.1, the overall imaging process consists of capturing the image several times for noise reduction, and this is heuristically reset by letting the uncontrolled system relax to equilibrium. In this case, the return trip is significantly longer in duration than the forward, contrast-producing trip. Thus, an interesting question is the time-minimal transfer from an arbitrary point to the north pole (or some other steady state, i.e. a point in the collinear set, §2.1.3). In the single-spin case, much of the analysis given in §2.2 can be employed and the optimal control synthesis is straightforward. In the two-spin, single-input case the analysis is more complex.

APPENDIX A PHYSICAL MODEL

The following description aims to briefly give an explanation of the physical model employed, enough to convey the basic idea of how the system behaves under no external influence, and how it can be controlled. Full details of this model are given in standard texts on NMR [26, 41].

The nucleus of an atom has two related properties which enable NMR techniques: magnetism and spin. A nucleus' magnetism interacts with magnetic fields, yet is weak and has negligible effect on the atom. The nuclear spin is an intangible quality which also has negligible effect on the atom. NMR techniques are used to manipulate and observe these qualities to yield information about a molecule's structure, motion, and chemical reactions without essentially altering these properties.

The model describes the time evolution of the net magnetic moment of a sampled substance under two magnetic fields. First let us understand the behavior of the magnetization of single nucleus in a single magnetic field.

The *magnetic moment* of a nucleus is represented by a vector $\mu = (\mu_x, \mu_y, \mu_z)^T \in \mathbb{R}^3$. This is collinear with the spin polarization of the nucleus, so although the model is of the magnetic moment, we refer to the spin interchangeably. Under the influence of a sufficiently strong magnetic field $\mathcal{B} \in \mathbb{R}^3$, the direction of which we set to be the z -axis of the coordinate system, the energy of the nucleus is $-\langle \mu, \mathcal{B} \rangle$. The magnetic field causes *precession*, which is the rotation of μ around the magnetic field at a constant angle which depends only on the initial spin polarization, forming the *cone precession* illustrated in Figure A.1. The frequency of this precession (called the Larmor frequency) is proportional to the strength of the field \mathcal{B} and the gyromagnetic ratio of the nucleus. In NMR, this frequency is on the order of megahertz.

Additionally, small fluctuating fields from the thermal environment cause perturbations in the cone precession, so that μ “wanders” about. This wandering is not random—it is biased toward a state of lower energy, and since this is $-\langle \mu, \mathcal{B} \rangle$, this means that μ tends to alignment with \mathcal{B} .

The net magnetic moment, $M = (M_x, M_y, M_z)^T$, is the sum of the magnetic moments in a sample. The net magnetization undergoes precession, and due to the “wandering” of individual moments, the net moment experiences *longitudinal relaxation* to alignment with \mathcal{B} . Additionally, the individual moments experience dephasing relative to each other such that the next xy -component of M decays with no net energy loss, called *transverse relaxation*. For protons in human tissue, the

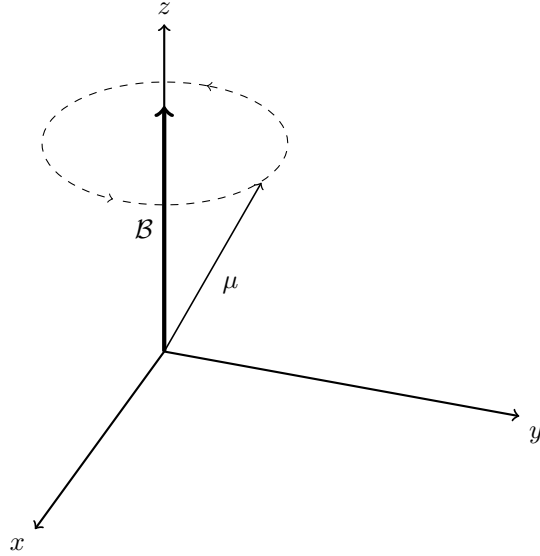


Figure A.1: Cone precession of a nuclear magnetic moment μ about a magnetic field \mathcal{B} .

time scale of relaxation is on the order of seconds. The initial value of M , under no influence of a magnetic field, is zero (it is the sum of randomly aligned vectors). Upon exposure to an external magnetic field, the net magnetization is initially zero then aligns with and grows along the z -axis due to relaxation. The units of M are normalized so that the thermal equilibrium is $M_{\text{eq}} = (0, 0, 1)^T$.

Now let us examine the behavior of the net magnetization in the case of an NMR experiment. There are two orthogonal magnetic fields: \mathcal{B}_0 , a strong, constant, and persistent field along the z -axis, and $\mathcal{B}_1(t)$, a weaker, time-varying, and temporarily-activated field lying in the xy -plane. Thus M will experience precession and relaxation with respect to the magnetic field $\mathcal{B}_0 + \mathcal{B}_1(t)$. Since M will always precess about \mathcal{B}_0 , we use a *rotating frame* for the coordinate system. We will assume that this frame rotates about the z -axis at the same frequency as the precession about \mathcal{B}_0 (i.e., the *resonance offset* is zero), so that the precession in this frame is stationary. Therefore only precession about \mathcal{B}_1 , when it is active, is accounted for in the model. Secondly, since \mathcal{B}_1 is weaker than \mathcal{B}_0 and the effects of relaxation are already minor compared to precession, we neglect relaxation with respect to \mathcal{B}_1 , and only model relaxation to alignment with \mathcal{B}_0 .

Therefore our physical model of the net magnetization accounts for two behaviors: rotation due to $\mathcal{B}_1(t)$ and relaxation to the equilibrium $(0, 0, 1)$ due to \mathcal{B}_0 . This is described by the *Bloch equation*,

which we will use for our mathematical model of the physical system:

$$\begin{cases} \frac{dM_x}{dt} = \omega_y M_z - M_x/T_2 \\ \frac{dM_y}{dt} = -\omega_x M_z - M_y/T_2 \\ \frac{dM_z}{dt} = -\omega_y M_x + \omega_x M_y - (M_z - 1)/T_1 \end{cases}$$

where $\omega_x = \omega \sin \phi$, $\omega_y = \omega \cos \phi$, and ω and ϕ are respectively the magnitude and angle in the $M_x M_y$ -plane of $\mathcal{B}_1(t)$. The magnitude is bounded by $|\omega| \leq \omega_{\max}$.

We will now abandon the usual notation for magnetization vector and relaxation times in favor of the coordinates $(x, y, z)^T = (M_x, M_y, M_z)^T$, parameters $\gamma = 2\pi/(T_1 \cdot \omega_{\max})$ and $\Gamma = 2\pi/(T_2 \cdot \omega_{\max})$, and $u = (u_1, u_2)$, $u = \omega/\omega_{\max}$. We view u as the *control* since it is the means of influencing the system in NMR. Then the Bloch equation is

$$\dot{q} = f(q, u, \gamma, \Gamma) = \begin{cases} \dot{x} = -\Gamma x + u_2 z \\ \dot{y} = -\Gamma y - u_1 z \\ \dot{z} = \gamma(1 - z) + u_1 y - u_2 x. \end{cases} \quad (\text{A.1})$$

As noted in the introduction (Remark 1), the parameters γ and Γ of a substance are subject to the physical constraint $2\Gamma \geq \gamma \geq 0$ [51]. With this constraint, the Bloch ball $|q| \leq 1$ is invariant for the dynamics. We additionally assume that $\gamma > 0$ (corresponding to finite relaxation times).

The system (A.1) is control-affine, i.e., it be split into *drift* and *control* vector fields as

$$\begin{aligned} \dot{q} &= F_0(q) + u_1 F_1(q) + u_2 F_2(q) \\ &= \begin{pmatrix} -\Gamma x \\ -\Gamma y \\ \gamma(1 - z) \end{pmatrix} + u_1 \begin{pmatrix} 0 \\ -z \\ y \end{pmatrix} + u_2 \begin{pmatrix} z \\ 0 \\ -x \end{pmatrix}. \end{aligned} \quad (\text{A.2})$$

The qualitative behavior of these vector fields is illustrated in Figure A.2, and its projection on the yz -plane for various strengths of the control u_1 is shown in Figure A.3.

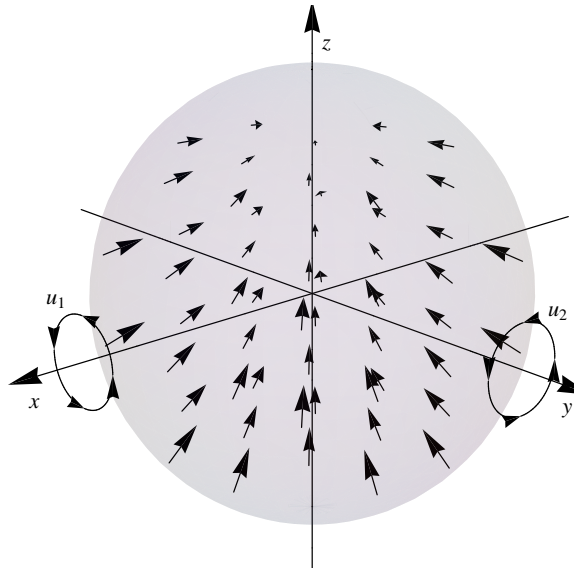


Figure A.2: Behavior of the components of the Bloch equation (A.2). The drift vector field F_0 is shown in the ball, and the rotation produced by the controls u_1 and u_2 about the y - and x -axes, respectively, is shown about the axes.

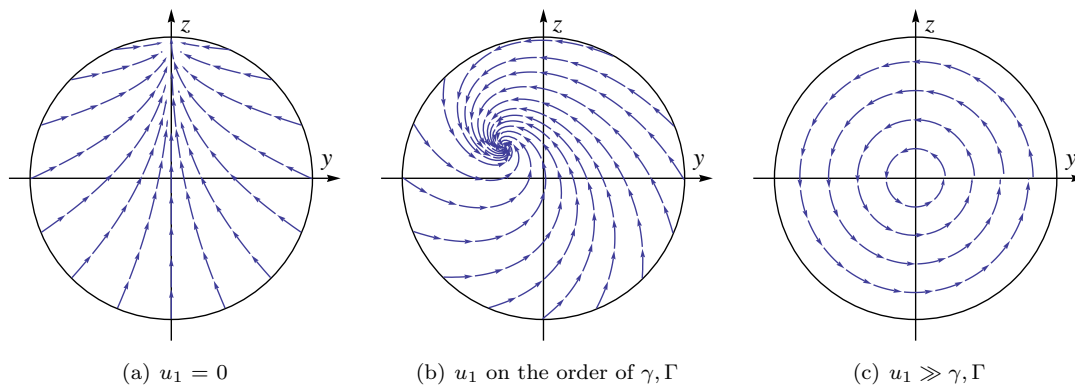


Figure A.3: Behavior of Bloch equation (A.1) in the yz -plane for various values of u_1 , with $u_2 \equiv 0$.

APPENDIX B

OPTIMAL CONTROL THEORY

Optimal control theory is an area of applied mathematics that was born out of application to physical problems, namely rocket guidance, in the 1950s and has since developed into a mature field with a rich framework. Although the subject has a fairly recent development, it traces a classical lineage. We will review a concise history from the calculus of variations to optimal control, and introduce optimal control theory. This material is well-established and covered in introductory texts [42, 50].

B.1 Calculus of variations

Optimal control theory traces its origin to the calculus of variations, an area which arose from the brachystochrone problem posed by Johann Bernoulli in the *Acta Eruditorum*, 1696:

Datis in plano verticali duobus punctis A & B, assignare Mobili M viam AMB, per quam gravitate sua descendens, & moveri incipiens a puncto A, brevissimo tempore perveniat ad alterum punctum B.

Paraphrased in English, this is to find the path AMB down which a movable point M must, by virtue of its weight, fall from A to B in the shortest possible time. This was accompanied with a flourishing challenge, and it attracted the responses of great mathematicians of the day: Jacob Bernoulli, l'Hôpital, Leibniz, Newton, and Tschirnhaus. This problem was a turning point since a geometric solution was not clear, and new techniques needed to be used. With the recently-developed tools of calculus, this problem was solved and its method of solution led to the development of the calculus of variations.¹ The brachystochrone problem is an example of the so-called “simplest problem” in calculus of variations, which we now state.

Problem 74 (Simplest problem in the calculus of variations). *Given $L \in \mathcal{C}^2(\mathbb{R}^{2n+1}, \mathbb{R})$ and $x_0, x_f \in \mathbb{R}^n$, minimize*

$$J(x) = \int_{t_0}^{t_f} L(t, x(t), \dot{x}(t)) dt$$

among all $x \in \mathcal{C}^1([t_0, t_f], \mathbb{R}^n)$ with $x(t_0) = x_0$ and $x(t_f) = x_f$.

¹The brachystochrone and other problems that are now seen as calculus of variations problems were considered even by the ancient Greeks, but were not solved in this framework (if at all). We take the viewpoint that calculus of variations was born when these problems were solved in this manner.

If the state $x \in \mathbb{R}^2$, this is briefly stated as finding a plane curve $x(\cdot)$ from a point x_0 to a point x_f which is optimal in the sense that it minimizes J . Generalizations can be made, and in particular we will see two of these: first, if $x(t_f)$ lies on a curve and second, if the cost contains a non-integral term.

Seeded by the brachystochrone problem, other problems and generalizations were studied and the calculus of variations saw development over the next few hundred years, and the sum of these developments very nearly brings us to optimal control theory. We list those relevant results with historical context here. For a more complete historical perspective, an excellent overview is given by Sussmann and Willems [54], and a complete picture is treated in introductory texts [42, 50].

Recall from finite-dimensional optimization that if x^* is a local minimum of a function $f : \mathbb{R}^n \rightarrow \mathbb{R}$ (assume that x^* is in the interior of the domain of f), we have several conditions for optimality. A first-order necessary condition for optimality is that $\nabla f(x^*) = 0$. A second-order necessary condition is that the Hessian matrix of f is positive semidefinite, i.e., $\nabla^2 f(x^*) \geq 0$. The second-order condition can be strengthened, giving the second-order sufficient condition for optimality, that if $\nabla f(x^*) = 0$ and $\nabla^2 f(x^*) > 0$ then x^* is a strict local minimum of f . Generalizing these concepts to the infinite-dimensional optimization of calculus of variations are the notions of the first and second variations of J .

A norm is needed in order to determine a local minimum $x(\cdot)$ of J . We will consider two norms: for $x \in C^0([t_0, t_f], \mathbb{R}^n)$, the 0-norm is $\|x\|_0 = \max_{t \in [t_0, t_f]} |x(t)|$ and for $x \in C^1([t_0, t_f], \mathbb{R}^n)$, the 1-norm is $\|x\|_1 = \max_{t \in [t_0, t_f]} |x(t)| + \max_{t \in [t_0, t_f]} |\dot{x}(t)|$. An extremum with respect to the 0-norm is called a *strong extremum*, and extremum with respect to the 1-norm is called a *weak extremum*. These are so-called since if x is a strong extremum it is necessarily a weak extremum (an ε -ball with respect to the 1-norm is contained in an ε -ball with respect to the 0-norm).

(CV 1) A first-order necessary condition for a weak extremum is found by calculating the first variation of J and setting it equal to zero. This is captured by the *Euler–Lagrange equation*. If $x(\cdot)$ is a local minimum then the Euler–Lagrange equation,

$$\frac{d}{dt} \frac{\partial L}{\partial \dot{x}}(t, x(t), \dot{x}(t)) = \frac{\partial L}{\partial x}(t, x(t), \dot{x}(t)), \quad (\text{B.1})$$

is satisfied for all $t \in [t_0, t_f]$. Solutions to (B.1) are candidates as local extrema, and are called *extremals*.

This relation was found by Euler in 1740, and the proof was improved upon by Lagrange in 1755.

- (CV 2) In the case of a variable endpoint, an additional first-order necessary condition for a weak extremum is the *transversality condition*. If the final condition is, instead of $x(t_f) = x_f$, that $(t_f, x(t_f))$ satisfies $\psi(t_f, x(t_f)) = 0$ where $\psi \in \mathcal{C}^1$, then

$$0 = \left[L \frac{\partial \psi}{\partial x} - \frac{\partial \psi}{\partial \dot{x}} \left(\frac{d\psi}{dt} + \frac{dL}{dt} \frac{\partial \psi}{\partial x} \right) \right] \Bigg|_{(t_f, x(t_f), \dot{x}(t_f))}$$

the transversality condition, must be satisfied.

- (CV 3) A second-order necessary condition for a weak minimum is found by computing the second variation and requiring that it is non-negative along a local minimum $x(\cdot)$, resulting in the *Legendre condition*. If $x(\cdot)$ is a local minimum then it satisfies the Legendre condition: $\frac{\partial^2 L}{\partial \dot{x}^2}(t, x(t), \dot{x}(t)) \geq 0$ for all $t \in [t_0, t_f]$. If this quantity is strictly positive, then $x(\cdot)$ satisfies the *strong Legendre condition*.

Legendre gave this in 1786, and incorrectly thought that the strong version was a sufficient condition. In 1797 Lagrange found a flaw with this assumption, and in 1837 Jacobi rectified the situation with the missing piece: the conjugate point condition, introduced next.

For a calculus of variations problem with a more general cost of the form $J = \int_{t_0}^{t_f} L(t, x(t), \dot{x}(t)) dt + \varphi(t_f, x(t_f))$, the analog to Legendre condition was given by Clebsch in 1858 [19].

- (CV 4) The strong Legendre condition is pointwise, and so this is a local condition. It is possible to construct counterexamples of an extremal $x(\cdot)$ that satisfies this local condition everywhere, yet is not optimal, therefore in addition to the strong Legendre condition, some global aspect of the solution must be considered. This is captured by the notion of a *conjugate point*. These are found by defining *Jacobi's equation*, denoted v , which is an accessory first-order differential equation defined by L and the candidate extremal. A point conjugate to the initial point is a root of Jacobi's equation with initial condition $v(t_0) = 0$, $v'(t_0) = 1$. With this, the second-order sufficient condition for optimality is that an extremal $x(\cdot)$ is a strict minimum if it satisfies the strong Legendre condition and there are no points conjugate to t_0 on the interval $[t_0, t_f]$.

(CV 5) In 1835, Hamilton proposed an alternate formalism by defining $p := \frac{\partial L}{\partial \dot{x}}(t, x, \dot{x})$ and the *Hamiltonian*

$$H(t, x, \dot{x}, p) := \langle p, \dot{x} \rangle - L(t, x, \dot{x}).$$

The coordinates x, p are called the canonical variables, and Hamilton's canonical equations are

$$\dot{x} = \frac{\partial H}{\partial p} \quad \text{and} \quad \dot{p} = -\frac{\partial H}{\partial x},$$

where the first is by definition of H and the second is by the Euler–Lagrange equation:

$$\frac{\partial p}{\partial t} = \frac{d}{dt} \frac{\partial L}{\partial \dot{x}}(t, x, \dot{x}) = \frac{\partial L}{\partial x}(t, x, \dot{x}) = -\frac{\partial H}{\partial x}(t, x, \dot{x}).$$

Thus in the canonical coordinates, the Euler–Lagrange has a simple formulation in the sense that the partial differential equation (B.1) is now a pair of first-order ordinary differential equations. We make two observations about H : first, by definition we have that

$$\frac{\partial H}{\partial \dot{x}} = p - \frac{\partial L}{\partial \dot{x}} = 0$$

and second, if neither \dot{x} nor L are time-dependent, then H is constant along extremals.

(CV 6) The previous conditions apply to weak minima of J . It is obviously desirable to consider a wider class (not necessarily \mathcal{C}^1) of functions to minimize over, and to find strong minima. A natural step is to consider continuous, piecewise- \mathcal{C}^1 functions. We call the points at which \dot{x} is discontinuous *corner points*. In this case, it can be seen that the Euler–Lagrange equation (in integral form) remains a necessary condition, and additionally the *Weierstraß–Erdmann corner conditions* (given by Weierstraß in 1865 but not published, and independently published by Erdmann in 1877) must hold: $\frac{\partial L}{\partial \dot{x}}$ and $\dot{x} \frac{\partial L}{\partial \dot{x}} - L$ must be continuous at each corner point of x (note that these are p and H in the Hamiltonian formalism).

A final result concerning piecewise- \mathcal{C}^1 strong minima is given by the Weierstraß excess function, a necessary condition given in 1879. This states that if $x(\cdot)$ is a strong minimum then

$$E(t, x, \dot{x}, y) \geq 0$$

at every non-corner point of x and all $y \in \mathbb{R}$, where

$$E(t, x, \dot{x}, y) = L(t, x, y) - L(t, x, \dot{x}) - (y - \dot{x}) \frac{\partial L}{\partial \dot{x}}(t, x, \dot{x}).$$

In the Hamiltonian formalism this is

$$E(t, x, \dot{x}, y) = H(t, x, \dot{x}, p) - H(t, x, y, p) \geq 0$$

for all $y \in \mathbb{R}$, i.e., that H is maximized pointwise by \dot{x} along an extremal.

B.2 Optimal control problem statement

Let us now see the advancement from a problem in calculus of variations to optimal control theory. The main distinguishing feature is that the derivative \dot{x} is replaced by a control u , which has greater freedom in the way that it influences the system. In particular, in the following discussion note the role of the Hamiltonian formalism in enabling this transition.

Definition 75. A *control system* consists of a state space $X \subseteq \mathbb{R}^n$ which is a smooth manifold, a control set $U \subseteq \mathbb{R}^m$, a class \mathcal{U} of admissible controls which are measurable and almost everywhere take values in U , and a dynamics $f : \mathbb{R} \times X \times U \rightarrow TX$. We assume that f is continuous in (t, x, u) , differentiable in x , and that each partial $\frac{\partial f}{\partial x}$ is continuous in (t, x, u) .

Definition 76. Let $u(\cdot) \in \mathcal{U}$ be defined on a time interval $[t_0, t_f]$, and let $x(\cdot)$ be the unique solution to $\dot{x} = f(t, x, u(t))$ with interval of definition $(t_1, t_2) \ni t_0$. Then $x(\cdot)$ is the trajectory associated to the control u , and the pair (x, u) is called an *admissible controlled trajectory*.

Remark 77. Since a control $u(\cdot) \in \mathcal{U}$ produces the associated trajectory $x(\cdot)$ through integration, two controls have the same associated trajectory if they differ only on a set of measure zero, and we can say that two such controls are equivalent.

Definition 78. We denote the target *set of terminal constraints* by $N = \{(t, x) \in \mathbb{R} \times X : \Psi(t, x) = 0\}$, where $\Psi = (\psi_0, \dots, \psi_k)$ is continuously differentiable and the gradients of the ψ_i are linearly independent on N .

Definition 79. The *objective* or *cost* functional, J , to minimize is

$$J(u) = \int_{t_0}^{t_f} L(t, x(t), u(t)) dt + \varphi(t_f, x(t_f))$$

where the Lagrangian L is continuous in (t, x, u) , differentiable in x , and $\frac{\partial L}{\partial x}$ is continuous in (t, x, u) and the penalty term φ is continuously differentiable. Optimal control problems with a cost of this form are known as *Bolza problems*, and are known as *Lagrangian* or *Mayer* problems if $\varphi = 0$ or $L = 0$, respectively.

With these definitions in hand, we can define an optimal control problem.

Problem 80 (Optimal control problem). *Among all admissible controlled trajectories (x, u) defined on $[t_0, t_f]$ such that $(t_f, x(t_f)) \in N$, find one that minimizes the cost $J(u)$.*

Notice that if an optimal control problem is Lagrangian and if $\dot{x} = u$, the problem is in fact the basic calculus of variations problem previously stated. Therefore the calculus of variations can be seen as a special case of optimal control theory.

B.3 Pontryagin maximum principle

The central result of optimal control theory, the Pontryagin maximum principle, was given in 1957 by a group of Russian mathematicians headed by Lev Pontryagin [47].

Proposition 81 (Pontryagin maximum principle). *Let (x^*, u^*) be an admissible controlled trajectory of Problem 80 which is optimal. Then there exist a constant $p^0 \leq 0$ and $p : [t_0, t_f] \rightarrow \mathbb{R}^n$ (an adjoint vector) such that the following conditions are satisfied.*

- (i) *Nontriviality of multipliers.* The pair $(p^0, p(t)) \neq 0$ for all $t \in [t_0, t_f]$.
- (ii) *Hamiltonian dynamics.* The dynamics of p is given by

$$\dot{p} = -\frac{\partial H}{\partial x}$$

where H is the control Hamiltonian function, defined as

$$H(t, p^0, p(t), x(t), u(t)) := \langle p(t), f(t, x(t), u(t)) \rangle + p^0 L(t, x(t), u(t)).$$

(iii) *Maximization condition.* For almost every $t \in [t_0, t_f]$,

$$H(t, p^0, p(t), x^*(t), u^*(t)) = \max_{v \in U} H(t, p^0, p(t), x^*(t), v).$$

(iv) *Transversality condition.* At the final time t_f , we have

$$(H + p^0 \varphi_t, -p + p^0 \varphi_x) \perp N.$$

Definition 82. A tuple (x, u, p, p^0) satisfying the first three conditions of the maximum principle is called an *extremal lift* (or simply *extremal*), and if it additionally satisfies the boundary conditions of the problem and transversality condition of the maximum principle it is a *BC-extremal*. We commonly use the coordinate z to denote an extremal lift. When p^0 and u are understood, we may omit them and just write $z = (x, p)$. An extremal lift is *normal* if $p^0 \neq 0$ and *abnormal* if $p^0 = 0$.

That optimal control is a generalization of calculus of variations is clear, and this relationship is also seen in the maximum principle which generalizes the necessary conditions (CV1) and (CV2), uses the Hamilton formalism as in (CV5), and contains the maximization condition (CV6). We will see the role of the (CV3) and (CV4) in §B.5 where the Legendre–Clebsch condition and the definition of a conjugate point are stated in the control setting.

Remark 83. If L and f are time-invariant, H as a function of t along an extremal is constant since $\frac{dH}{dt} = 0$. If furthermore φ and Ψ are time-invariant (and therefore the final time cannot be fixed), then H is zero along an extremal by the transversality condition.

Remark 84. In a time-optimal control problem, we have $H = \langle p, f \rangle + p^0$ since $L = 1$, which is identically zero along an extremal by the previous remark. If $p(t) = 0$ for some t , then $p^0 = 0$ as well, violating the nontriviality condition of the maximum principle. Therefore, in a time-optimal control problem $p(t) \neq 0$ for all $t \in [t_0, t_f]$.

B.4 Optimal control computation

Let us now discuss the computation of an optimal control in a particular setting: assume that the dynamics is *autonomous* (time-invariant) and *control-affine*, i.e., that

$$\dot{x} = f(x, u) = F_0(x) + \sum_{i=1}^m u_i F_i(x) \quad (\text{B.2})$$

for some continuously differentiable vector fields F_i , $i = 0 \dots m$, that the control is bounded— for simplicity we will assume $|u| \leq M = 1$, and that the integral cost L is constant. This setting encompasses many optimal control problems: the control-affine, autonomous dynamics and bounded control are common in applications, and the assumption on L includes Mayer-type problems ($L \equiv 0$) and time-optimal problems ($L \equiv 1$).

B.4.1 Definitions

Definition 85. Given a fixed initial point x_0 and a final time T , the *end-point mapping*, denoted $E^{x_0, T}$, of a system $\dot{x} = f(x, u)$ is the mapping $u \mapsto x(x_0, T, u)$ where $x(x_0, T, u)$ is the solution of the system with initial point x_0 associated to the control $u \in \mathcal{U}$ at time t .

If \mathcal{U} is endowed with the L^∞ topology, then the mapping $E^{x_0, T}$ is smooth. Furthermore, if $x(\cdot)$ is the trajectory associated to a smooth control $u : [0, T] \rightarrow U$, then u can be smoothly extended to $\tilde{u} : [0, T + \varepsilon] \rightarrow U$, where $\varepsilon > 0$ is fixed.

Definition 86. Given a Hamiltonian function $H(x, p)$, we denote the Hamiltonian vector field on T^*X by \vec{H} , where

$$\vec{H} = \left(\frac{\partial H}{\partial p}, -\frac{\partial H}{\partial x} \right).$$

When the control $u(\cdot)$ can be calculated as a feedback control in terms of x and p (discussed below), its expression can be inserted into H to define the *true Hamiltonian* H_r , yielding \vec{H}_r in the natural way.

Definition 87. Let $z(t, z_0)$ denote the trajectory of a true Hamiltonian \vec{H}_r such that $z(0, z_0) = z_0 = (x_0, p_0)$. The *exponential map*, $\exp_{x_0, t}(p_0)$, is the map $p_0 \mapsto x(t, x_0, p_0)$ where $x(t, x_0, p_0)$ is the state components of the true Hamiltonian flow from the initial point z_0 at time t .

Definition 88. In the single-input case $m = 1$, if a control is valued in the set $\{-1, +1\}$ and there are only finitely many changes, called *switchings*, between these values then the control is called *bang-bang*.

Definition 89. Relaxing the control bound, a control $u : [t_0, t_f] \rightarrow \mathbb{R}^m$, $u \in L^\infty([t_0, t_f])$ is called *singular* on $[t_0, t_f]$ if the Fréchet derivative of E^{x_0, t_f} is not of full rank.

Remark 90. Given a system of the form (B.2), we denote the Hamiltonian vector fields $H_i(x, p) := \langle p, F_i(x) \rangle$, $i = 1 \dots m$. Similarly, we denote $H_X = \langle p, X \rangle$ for some vector field X .

Definition 91. Given a Hamiltonian $H(q, p)$, we denote the Hamiltonian vector field on T^*M by \vec{H} , where

$$\vec{H} = \left(\frac{\partial H}{\partial p}, -\frac{\partial H}{\partial q} \right).$$

Definition 92. The *Lie bracket* of two differentiable vector fields X and Y is the operator $[X, Y] = XY - YX$. In coordinates, this is

$$[X, Y](x) = \frac{\partial Y}{\partial x} \cdot X(x) - \frac{\partial X}{\partial x} \cdot Y(x).$$

Definition 93. Given two Hamiltonian vector fields H_1 and H_2 , the *Poisson bracket*, $\{H_1, H_2\}$, is defined as $\{H_1, H_2\} = dH_1(\vec{H}_2)$. In coordinates, this is $\{H_1, H_2\}(x, p) = \langle p, [F_1, F_2](x) \rangle$.

B.4.2 Single-input case

In the single-input case, i.e. $m = 1$, we write the vector fields as $F = F_0$ and $G = F_1$, thus the dynamics is $\dot{x} = F + uG$. By the maximization condition of the maximum principle, for an optimal control $u(\cdot)$ with associated trajectory $x(\cdot)$ we have that for all $t \in [t_0, t_f]$

$$\begin{aligned} H(t, p^0, p(t), x(t), u(t)) &= \max_{v \in U} H(t, p^0, p(t), x(t), v) \\ &= \max_{v \in U} (\langle p(t), F(x(t)) + vG(x(t)) \rangle + p^0 L(t, x(t), u(t))) \\ &= \langle p(t), F(x(t)) \rangle + p^0 L(t, x(t), u(t)) + \max_{v \in U} v \langle p(t), G(x(t)) \rangle \end{aligned}$$

so in particular the maximization of H over $v \in U$ amounts to maximizing just the quantity $v \langle p, G \rangle$ and to this end we define the *switching function* $\Phi(t) := \langle p(t), G(x(t)) \rangle$. Clearly, if $\Phi(t)$ is nonzero, $u(t) = \text{sgn } \Phi(t)$, i.e., $u(t) = \pm 1$, and if $\Phi(t) = 0$ this condition gives no immediate information about

the value of $u(t)$. If this occurs only at a point, i.e., $\Phi(t) = 0$ but $\dot{\Phi}(t)$ exists and is nonzero, then $u(t)$ is defined everywhere on a neighborhood of t except at the point t , and by Remark 77 this is sufficient to define u on this interval. Aside from situations where the times t such that $\Phi(t) = 0$ accumulate, the control is bang-bang.

If however $\Phi(t) = 0$ on an interval, then we are in the singular case and the above straightforward observation does not define the value of the control. Fortunately, further relations are found by the fact that since Φ is identically zero, all derivatives are also zero, i.e., $\frac{d^k \Phi}{dt^k}(t) = 0$ for all t in this interval and $k \in \mathbb{Z}^+$. This first derivative is

$$\begin{aligned}
\frac{d\Phi}{dt} &= \left\langle \frac{dp}{dt}, G \right\rangle + \left\langle p, \frac{dG}{dt} \right\rangle \\
&= -\frac{\partial H}{\partial x} \cdot G + \left\langle p, \frac{\partial G}{\partial x} \frac{dx}{dt} \right\rangle \\
&= -\frac{\partial(\langle p, F + uG \rangle + p^0 L)}{\partial x} \cdot G + \left\langle p, \frac{\partial G}{\partial x} \cdot (F + uG) \right\rangle \\
&= -\left\langle p, \frac{\partial F}{\partial x} \cdot G \right\rangle - u \left\langle p, \frac{\partial G}{\partial x} \cdot G \right\rangle + \left\langle p, \frac{\partial G}{\partial x} \cdot F \right\rangle + u \left\langle p, \frac{\partial G}{\partial x} \cdot G \right\rangle \\
&= \left\langle p, \frac{\partial G}{\partial x} \cdot F - \frac{\partial F}{\partial x} \cdot G \right\rangle + u \left\langle p, \frac{\partial G}{\partial x} \cdot G - \frac{\partial G}{\partial x} \cdot G \right\rangle.
\end{aligned}$$

Although the last term is zero we include it since recalling Definition 92, we see that the previous computation is neatly captured by the Lie bracket: $\dot{\Phi} = \langle p, [F, G] \rangle + u \langle p, [G, G] \rangle = \langle p, [F, G] \rangle$. More generally, the above steps guide the proof of the following lemma [53].

Lemma 94. *If X is a differentiable vector field and p is a solution to the adjoint equation, then*

$$\frac{d}{dt} \langle p, X \rangle = \langle p, [F, X] \rangle + u \langle p, [G, X] \rangle.$$

We are now equipped to calculate the singular control. As above, $0 = \dot{\Phi} = \langle p, [F, G] \rangle$, and differentiating once more shows that

$$0 = \ddot{\Phi} = \langle p, [F, [F, G]] \rangle + u \langle p, [G, [F, G]] \rangle, \tag{B.3}$$

and if $\langle p, [G, [F, G]] \rangle \neq 0$, this gives the value of the singular control u_s ,

$$u_s(t) = -\frac{\langle p, [F, [F, G]] \rangle}{\langle p, [G, [F, G]] \rangle}.$$

This is called a *singular control of order 1*, higher orders occurring when $\langle p, [G, [F, G]] \rangle$ is zero and further differentiation is required to compute the value of u . When doing so, it is immediately seen that only even-numbered derivations give relations on the control. A control defined by the $(2n)$ th is called an order n singular control. We omit further discussion of higher-order cases (or other more pathological situations) for two reasons: first, this work employs only order 1 singular controls and second, singular extremals are generically of order 1 [7]. Using Definition 93, the value of a order 1 singular control is expressed as

$$u_s = -\frac{\{H_F, \{H_F, H_G\}\}}{\{H_G, \{H_F, H_G\}\}}. \quad (\text{B.4})$$

Remark 95. The properties “bang-bang” or “singular” are properties of an extremal lift since they depend on the state and adjoint vectors. We commonly refer to the state and control of such an extremal lift as, e.g., a singular trajectory (or arc) and control.

B.4.3 Bi-input case

In the case where the number of controls is 2, the system is written as

$$\dot{x} = F_0(x) + u_1 F_1(x) + u_2 F_2(x),$$

with $|u| \leq 1$. By the maximization condition of the maximum principle, $u_1 H_1 + u_2 H_2$ is to be maximized among $|u| \leq 1$, i.e., u must be of maximum magnitude and collinear with the vector (H_1, H_2) , so

$$u_1 = \frac{H_1}{\sqrt{H_1^2 + H_2^2}}, \quad u_2 = \frac{H_2}{\sqrt{H_1^2 + H_2^2}}$$

is a parameterization of the control outside the switching surface Σ , $\Sigma = \{z : H_1 = H_2 = 0\}$. Substituting this value of u into H gives the *true Hamiltonian* H_n ,

$$H_n = H_0 + (H_1^2 + H_2^2)^{1/2},$$

the smooth solutions of which are extremals of order zero.

Defining the system with extended state coordinate (x, α) and control v by $u_1 = \sin \alpha$, $u_2 = \cos \alpha$, and $\dot{\alpha} = v$, we have the following result [5, 14].

Proposition 96. (i) *Extremal controls of order zero correspond to the singularities of the end-*

point map $E^{x_0, T} : u \in L^\infty[t_0, t_f] \cap \{|u| = 1\} \mapsto x(T, x_0, u)$, i.e., restricting the controls to the unit sphere S^1 .

(ii) Extremal curves of order zero are projections on the x -space of smooth singular trajectories of the end-point mapping of the extended system $v \mapsto (x(t, v, x_0, \alpha_0), \alpha(t, v, x_0, \alpha_0))$.

B.5 Second-order conditions

To complete our general discussion of optimal control theory, we state the generalizations of (CV3) and (CV4). The Legendre–Clebsch condition is standard [1, 7, 34], and the relation of conjugate points to optimal control is now well-established [1, 6, 14, 49]. In this section we relax the constraints on the domain of control values, $U = \mathbb{R}^m$.

Definition 97. Consider a trajectory $x(\cdot)$ associated to the control u defined on $[0, T]$ with $x(0) = x_0$, and write the objective cost for this control as $J(T, u)$.

- If T is fixed, $x(\cdot)$ is said to be locally optimal in the L^∞ topology if it is optimal in a neighborhood of u in the L^∞ topology.
- If T is fixed, $x(\cdot)$ is said to be locally optimal in the \mathcal{C}^0 topology if it is optimal in a neighborhood of $x(\cdot)$ in the \mathcal{C}^0 topology.
- If T is not fixed, $x(\cdot)$ is said to be locally optimal in the L^∞ topology if for every neighborhood V of u in $L^\infty([0, T + \varepsilon], U)$, every $\tau \in \mathbb{R}$ such that $|\tau| < \varepsilon$, and every $v \in V$ such that $E(x_0, T + \tau, v) = E(x_0, T, u)$, we have that $J(T + \tau, v) \geq J(T, u)$.
- If T is not fixed, $x(\cdot)$ is locally optimal in the \mathcal{C}^0 topology if for every neighborhood Y in M of $x(\cdot)$, every $\tau \in \mathbb{R}$ such that $|\tau| < \varepsilon$, and every $y(\cdot) \in Y$ associated to a control v on $[0, T + \tau]$ satisfying $y(0) = x_0$ and $y(T + \tau) = x(T)$, we have that $J(T + \tau, v) \geq J(T, u)$.

Remark 98. If $x(\cdot)$ is the globally optimal solution trajectory, then it is clearly locally optimal in the \mathcal{C}^0 topology, and since this includes all neighboring trajectories (even those not associated to a neighboring control), this implies that it is locally optimal in the L^∞ as well.

B.5.1 Legendre–Clebsch condition

Proposition 99. *Let (x, u) be an admissible controlled trajectory defined on $[t_0, t_f]$. If $x(\cdot)$ is optimal in the L^∞ topology then the Legendre–Clebsch condition,*

$$\frac{\partial^2 H}{\partial u^2}(x, p, p^0, u)(v, v) \leq 0 \quad \forall v \in \mathbb{R}^m,$$

holds along every extremal lift (x, p, p^0, u) of $x(\cdot)$.

If the strong Legendre–Clebsch condition, that there exists $\alpha > 0$ such that

$$\frac{\partial^2 H}{\partial u^2}(x, p, p^0, u)(v, v) \leq -\alpha \|v\|^2 \quad \forall v \in \mathbb{R}^m, \tag{B.5}$$

holds, then $x(\cdot)$ is locally optimal in the L^∞ topology on $[0, \varepsilon]$ for some $\varepsilon > 0$. If the extremal is normal ($p^0 < 0$) then $x(\cdot)$ is locally optimal in the C^0 topology for some $\varepsilon > 0$.

For a control-affine system, $\frac{\partial^2 H}{\partial u^2} \equiv 0$ and this theorem provides no classification. In this case the higher-order maximum principle is used to derive the generalized Legendre–Clebsch condition [34], stated here as it applies to the problem assumptions used in §B.4.

Proposition 100 (generalized Legendre–Clebsch condition). *If (x, u) is a extremal which minimizes J and u is singular on an interval $[t_1, t_2] \subseteq [t_0, t_f]$, then there exists an adjoint p such that*

$$\langle p(t), [G, [F, G]](x(t)) \rangle \geq 0 \text{ for all } t \in [t_1, t_2],$$

and we say that the extremal lift (x, p, u) satisfies the generalized Legendre–Clebsch condition. If this value is strictly positive on this interval, the extremal lift satisfies the strong generalized Legendre–Clebsch condition.

B.5.2 Conjugate points

We will define the concept of a conjugate point in the control setting, with the central result that the first conjugate point of an extremal solution is the point at which an extremal is no longer locally optimal. The discussion here of conjugate points follows the presentation of Bonnard, Caillaud, and Trélat [6]. Let $z = (x, u, p, p^0)$ be a reference extremal lift defined on a time interval $[0, T]$. We say that u is corank one if the derivative of the end-point mapping with respect to u is of codimension

one, and in this case we say that the extremal is of corank one as well.

Definition 101. We denote by Q_t , $t \in [0, T]$, the intrinsic second-order derivative of the end-point mapping with respect to u . The *first conjugate point* along an extremal is the supremum of times t such that Q_t is positive definite.

Theorem 102. *Suppose that $z(\cdot)$ is of corank one, and let t_c be the first conjugate time along this extremal.*

(i) *If the (generalized) strong Legendre–Clebsch condition holds along $z(\cdot)$, then $x(\cdot)$ is locally optimal in the L^∞ topology on $[0, t_c]$. If moreover the extremal lift is normal ($p^0 < 0$), then $x(\cdot)$ is locally optimal in the C^0 topology on $[0, t_c]$.*

(ii) *If the control is of corank one on every subinterval $[t_1, t_2] \subseteq [0, T]$, then $z(\cdot)$ is not locally optimal in the L^∞ topology on $[0, t]$ for all $t > t_c$.*

Definition 103. Let \vec{H} be a Hamiltonian vector field on T^*M and let $z(\cdot)$ be a trajectory of \vec{H} defined on $[t_0, t_f]$, i.e. $\dot{z}(t) = \vec{H}(z(t))$ for $t \in [t_0, t_f]$. The differential equation

$$\hat{\delta}z(t) = d\vec{H}(z(t))\delta z(t)$$

is called the *Jacobi equation* along $z(\cdot)$.

Definition 104. A *Jacobi field* $\delta z(\cdot) = (\delta x(\cdot), \delta p(\cdot))$ is a nontrivial solution of the Jacobi equation along $z(\cdot)$. It is said to be *vertical at time t* when $\delta x(t) = 0$. A time t_c is *geometrically conjugate* if there exists a Jacobi field that is vertical at times t_0 and t_c , and in this case we say that the point $x(t_c)$ is *geometrically conjugate* to $x(t_0)$.

Proposition 105. *Let $(x_0, p_0) = z(0)$, $L_0 := T_{x_0}^*\mathbb{R}^n$, and $L_t := \exp_t(\vec{H})(L_0)$. Then L_t is a Lagrangian submanifold of $T^*\mathbb{R}^n$ whose tangent space is spanned by Jacobi fields initiated at L_0 . Moreover, $x(t_c)$ is geometrically conjugate to x_0 if and only if the mapping $\exp_{t_c}(x_0, \cdot)$ is not an immersion at p_0 .*

Theorem 106. *Assume that the strong Legendre condition holds along $z(\cdot)$, and assume strong regularity: that u is of corank one along every subinterval $[t_1, t_2] \subseteq [0, T]$. Then the first geometric conjugate time is the first conjugate time along $z(\cdot)$, denoted t_c . Therefore $x(\cdot)$ is locally optimal on*

$[0, t_c)$ in the L^∞ topology (in the C^0 topology if $p^0 < 0$), and if $t > t_c$, $x(\cdot)$ is not locally optimal on $[0, t]$ in the L^∞ topology.

Proposition 105 provides a way of constructing an algorithm for the detection of geometric conjugate points, and Theorem 106 shows that under proper assumptions these are conjugate times.

BIBLIOGRAPHY

- [1] A. A. Agrachev and Y. L. Sachkov. *Control theory from the geometric viewpoint*, volume 87 of *Encyclopaedia of Mathematical Sciences*. Springer-Verlag, Berlin, 2004.
- [2] F. J. Bonnans, P. Martinon, and V. Grélard. Bocop – a collection of examples. Technical report, INRIA RR-8053, 2012.
- [3] B. Bonnard. Feedback equivalence for nonlinear systems and the time optimal control problem. *SIAM J. Control Optim.*, 29(6):1300–1321, 1991.
- [4] B. Bonnard. Quadratic control systems. *Math. Control Signals Systems*, 4(2):139–160, 1991.
- [5] B. Bonnard, J.-B. Caillau, and E. Trélat. Geometric optimal control of elliptic Keplerian orbits. *Discrete Contin. Dyn. Syst. Ser. B*, 5(4):929–956 (electronic), 2005.
- [6] B. Bonnard, J.-B. Caillau, and E. Trélat. Second order optimality conditions in the smooth case and applications in optimal control. *ESAIM Control Optim. Calc. Var.*, 13(2):207–236 (electronic), 2007.
- [7] B. Bonnard and M. Chyba. *Singular trajectories and their role in control theory*, volume 40 of *Mathématiques & Applications*. Springer-Verlag, Berlin, 2003.
- [8] B. Bonnard, M. Chyba, and J. Marriott. Singular trajectories and the contrast imaging problem in nuclear magnetic resonance. *SIAM J. Control Optim.*, 51(2):1325–1349, 2013.
- [9] B. Bonnard, M. Chyba, and J. Marriott. Feedback equivalence and the contrast problem in nuclear magnetic resonance imaging. *Pacific Journal of Optimization*, to appear 2013.
- [10] B. Bonnard, M. Chyba, and D. Sugny. Time-minimal control of dissipative two-level quantum systems: the generic case. *IEEE Trans. Automat. Control*, 54(11):2598–2610, 2009.
- [11] B. Bonnard, M. Claeys, O. Cots, and P. Martinon. Comparison of numerical methods in the contrast imaging problem in NMR. In *Decision and Control and European Control Conference (CDC-ECC), 2013 52nd IEEE Conference on*, to appear 2013.

- [12] B. Bonnard and O. Cots. Geometric numerical methods and results in the contrast imaging problem in nuclear magnetic resonance. *Mathematical Models and Methods in Applied Sciences*, 23:1–26, 2013.
- [13] B. Bonnard, A. Jacquemard, M. Chyba, and J. Marriott. Algebraic geometric classification of the singular flow in the contrast imaging problem in nuclear magnetic resonance. *Mathematical Control and Related Fields*, 3(4):397–432, 2013.
- [14] B. Bonnard and I. Kupka. Théorie des singularités de l’application entrée/sortie et optimalité des trajectoires singulières dans le problème du temps minimal. *Forum Math.*, 5(2):111–159, 1993.
- [15] B. Bonnard and D. Sugny. Time-minimal control of dissipative two-level quantum systems: the integrable case. *SIAM J. Control Optim.*, 48(3):1289–1308, 2009.
- [16] P. Brunovský. A classification of linear controllable systems. *Kybernetika (Prague)*, 6:173–188, 1970.
- [17] Bruno Buchberger. Bruno Buchberger’s PhD thesis 1965: An algorithm for finding the basis elements of the residue class ring of a zero dimensional polynomial ideal. *Journal of Symbolic Computation*, 41(3–4):475–511, 2006.
- [18] J.-B. Caillaud, O. Cots, and J. Gergaud. Differential pathfollowing for regular optimal control problems. *Optim. Methods Softw.*, 27:177–196, 2012.
- [19] R. F. A. Clebsch. *J. für Math.*, 55:254, 1858.
- [20] S. Conolly, D. Nishimura, and A. Macovski. Optimal control solutions to the magnetic resonance selective excitation problem. *Medical Imaging, IEEE Transactions on*, 5(2):106–115, 1986.
- [21] D. Cox, J. Little, and D. O’Shea. *Ideals, varieties, and algorithms*. Undergraduate Texts in Mathematics. Springer, New York, third edition, 2007.
- [22] J. A. Dieudonné and J. B. Carrell. Invariant theory, old and new. *Advances in Math.*, 4:1–80, 1970.
- [23] D. S. Dummit and R. M. Foote. *Abstract algebra*. John Wiley & Sons Inc., Hoboken, NJ, third edition, 2004.

- [24] D. Eisenbud. *Commutative algebra*, volume 150 of *Graduate Texts in Mathematics*. Springer-Verlag, New York, 1995.
- [25] D. Eisenbud, C. Huneke, and W. Vasconcelos. Direct methods for primary decomposition. *Invent. Math.*, 110(2):207–235, 1992.
- [26] R. R. Ernst, G. Bodenhausen, and A. Wokaun. *Principles of Nuclear Magnetic Resonance in One and Two Dimensions*. International series of monographs on chemistry. Clarendon Press, 1990.
- [27] A. Garon, S. J. Glaser, and D. Sugny. Revealing the geometric nature of spin dynamics with relaxation: Vector fields, magic plane and steady-state ellipsoid. *J. Magn. Reson.*, submitted 2013.
- [28] P. Gianni, B. Trager, and G. Zacharias. Gröbner bases and primary decomposition of polynomial ideals. *J. Symbolic Comput.*, 6(2-3):149–167, 1988.
- [29] A. Jacquemard and M. A. Teixeira. Effective algebraic geometry and normal forms of reversible mappings. *Rev. Mat. Complut.*, 15(1):31–55, 2002.
- [30] J. A. Jones and M. Mosca. Implementation of a quantum algorithm on a nuclear magnetic resonance quantum computer. *The Journal of Chemical Physics*, 109(5):1648–1653, 1998.
- [31] N. Khaneja, R. Brockett, and S. J. Glaser. Time optimal control in spin systems. *Phys. Rev. A*, 63:032308, Feb 2001.
- [32] N. Khaneja, S. J. Glaser, and R. Brockett. Sub-riemannian geometry and time optimal control of three spin systems: Quantum gates and coherence transfer. *Phys. Rev. A*, 65:032301, Jan 2002.
- [33] N. Khaneja, T. Reiss, C. Kehlet, T. Schulte-Herbrüggen, and S. J. Glaser. Optimal control of coupled spin dynamics: design of NMR pulse sequences by gradient ascent algorithms. *Journal of Magnetic Resonance*, 172(2):296–305, 2005.
- [34] A. J. Krener. The high order maximal principle and its application to singular extremals. *SIAM J. Control Optim.*, 15(2):256–293, 1977.

- [35] I. Kupka. Geometric theory of extremals in optimal control problems. I. The fold and Maxwell case. *Trans. Amer. Math. Soc.*, 299(1):225–243, 1987.
- [36] M. Lapert, Y. Zhang, M. Braun, S. J. Glaser, and D. Sugny. Geometric versus numerical optimal control of a dissipative spin 1/2 particle. *Phys. Rev. A*, 82(6):063418, December 2010.
- [37] M. Lapert, Y. Zhang, M. Braun, S. J. Glaser, and D. Sugny. Singular extremals for the time-optimal control of dissipative spin $\frac{1}{2}$ particles. *Phys. Rev. Lett.*, 104(8):083001, Feb 2010.
- [38] M. Lapert, Y. Zhang, M. A. Janich, S. J. Glaser, and D. Sugny. Exploring the physical limits of saturation contrast in magnetic resonance imaging. *Scientific Reports*, 2, August 2012.
- [39] Jean B. Lasserre, Didier Henrion, Christophe Prieur, and Emmanuel Trélat. Nonlinear optimal control via occupation measures and LMI-relaxations. *SIAM J. Control Optim.*, 47(4):1643–1666, 2008.
- [40] J. M. Lee. *Manifolds and differential geometry*, volume 107 of *Graduate Studies in Mathematics*. American Mathematical Society, Providence, RI, 2009.
- [41] M. H. Levitt. *Spin dynamics*. John Wiley & Sons, Ltd, second edition, 2008.
- [42] D. Liberzon. *Calculus of variations and optimal control theory*. Princeton University Press, Princeton, NJ, 2012.
- [43] L. Markus. Quadratic differential equations and non-associative algebras. In *Contributions to the theory of nonlinear oscillations, Vol. V*, pages 185–213. Princeton Univ. Press, Princeton, N.J., 1960.
- [44] P. Martinon. Bocop – the optimal control solver. <http://bocop.org/>.
- [45] H. Melenk, H. M. Moller, and W. Neun. Symbolic solution of large stationary chemical kinetics problems. *IMPACT Comput. Sci. Eng.*, 1(2):138–167, May 1989.
- [46] D. Mumford, J. Fogarty, and F. Kirwan. *Geometric invariant theory*, volume 34 of *Ergebnisse der Mathematik und ihrer Grenzgebiete (2) [Results in Mathematics and Related Areas (2)]*. Springer-Verlag, Berlin, third edition, 1994.

- [47] L. S. Pontryagin, V. G. Boltyanskii, R. V. Gamkrelidze, and E. F. Mishchenko. *The mathematical theory of optimal processes*. Translated from the Russian by K. N. Trirogoff; edited by L. W. Neustadt. Interscience Publishers John Wiley & Sons, Inc. New York-London, 1962.
- [48] A. O. Remizov. Implicit differential equations and vector fields with nonisolated singular points. *Mat. Sb.*, 193(11):105–124, 2002.
- [49] A. V. Saryčev. Index of second variation of a control system. *Mat. Sb. (N.S.)*, 113(3):464–486, 496, 1980.
- [50] H. Schättler and U. Ledzewicz. *Geometric optimal control*, volume 38 of *Interdisciplinary Applied Mathematics*. Springer, New York, 2012.
- [51] S. G. Schirmer and A. I. Solomon. Constraints on relaxation rates for n -level quantum systems. *Phys. Rev. A*, 70:022107, August 2004.
- [52] M. Spivak. *A comprehensive introduction to differential geometry. Vol. I*. Publish or Perish Inc., Wilmington, Del., second edition, 1979.
- [53] H. J. Sussmann and G. Tang. Shortest paths for the Reeds-Shepp car: A worked out example of the use of geometric techniques in nonlinear optimal control. Technical report, Rutgers University, 1991.
- [54] H. J. Sussmann and J. C. Willems. 300 years of optimal control: from the brachystochrone to the maximum principle. *Control Systems, IEEE*, 17(3):32–44, June 1997.
- [55] L. M. K. Vandersypen and I. L. Chuang. NMR techniques for quantum control and computation. *Rev. Mod. Phys.*, 76:1037–1069, Jan 2005.